Longshore transport of coarse-grained material

An assessement of the longshore transport
behavior of the dynamic rock slope
at Maasvlakte 2

T. Olthoff

TUDelft

Van Oord
Marine ingenuity

Longshore transport of coarse-grained material

An assessment of the longshore transport behavior of the dynamic rock slope at Maasvlakte 2

by

T. Olthoff

to obtain the degree of Master of Science
at the Delft University of Technology,
to be defended publicly on Monday January 14, 2019 at 10:00 AM.

TUDelft

Van Oord

Marine ingenuity

Acknowledgements

With this thesis report I conclude my Master of Science in Hydraulic Engineering at the Delft University of Technology.

My sincere gratitude goes out to my thesis committee for their guidance and fruitful discussions throughout my thesis work; Stefan Aarninkhof for your limited time and on-point feedback, Greg Smith for your feeling for overview and simultaneous attention to detail and Bas Hofland for your infinite amount of solutions which you brought to the table every time we met. I explicitly want to thank my daily supervisor at Van Oord, Dennis van Kester. Dennis, I learned a lot from your enthusiastic, down-to-earth and pragmatic approach and will take these matters along in my future work at Van Oord.

Next to my committee, I would like to express my gratitude to all the friendly and helpful people at Van Oord for assisting me whenever necessary. I also would like to thank Van Oord as a company for giving me the opportunity to immediately start working there after my graduation.

Finally I want to thank my family and friends for their unconditional support throughout the last 9 months. A special thanks goes out to my roommates, who coped with me and my roller coaster of different moods, which I experienced throughout my thesis research.

T. (Tymen) Olthoff
Rotterdam, January 2019

Abstract

Introduction

The consortium Projectorganisatie Uitbreiding Maasvlakte (PUMA), consisting out of Van Oord and Boskalis, constructed a hard sea defence for the protection of Maasvlakte 2, which is the expansion of the Port of Rotterdam. This hard sea defence consists of a Dynamic Rock Slope (DRS) with a Block Dam (BD) situated in front of it. The BD is build up out of large concrete blocks which were recycled from Maasvlakte 1. The Dynamic Rock Slope behind it protects the hinterland through an approximate three to four meter thick layer of quarry rock. When waves travel obliquely through this Block Dam and interact with the Dynamic Rock Slope, stones are transported in alongshore direction. This process is called Longshore Transport (LT) and will have erosion and accretion of stones to effect along the DRS. In order to maintain the layer thickness of this stone layer, PUMA made a prognosis on LT for the coming 50 years after construction. From this prognosis a nourishment campaign was set-up, consisting of volumes of stone PUMA expected to nourish every 2.5 years.

Goal of this research

After a maintenance period of five years it was concluded by PUMA that the nourishment volumes were lower than expected. Therefore Van Oord asked to assess where differences in the prognosis of PUMA on Longshore Transport and the observed Longshore Transport rates over the period 2013 to 2018 come from. Within their prognosis, PUMA made use of a dimensional Longshore Transport relation. As this specifically calibrated Longshore Transport relation is only applicable for the computation of LT rates at a structure containing the characteristics of the DRS at Maasvlakte 2, this research looked into the possibilities of using a non-dimensional Longshore Transport relation for the computation of Longshore Transport rates at the DRS of Maasvlakte 2. Would such an equation be applicable to the case of Maasvlakte, it would subsequently be usable when designing a new Dynamic Rock Slope, containing different characteristics than those of the DRS at Maasvlakte 2.

Two Longshore Transport Relations

In order to calibrate the dimensional Longshore Transport relation of PUMA, HR Wallingford executed scale model tests on Longshore Transport, in assignment of PUMA (HR Wallingford, 2007a)(HR Wallingford, 2007b) (HR Wallingford, 2009c)(HR Wallingford, 2009d). By means of these scale model tests it was shown in this research the non-dimensional General Longshore Transport (GLT) relation of Tomasicchio et al. (2016) is able to predict Longshore Transport rates following from these tests. As the GLT relation showed promising results regarding the prediction of Longshore Transport at a Dynamic Rock Slope for these scale model tests, this relation and the PUMA relation, were both taken into the assessment of the Longshore Transport behavior of the Dynamic Rock Slope at Maasvlakte 2.

Methodology

Computing Longshore Transport rates that follow from the two Longshore Transport relations over the period 2013 to 2018 required a calculation model. This calculation model made use of the wave data following from a SWAN run. The input wave data was taken at the Europlatform, situated approximately 50 kilometers offshore of Maasvlakte 2. The output of the SWAN run consisted of a representative wave climate for every 100 meters along the DRS, situated at the toe of the DRS. Consecutively, the calculation model altered the three main forcing parameters, wave height, wave direction and peak period, as a result of the limiting water depth and interaction with the Block Dam. In this way the transport rates following from the wave climate over the period 2013 to 2018 were computed. All the corresponding characteristics regarding the specific case of the Dynamic Rock Slope at Maasvlakte 2, for the period of 2013 to 2018, were taken into account.

Next to the sole computation of wave data over the period 2013 to 2018, survey data over this period was analysed. This survey data shows the actual occurred changes in volumes of stone along the interest area of the DRS at Maasvlakte. The displaced volumes over the different survey periods represent the amounts of erosion or accretion a section of a 100 meters experienced over these survey periods. By comparison of the displaced volumes to the computed Longshore Transport, following from both the LT relations, the predictive

abilities of both relations was assessed. In other words, a validation was carried out on both the PUMA and the GLT relation.

Results PUMA relation
Following from computations using the wave climate of 2013 to 2018, it was seen this wave climate produces 32% less Longshore Transport over the interest area along the DRS at Maasvlakte 2, with respect to the prognosis of PUMA. For this prognosis, PUMA used the wave climate of 1979 to 2005. The cause for differences in wave climate, being the first reason for the lower computed transport rates, are twofold. Firstly it was seen the wave climate over the period 2013 to 2018 solely consisted of 1:5 year storm events, making this period a relatively mild wave climate, compared with the design storms on which the DRS was designed. Next to a milder wave climate, a difference in refraction is present when comparing the two different periods. This difference in refraction is the result of the morphodynamically active foreshore of Maasvlakte 2. As the effect of storm events on the computation of Longshore Transport appeared to be severe, the milder wave climate over the recent period is seen as the normative reasoning for the lower occurred transport rates over the period 2013 to 2018. The second reason for the lower computed transport rates over the period 2013 to 2018, is the higher placement of the Block Dam. During executing the concrete blocks forming the Block Dam were placed higher than was opted in design. Computed transport rates showed that, would the design be followed exactly, Longshore Transport would be approximately 2 times the amount of transport as is currently observed.

Following from the validation of the PUMA relation, it was concluded the PUMA relation was able to compute the areas over which erosion or accretion will occur. With respect to the accuracy of the PUMA relation, an approximate accuracy of a factor 2 was obtained. Meaning a computed volume of displaced stones over a section of a 100 meters can be twice as high or two times as small as the occurred stone displacement. The validation showed the differences in prognosis and currently observed Longshore Transport at the DRS are circumstantial and are not due to the predictive abilities of the PUMA relation.

Results General Longshore Transport (GLT) relation
The General Longshore Transport (GLT) relation of Tomasicchio et al. (2016) appeared to compute approximately similar amount of transport rates over the period 2013 to 2018, compared to the PUMA relation. On average the GLT relation computed 9% less transport over this period. Thereby it was concluded the non-dimensional GLT relation is applicable for the case of the Dynamic Rock Slope at Maasvlakte 2.
As the GLT relation computes approximately similar amounts of Longshore Transport with respect to the PUMA relation, the accuracy in predicting amounts of erosion or accretion over the different survey periods appeared to be similar as to accuracy of the PUMA relation. The accuracy over the period 2013 to 2018 therefore again amounted to a factor 2. Thereby the GLT relation and the PUMA relation are equally validated within this research, keeping in mind this validation holds for the specific case of the Dynamic Rock Slope at Maasvlakte 2 and the period of 2013 to 2018.

Recommendations
Resulting from this research, multiple recommendations regarding the Longshore Transport behavior of the Dynamic Rock Slope at Maasvlakte 2 were given. Firstly it is recommended to acquire more field data on actual Longshore Transport processes behind the Block Dam. Such field data would give more insight into the processes leading to Longshore Transport and could consequently be used in an update of the maintenance plan of the DRS. Secondly, this more specific knowledge on LT processes at the DRS could contribute in quantifying the effect of the changing foreshore on Longshore Transport. Lastly, it is recommended that with regard to the current maintenance plan, a pragmatic approach should be maintained. This research showed storm events have a severe influence on the alongshore displacement of stones following from such an event. One must be aware intensive maintenance will be required, would a severe storm event occur.

For further research on the topic of Longshore Transport of coarse-grained material at a Dynamic Rock Slope, it is recommended more field and scale model test data is required for the calibration of the General Longshore Transport relation of Tomasicchio et al. (2016). It is important to investigate the performance of the GLT relation - and other Longshore Transport relations - when applying it on a case of a Dynamic Rock Slope which does not include a Block Dam and which preferably holds different characteristics, e.g. slope, orientation and stone size.

Contents

Nomenclature

Abbreviations

Symbol	Description	Unit
BD	Block Dam	-
DRS	Dynamic Rock Slope	-
LT	Longshore Transport	-
MV2	Maasvlakte 2	-
PUMA	Projectorganisatie Uitbreiding Maasvlakte	-
SMT	Scale model test	-
SP	Setting Period	-

Symbols

Symbol	Description	Unit
α	Slope angle	$^\circ$
β	Angle of wave incidence	$^\circ$
Δ	Relative density ($= \frac{\rho_s - \rho_w}{\rho_w}$)	-
γ_b	Breaker depth index	-
$\gamma_{b,T}$	Breaker depth index of Tomasicchio et al. (2016)	-
ξ_p	Breaking parameter	-
A	Surface area	m
B	Crest width	m
c	Wave celerity	m/s
C_k	Characteristic wave height constant.	-
C_t	Wave transmission coefficient	-
c_{avg}	Average crest height	m
D	Diameter of a sediment particle	m
d	Local water depth	m
D_n	Nominal diameter of a sediment particle	m
D_{50}	50% representative of the grain diameter	m
D_{90}	90% representative of the grain diameter	m
$D_{n,50}$	50% representative of the nominal grain diameter ($D_{n,50} = (M_{50}/\rho_s)^{1/3}$)	m
$Dir_{10\%}$	10% of the wave direction	$^\circ N$

$Dir_{90\%}$	90% of the wave direction	$°N$
Dir_{av}	Average wave direction	$°N$
e	Void ratio	-
g	Gravitational acceleration (9.81)	m/s^2
h	Water level	m
H_s	Significant wave height	m
$H_{s,d}$	Local significant wave height	m
k	Wave number ($k = 2\pi/L_p$)	m^{-1}
K_s	Shoaling factor	-
L	Wavelength	m
l_d	Displacement length	m
L_{BK}	Riblength of concrete cubes	m
N	Number of waves	-
n	Porosity	-
N_s	Stability number (= H_o).	-
N_s^{**}	Updated stability number	-
N_{od}	Damage parameter	-
$Q_{LT,N}$	Longshore Transport in volume per unit time according to Tomasic-chio et al. (2013)	m^3/s
R_c	Freeboard	m
s_m	Mean wave steepness	-
$S_{LT,m}$	Longshore Transport rate of the immersed mass per unit time	kg/s
$S_{LT,N}$	Longshore Transport as units per wave	-
$S_{LT,P}$	PUMA's Longshore Transport rate of the immersed mass per unit time	kg/s
S_{LT}	Longshore Transport rate in volume per unit time	m^3/s
$s_{m,0}$	Offshore mean wave steepness	-
$s_{m,k}$	Characteristic mean wave steepness	-
SLR	Sea Level Rise	m
SWL	Still Water Level	$m \pm NAP$
T_m	Mean wave period	s
T_s	Significant wave period	s
$T_{m-1,0}$	Wave period calculated from the first negative moment of the spectrum	s
T_{op}	Wave period parameter ($T_{op} = T_p\sqrt{g/D_{n50}}$)	-
V	Volume	m^3

| z_{BK} | Settlement Block Dam | m |

General Subscripts

Symbol	Description	Unit
0	Offshore	-
b	Breaker	-
BK	Concrete cube shaped blocks	-
d	Deposition	-
i	Incoming	-
k	Characteristic	-
m	Mean	-
p	Peak	-
s	Significant	-
t	Transmission	-

List of Figures

List of Tables

Introduction

1.1. Breakwater types

Breakwaters are generally used to protect hinterland from the sea. This hinterland often contains economic or aesthetic value, like a port, a residential area or world heritage site. In the end breakwaters are nothing more than man-made structures built from sand, clay, rocks or even concrete. To protect the sea-facing side of a breakwater against incoming waves an armour layer is used. This armour layer is often made out of rocks or concrete casted blocks, which nowadays come in several shapes and sizes.

In general The Rock Manual classifies four different types of breakwaters (CIRIA, CUR, 2007):

1. Caissons or seawalls

2. Statically stable breakwaters

3. Dynamically stable structures

4. Dynamic rock slopes and beaches
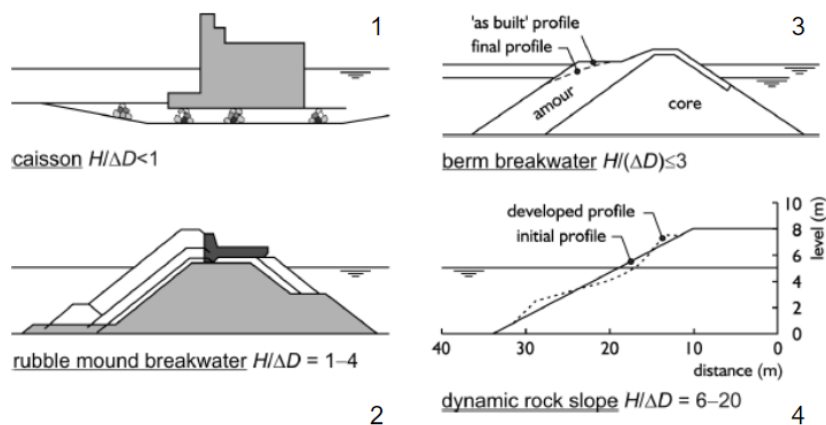
Figure 1.1: Different type of breakwater structures (CIRIA, CUR, 2007).

This classification is based on a damage level which is allowed. In the case of a caissons there is no damage allowed, statically stable breakwaters allow for only very little damage; think of minor displacements of the concrete armour layer. Dynamically stable structures are said to be stable after reshaping of the outer rock layer, so no mayor damage will occur after reshaping. Dynamic rock slopes are in a sense constantly damaged by the waves due to the small stone size of the outer layer of the breakwater and therefore continually moving. The same holds for the sediment on a beach.

As can be seen from Figure 1.1 the classification is quantified by a stability number $\frac{H}{\Delta D} = N_s = H_o$ which will be discussed more extensively in Appendix A.

1.2. The dynamic rock slope concept

In this thesis the focus lies on the Dynamic Rock Slope concept (henceforth also referred to as "DRS"). The armour stones of a DRS are relatively small and will therefore reshape due to wave attack. The idea is to apply a layer of stones as an armour layer on a slope that is thick enough so that the underlying material, often sand, will not surface and wash out.

Waves will attack a DRS and replace the exposed material on the outer slope. When waves would attack this DRS shorenormal, only cross shore transport of sediment, e.g. stones, will take place. In time a cross-sectional profile will form until an equilibrium state is reached. Due to the shore normal wave attack a cross sectional volume balance must hold. Using this volume balance it is possible to predict a so-called S-shaped equilibrium profile. Nowadays this can be done with a numerical model like BREAKWAT, applying the method of Van der Meer (1990b).

Size range [mm]	Sediment
Smaller-$\frac{1}{256}$	Clay
$\frac{1}{256}$ - $\frac{1}{16}$	Silt
$\frac{1}{16}$-2	Sand
2-64	Gravel
64-256	Cobble

Table 1.1: Classification of sediments (Wentworth, 1922).

1.2.1. Longshore Transport of coarse-grained material

In reality waves are more randomly distributed and will attack the shore with a certain obliqueness. This oblique wave incidence causes sediment to be transported alongshore and not solely cross shore. At a DRS this will also be the case for the sediment on the outer layer. Rock in the form of gravel, cobbles or even larger sediment will be displaced and the slope will deform. For the remainder of this thesis it is important to classify the different sediment materials. Table 1.1 shows this classification based on Wentworth (1922).

A schematisation of the Longshore Transport (henceforth also referred to as "LT") process is shown in Figure 1.2. Coarse grained particles are picked up and transported inside the swash zone. It can already be seen that parameters like grain size, wave direction and wave height play a role in the final length of the displacement and therefore are governing parameters when it comes to Longshore Transport.
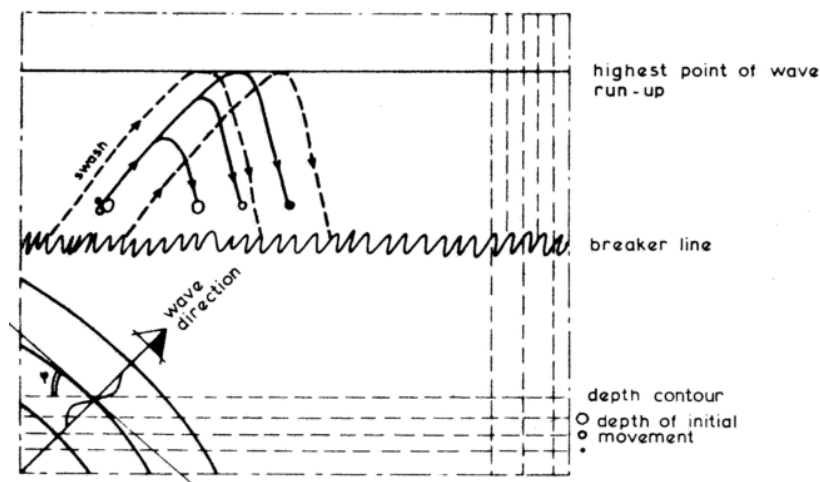
Figure 1.2: Schematic presentation of Longshore Transport of coarse grained material (van Hijum and Pilarczyk, 1982).

1.3. Introducing Maasvlakte 2

Nowadays the application of a DRS is getting more widespread. When the availability of rock is not a limiting factor, often a DRS is economically more interesting than casting a large amount of concrete armour blocks. This was the case for the DRS which was constructed at Maasvlakte 2 (henceforth also referred to as "MV2"). The Maasvlakte 2 is an expansion of the port of Rotterdam, which was initiated by The Port of Rotterdam and executed by the consortium Projectorganisatie Uitbreiding Maasvlakte (henceforth also referred to as "PUMA"); consisting of Van Oord and Boskalis. Construction was completed in 2013.

Figure 1.3: MV2 situated in the Netherlands (Port of Rotterdam, 2018a).

1.3.1. The DRS at Maasvlakte 2

Within the Maasvlakte 2 project a DRS slope was designed and constructed. The DRS construction is situated at the northwestern part of MV2, delineated in Figure 1.4. The main reason for constructing a DRS, besides economical reasons, is the relatively steep slope which can be attained using quarry rock compared to a sand beach. The usage of stone makes it possible to reach the required height of the breakwater, without an extensive sandy foreshore. Such a sandy foreshore would result in easterly directed sediment transport towards the entrance channel of the Rotterdam port. Due to the placement of the DRS this sediment transport is blocked and the inlet of the Rotterdam port can retain its depth and will not become a limiting factor for the draught of passing ships.

The 3,5 km long hard seawall is constructed from 7 million tonnes of quarry stone (Port of Rotterdam, 2018a). The four meter thick quarry stone layer is situated on top of a foundation consistent of two types of sand. The DRS has a 1:7,5 slope and is partially protected by 20,000 concrete blocks, which are recycled from Maasvlakte 1. These concrete blocks form a dam in front of the DRS. On this Block Dam (hereafter also referred to as "BD") most waves break, which causes wave energy to dissipate before hitting the slope consisting of quarry rock.

The block dam will never fully prevent the impact of waves on the DRS behind it. Especially with high water levels, i.e. during storms, waves will brake behind the BD or even on the DRS itself. This causes transport of sediment in the cross-shore and longshore direction, resulting in deformation of the DRS profile.

Figure 1.4: Topview of MV2 (Port of Rotterdam, 2018b).

Figure 1.5: Cross-sectional design of the DRS at MV2 (Projectorganisatie Uitbreiding Maasvlakte, 2011c).

1.3.2. DRS design

In Figure 1.5 the cross-sectional design of the hard sea defence of MV2 is shown. The structure is based on dredged material of sand with a D_{50} of 370 μm, indicated in light orange. The remaining structure generally consists of two parts; the actual dynamic rock slope and the Block Dam in front of it, including its base layers.

On top of the base layer, a layer of sand, indicated in yellow, is situated. This sand layer is slightly coarser with a minimum D_{50} of 150 μm. On this sand layer a quarry rock layer - on average 4 meters thick - is constructed, which forms the actual DRS and extends under the Block Dam, serving as a part of its bottom protection. This quarry rock has a D_{n50} of 65 mm and a wide grading of 20-135 mm.

The block dam rests on multiple layers of quarry rock shown in brown, blue and green respectively, representing the grading of 5-70 kg, 150-800 kg and 1-10 tons. Square shaped concrete armour units retrieved from Maasvlakte 1, weighing on average 38 to 46 tons, are placed on top of these quarry rock layers, completing the Block Dam.

Important to notice is the distinction PUMA made in sections ranging from KP -0.200 to KP +3.495 along the hard sea defence of MV2. This distinction will be used throughout this thesis in order to indicate the exact location along the DRS and is presented in Figure 1.6.

Figure 1.6: Top view of the Dynamic Rock Slope design at Maasvlakte 2.

1.3.3. Nourishment prognosis

By attaining the project of MV2, PUMA became not only responsible for design and construct, but also for maintenance of the DRS for the following 30 years. The DRS slope at MV2 requires maintenance in the form of regular nourishment of quarry rock, thereby maintaining the layer thickness of the armour layer and preventing erosion of the underlying sand.

Four steps of PUMA

To estimate the required nourishment volumes an extensive prognosis was made (Projectorganisatie Uitbreiding Maasvlakte, 2012). Multiple steps were taken to go from the offshore wave climate to a prognosis of the required nourishment volumes.

Generally PUMA took four steps to estimate the required nourishment volumes. Figure 1.7 shows these steps schematically. First the historical wave climate of the period ranging from 1979 to 2005 was translated to nearshore wave conditions. Next, the interaction of the nearshore wave climate and the Block Dam was assessed, resulting in wave characteristics which represent the waves occurring behind the dam and which attack the DRS. With these wave conditions a prognosis of Longshore Transport was established. For this prognosis a predictive LT formula - represented as S_y in Figure 1.7 - was calibrated. This calibration was based on scale model tests executed by HR Wallingford. The remaining step for PUMA was to translate these LT predictions to a maintenance program containing yearly nourishment volumes.

Figure 1.7: Four main steps taken by PUMA within their nourishment volume estimation.

The MV2 project was rather extensive and worked on by multiple parties. This resulted in substantial documentation on design, construct and maintenance subjects. To give insight in the approach of PUMA to estimate the nourishment volumes, the presented steps will be discussed in more detail in Appendix B. Here only the prognosis for the Longshore Transport is presented in Figure 1.8. Following from this prognosis a maintenance campaign on nourishment values was set by PUMA. The main conclusions after a five year maintenance period will be presented in the following section.
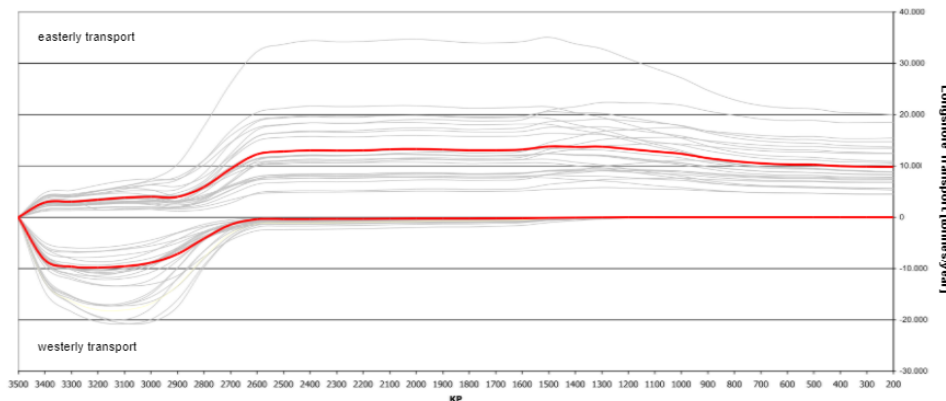
Figure 1.8: Longshore Transport prediction of PUMA with a Block Dam height of 2 m + NAP and 0.35 m of Sea Level Rise. (Projectorganisatie Uitbreiding Maasvlakte, 2012)

1.3.4. PUMA's conclusions after a five-year maintenance period

Five years after construction of MV2, PUMA drew multiple conclusions regarding the first maintenance period (Projectorganisatie Uitbreiding Maasvlakte, 2018). PUMA made a cross sectional division for assessing the stone volumes along the DRS of MV2. The reason for this being that the area above 8 m + NAP will never be exposed to hydraulic forcing. This division will be followed equally within this thesis. In other words, when discussing loss of stone, all matters refer to the dynamic part of the DRS, that part which is affected by hydraulic loading, i.e. the part of the DRS lower than NAP + 8 m.

Stone volume above NAP + 8 meter.
The expectation by PUMA was that the volume of stones above NAP + 8 meter would not decrease as no hydraulic loading would be present at this higher part of the DRS. The measured stone volumes reveal a slight decrease in volume due to the settlement of the subsoil.

Stone volume below NAP + 8 meter.
In the section below NAP + 8 meter stones will be transported along the DRS for which a prognosis was made. During the Setting Period (henceforth also referred to as "SP"), which is the period of 2013 to 2018, the nourishment volumes which were needed for the part below NAP + 8 m, turned out to be lower than expected, as can be seen in Table 1.2.

Year	Proposed nourishment [kton]	Executed nourishment [kton]
2014	-	-
2015	-	-
2016	34.3	10.0
2017	-	-
2018	37.6	16.0[1]

Table 1.2: Nourishment campaign set by PUMA for the first 5 years after construction.
1) Expected nourishment volumes based on the volumes present.

PUMA gives the following reasoning for the lower nourishment volumes:

- The maximum crest height of the block dam is set to approximately 3.2 m above NAP during construction. This is higher than the maximum crest height of 2.6 m + NAP which was used within the prognosis of Longshore Transport, as explained in Appendix B.

- Locally the settlement of the subsoil can vary with respect to the expected settlement of 0.02 m per year during the so called Setting Period, which is the first 5 years after construction.

- The hydraulic loading varies along the DRS.

- A deviation in degradation of the cobble stones.

The reasoning mentioned above is not substantiated by PUMA. Therefore it is requested by PUMA to assess what the reasons for the lower nourishment volumes could be.

2

Research approach

Here the set-up for the research will be given, therewith providing a scope through the report. As a result of the problem definition a research objective is set. In order to reach this objective, multiple research questions are presented. These questions are used as a general gist throughout the remainder of this thesis. As a last part of the research approach, the outline of the report is briefly explained.

2.1. Problem definition

Van Oord, as part of the consortium PUMA, made a prognosis of Longshore Transport at the DRS of Maasvlakte 2. Based on this prognosis maintenance requirements were set. After five years of maintenance and surveys it has become clear that the nourishment volumes turn out to be lower than expected. These lower nourishment values are the consequence of lower amounts of transported volumes along the DRS of Maasvlakte 2. Van Oord has asked to assess these differences and to give insight in the processes leading to these differences.

PUMA used a dimensional relation in their LT prognosis. This relation is only applicable for the DRS at Maasvlakte 2, as it is specifically calibrated for the characteristics present at the Maasvlakte 2. Would Van Oord want to design a Dynamic Rock Slope in a new project, then a dimensional relation would not be applicable. Therefore it is of interest to investigate if there is a non-dimensional relation that is able to describe Longshore Transport at a Dynamic Rock Slope.

2.2. Data availability

The Dynamic Rock Slope at MV2 was constructed five years ago. In that time multiple nourishments of stones have taken place. Besides nourishments Van Oord also executed surveys of the DRS. These were executed approximately every year and are meant to assess the development of the quarry stones on the DRS. With this survey data the necessary amount of stones for the individual nourishments are determined.

Next to the survey data on stone volumes on the DRS slope, there is also the availability of wave measurements offshore of MV2. The wave data of the past five years that will be used are measured at the Europlatform, approximately 50 km offshore of MV2. This is the same location as Svasek used in their assessment of the wave climate at the time of design of the DRS.

2.3. Objective

The objective for this research is stated as follows:

> *Analyse where differences in predicted and observed transport rates come from and assess if it possible to validate a non-dimensional relation which describes Longshore Transport at the Dynamic Rock slope of Maasvlakte 2.*

The objective of this research is build up out of two parts. Partly an analysis is carried out in order to show where differences in transport following from the prognosis of PUMA and the actual observed transport rates come from. Next to this objective there is the objective of investigating if there is a Longshore Transport relation next to the PUMA relation, which is able to describe Longshore Transport at the DRS of Maasvlakte. Such a non-dimensional relation would then be usable when designing a new Dynamic Rock SHahlope.

2.4. Research questions

In order to reach the set objective for this research, multiple research questions are proposed. The three research questions are:

1. Can wave and survey data of Maasvlakte 2 show where the differences in predicted and observed transport rates at the Dynamic Rock Slope of Maasvlakte 2 come from?

2. Is there a non-dimensional Longshore Transport relation which is able to describe Longshore Transport at the Dynamic Rock Slope of Maasvlakte 2?

3. Is it possible to validate a relation which describes Longshore Transport of stones at the Dynamic Rock Slope of Maasvlakte 2?

2.5. Structure report

In order to reach the objective set for this research and to constitute an answer on the proposed research questions, an approach is necessary. This approach is presented through a description of the consecutive chapters in this report.

Chapter 3: **Literature on Longshore Transport**
Here foregoing research on Longshore Transport of coarse-grained material is presented. A general Longshore Transport model of Tomasicchio et al. (2013) will be introduced.

Chapter 4: **Historic scale model testing**
Results from historic scale model tests are discussed. On the basis of these tests conclusions are drawn regarding the applicability of different formulas to estimate Longshore Transport at the Dynamic Rock Slope of Maasvlakte 2.

Chapter 5: **Wave climate analysis**
The main focus in this chapter is the analysis of the wave data over the period 2013 to 2018. This data will be compared to the wave data over the period of 1979-2005 which were used by PUMA to estimate Longshore Transport rates. An analysis of the year-round wave conditions and storm events will be given.

Chapter 6: **Methodology of calculating transport rates**
Using the year-round wave conditions from Chapter 5 Longshore Transport rates are calculated. An explanation of the calculation model, used to compute these LT rates, will be given within this chapter.

Chapter 7 **Results PUMA relation**
In this Chapter the output following from Chapter 6 by means of the PUMA relation is discussed. The first part of this chapter discusses the prognosis PUMA made and the differences w.r.t. the computed transport rates over the period 2013 tot 2018. Within the second part of this chapter the influences of different parameters on computed LT rates for the PUMA relation are assessed. The last part of this chapter introduces actual occurred gradients in transport along the DRS over the period 2013 to 2018. By comparing computed gradients in transport to observed gradients in transport a validation of the PUMA relation is carried out.

Chapter 8: **Results General Longshore Transport relation**
In this Chapter the output following from Chapter 6 by means of the General Longshore Transport (GLT) relation is discussed. This chapter comprises of two parts. The first part discusses the theoretical performance of the GLT relation with respect to the PUMA relation and assess the influence of different parameters on the output of Longshore Transport. Within the second part of this chapter the GLT relation is again validated on the basis of observed transport gradients along the DRS, analogous to the validation which was carried out for the PUMA relation in the previous chapter.

Chapter 9: **Conclusions and recommendations**
Conclusions are drawn with respect to this thesis research. Based on these conclusions multiple recommendations for further research are presented.

3

Literature on Longshore Transport

3.1. Longshore Transport methods

Generally three methods are presently accepted for assessing Longshore Transport (Tomasicchio et al., 2013):

1. Energetics method; divided into the energy flux approach and the stream power approach.

2. Force-balance method.

3. Dimensional analysis method.

Below the dimensional analysis method is treated extensively as this is the method which falls in the scope of this research. The other methods are briefly treated in Appendix C.

3.1.1. Dimenisonal analysis method

The third and most extensively used LT method is that of the dimensional analyses. These deterministic formulae are generally derived from laboratory experiments. When it comes to Longshore Transport of coarse material, Van Hijum and Pilarczyk were the first to apply this method and came up with the following formula following from their experiments (van Hijum, 1977)(van Hijum and Pilarczyk, 1982):

$$\frac{S_{LT}}{gD_{90}^2 T_s} = 7.12 \cdot 10^{-4} \frac{H_{s,d} cos^{1/2}(\beta)}{D_{90}} \left[\frac{H_{sd} cos^{1/2}(\beta)}{D_{90}} - 8.3 \right] \frac{sin(\beta)}{tanh(\frac{2\pi d}{L})} \qquad [stones/wave] \qquad (3.1)$$

where S_{LT} is the transport in $[m^3/s]$, D_{90} is the 90% representative of the grain diameter, T_s is the significant wave period, $H_{s,d}$ is the local significant wave height, β is the wave angle, d is the water depth and L is the wave length.

Later Van Wellen et al. (Van Wellen et al., 2000) noted the implications which arise by using wave parameters measured at an offshore location and at the toe of the model beach of Van Hijum and Pilarczyk. Van der Meer (Van der Meer, 1990a) equally recognized these complications and re-calibrated Equation 3.1 to come up with his own LT formula, which he finally adjusted resulting into an equation which distinguishes different types of beaches (Van der Meer and Veldman, 1992):

Gravel/shingle beach; $\quad H_s/\Delta D_{n50} > 50 \quad$ up to sand beaches $\hspace{6cm}$ (3.2)

$$S_{LT,N} = 0.0012\pi H_s C_{op} sin(2\beta_b) \hspace{4cm} [stones/wave] \quad (3.3)$$

Rock/gravel beach; $\quad 10 < H_s/\Delta D_{n50} > 50 \hspace{7cm}$ (3.4)

$$\frac{S_{LT}}{gD_{n50}^2 T_p} = 0.0012 \frac{H_s\sqrt{cos\beta}}{D_{n50}} \left(\frac{H_s\sqrt{cos\beta}}{D_{n50}} - 11 \right) sin\beta \hspace{2cm} [stones/wave] \quad (3.5)$$

Berm breakwater; $\quad H_s/\Delta D_{n50} < 10$, for angles of 15-40° $\hspace{5cm}$ (3.6)

$$S_{LT,N} = 0 \hspace{2cm} H_o T_{op} < 105 \hspace{5cm} (3.7)$$

$$S_{LT,N} = 0.00005(H_o T_{op} - 105)^2 \hspace{3cm} [stones/wave] \quad (3.8)$$

in which $H_o = \frac{H_s}{\Delta D_{n50}}$ again and $T_{op} = T_p \sqrt{g/D_{n50}}$. In above-mentioned equations H_s represents the significant wave height, Δ is the relative density, $D_{n,50}$ is the nominal diameter.

Besides Van der Meer, Chadwick (Chadwick, 1989) altered the data resulting from the Van Hijum and Pilarczyk experiments to give:

$$S_{LT} = 0.0013\left(gD_{90}^2 T_s\right)W(W - 8.3)sin\beta_b \qquad [m^3/s] \qquad\qquad \text{where} \qquad W = \frac{H_{s,b}\sqrt{cos\beta}}{D_{90}} \qquad (3.9)$$

Later Alikhani et al. (1996) proposed a formula for a berm breakwater that is also dependent on the wave angle, resulting in:

$$S_{LT,N} = 0.8 \cdot 10^{-6}\sqrt{cos\beta}(H_o T_{op}\sqrt{sin2\beta} - 75)^2 \qquad [stones/wave] \qquad\qquad (3.10)$$

Mulders adjusted the coefficient $0.8 \cdot 10^{-6}$ to $0.8 \cdot 10^{-4}$, as he found a better fit for the berm breakwater data available from literature and his own tests (Mulders, 2010). This logically resulted in the following equation applicable for berm breakwaters:

$$S_{LT,N} = 0.8 \cdot 10^{-4}\sqrt{cos\beta}(H_o T_{op}\sqrt{sin2\beta} - 75)^2 \qquad [stones/wave] \qquad\qquad (3.11)$$

Above-mentioned equations are stated because of their applicability to estimate LT rates of coarse-grained material. Within this thesis only formulas belonging to the dimensional analysis method will be used to estimate LT rates. The main reason being that this method was used to calibrate the non-dimensional formula of PUMA to estimate LT rates, as will be explained in the remainder of this report.

Most of the equations mentioned in Section 3.1.1 are based on the stability number N_s, explained in Section 1.1. Tomasicchio attempted to combine multiple data sets to come up with a general Longshore Transport (henceforth also referred to as "GLT") model, which is applicable for any sediment size and stability number. The GLT model is treated in the following section.

3.2. General Longshore Transport model

Following from experiments at the Danish Hydraulic Institute in 1995, Tomasicchio et al. formulated a general model for the assessment of Longshore Transport. These tests showed a relation between the damage of the profile and that of the earlier mentioned stability number N_s. Also the wave steepness showed to be of influence to the damage (Tomasicchio et al., 1994). Therefore an updated stability number was presented:

$$N_s^{**} \propto N_s \cdot s_m^{-1/5} \tag{3.12}$$

here s_m is the mean wave steepness. In order to catch the influence of wave obliquity within the model, a dependence of β was introduced. This lead to the following *modified stability number*:

$$N_s^{**} = \frac{H_k}{C_k \Delta D_{n50}} \cdot \left(\frac{s_{m,0}}{s_{m,k}}\right)^{-1/5} \cdot (\cos\beta_0)^{2/5} \tag{3.13}$$

where $H_k = C_k \cdot H_s$ is the characteristic breaker height, C_k is a constant of 1.55, D_{n50} is the nominal diameter of the material, $s_{m,0}$ and $s_{m,k}$ represent the offshore and characteristic wave steepness respectively and β_0 is the wave angle w.r.t. shore normal. A reference wave steepness $s_{m,k}$ of 0.03 was assumed.

The general model of Tomasicchio et al. is based on the amount of damage N_{od}. Two areas of damage are distinguished. The one where $N_s^{**} \leq 23$ describes damage from berm breakwaters up to gravel beaches and the area $N_s^{**} > 23$ which describes damage for sandy beaches.

$$N_{od} = \begin{cases} 20N_s^{**}(N_s^{**} - 2)^2 & N_s^{**} \leq 23 \\ exp[2.72ln(N_s^{**}) + 1.12] & N_s^{**} > 23 \end{cases} \tag{3.14}$$

Longshore Transport as a result of wave obliquity is being related to the mobility level of the particles out of which the breakwater is constructed. To generalize the Longshore Transport process, a schematic formulation was set-up. In this model a particle is assumed to pass through a certain control section in a small time interval Δt if and only if it is removed from an updrift area of extension equal to the longitudinal component of the displacement length, $l_d \sin\beta_d$ (Tomasicchio et al., 2016). Here the displacement length is defined as l_d and wave obliquity as β_d, both visually represented in Figure 3.1. l_d is computed as follows:

$$l_d = \frac{(1.4N_s^{**} - 1.3)}{tanh^2(kd)} D_{n50} \tag{3.15}$$

where k is the wave number and d is the local depth.
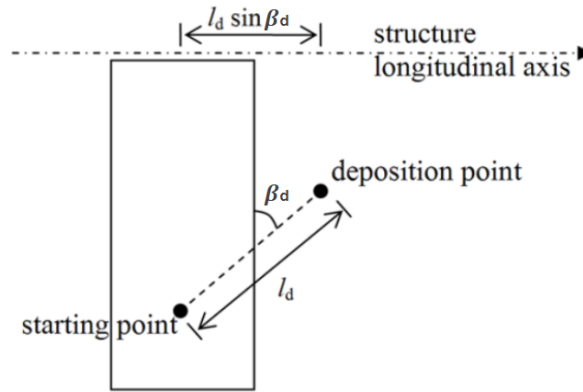
Figure 3.1: Visual representation of general Longshore Transport model (Tomasicchio et al., 2016).

Finally the actual transport $S_{LT,N}$, i.e. the number of units travelling across the control unit, is found through Equation 3.16. In this Equation $S_{LT,N}$ is the amount of N_{od} in 1000 waves per one diameter long strip. Tomasicchio et al. formulated this as Equation 3.16.

$$S_{LT,N} = \frac{l_d}{D_{n50}} \cdot \frac{N_{od}}{1000} \cdot \sin\beta_{k,b} \qquad [stones/wave] \tag{3.16}$$

The Longshore Transport rate $S_{LT,N}$ is related to the mass transport in $[m^3/s]$ through:

$$Q_{LT,N} = \frac{S_{LT,N}D_{n50}^3}{(1-n)T_m}$$

(3.17)

in which T_m represents the mean wave period.

3.2.1. Historical Longshore Transport data

Tomasicchio et al. (2016) provided the general Longshore Transport model with data of foregoing researchers. By doing so, a clear distinction of regions for the updated stability numbers became clear. The separation of regions for berm breakwaters, shingle and sandy beaches, which is provided by Tomasicchio, is shown in Figure 3.2.

Within the GLT model of Tomasicchio et al. the data for shingle beaches is limited, as can be seen in Figure 3.2. Therefore the data of this study could contribute by giving insight in the performance of the model in that specific region.
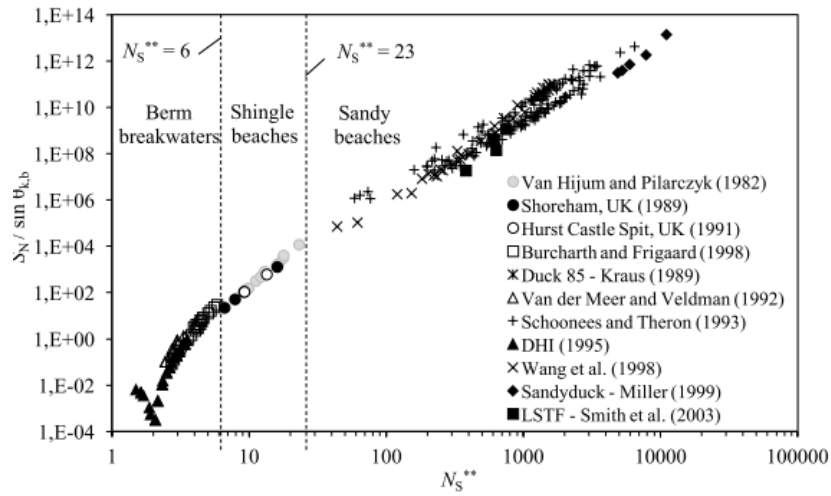
Figure 3.2: Region of N_s^{**} for historic scale model tests. (Tomasicchio et al., 2016).

<div align="right">

4

</div>

Historic scale model testing

For the calibration of PUMA's Longshore Transport formula HR Wallingford was asked to perform scale model tests with the focus on the Longshore Transport process. This chapter describes Wallingford's tests and assess the applicability of different Longshore Transport relations to the Maasvlakte 2 data. A comparison is made between the results of historical scale model tests and the newly obtained scale model test data executed by Wallingford.

4.1. Type of structure

Through the years many Longshore Transport relations on LT were established, all describing LT for different structures, each with its own characteristics. The division of structure types was formerly based on the stability number N_s, as mentioned in Section 1.1.

$$N_s = \frac{H_s}{\Delta D_{n50}} \tag{4.1}$$

The choice of historic formula to use in the remainder of this research will therefore be based on this distinctive parameter. In the case of Maasvlakte 2 the Block Dam alters the significant wave height considerably. Because of this reduction in H_s the stability numbers are reduced equally, making the distinction of structure type and therewith the choice of LT relation more troublesome.

This can easily be shown by taking a range of standard wave heights for the North Sea and computing the corresponding stability numbers, using the characteristics of the DRS at Maasvlakte 2. For input parameters a range of wave heights from 0.5 up to 4 meters at the toe of the DRS, the D_{n50} applied at the DRS of 65 mm and a Δ of 1.6 are used. Now the range of stability numbers is approximately 5 to 40, making the DRS a rock or gravel beach according to Van der Meer and Veldman (1992). When the transmitted wave height is taken into account the stability numbers are reduced. PUMA calibrated a wave transmission formula for the BD with a reduction of the wave height that lies between 0.075 and 0.85 as can be obtained from Appendix B. When applying this minimum and maximum reduction of wave heights, the range of stability numbers is narrowed down to 0 - 33. When looking at the average of the both ranges in Table 4.1 it is clearly obtainable the DRS would be classified as a berm breakwater.

Stability Number	Location H_s	Range	Average	Type of structure
N_s	At toe	5 - 40	22	Rock/gravel beach
N_s	Transmitted	0 - 33	9	Berm breakwater

Table 4.1: Stability numbers N_s for the DRS at MV2 and corresponding structure types (Van der Meer and Veldman, 1992).

With this lower stability region for the DRS it is necessary to assess if a berm breakwater relation can be used to compute transport rates at the DRS. In order to make this assessment the berm breakwater relation of Alikhani, which was later updated by Mulders, will be taken into account.

4.2. Scale model tests Wallingford

In order for PUMA to get more insight into the governing parameters with respect to the Longshore Transport processes at the DRS of Maasvlakte 2, scale model tests were executed by HR Wallingford (HR Wallingford, 2007a)(HR Wallingford, 2007b)(HR Wallingford, 2009c)(HR Wallingford, 2009d). The specific conditions under which the scale model tests were executed are presented in Table 4.2. Results of these tests were used to calibrate the dimensional Longshore Transport relation of PUMA which was used for the prognosis of LT specifically at the DRS of Maasvlakte 2.

Test	Scale	Material	D_{50} [mm]	D_{n50} [mm]	ρ_s [kg/m^3]	H_s [m]	T_p [s]	β [°]
EX 5474	1:20	Anthracite	11.0	9.3	1400	0.1, 0.175, 0.25	1.48, 1.81, 2.09	30, 45
EX 5828	1:20	Limestone	6.0	5.0	2700	0.1, 0.175	1.48, 1.81	15, 30
EX 5858 2a	1:20	Limestone	3.54	3.0	2628	0.1, 0.175, 0.25	1.48, 1.81, 2.09 1.59, 1.99	30
EX 5858 2b	1:20	Limestone	3.54	3.0	2628	0.1, 0.175, 0.25	1.48, 1.81, 2.09	15, 45

Table 4.2: Different scale model test parameters of Wallingford.

Important to notice is the execution of test EX5474, which was done with the material Anthracite (HR Wallingford, 2007b). According to Kamphuis (1985) this lightweight material is not suitable for scale model testing. The specific density of this material is not scaled right. Therefore no conclusions will be drawn with respect to the results of test EX5474.

4.3. Berm Breakwater relations

In order to make a comparison of the applicability of berm breakwater relations to compute transport rates at the DRS of Maasvlakte 2, historic data of scale model tests are retrieved. To recap the berm breakwater formulas for Alikhani, Equation 4.2, and that of Mulders, Equation 4.3, are given below. The only difference being the order of magnitude of the coefficient by which the formula is multiplied.

$$S_{LT,N} = 0.8 \cdot 10^{-6} \sqrt{cos\beta} (H_o T_{op} \sqrt{sin2\beta} - 75)^2 \qquad [stones/wave] \qquad (4.2)$$

$$S_{LT,N} = 0.8 \cdot 10^{-4} \sqrt{cos\beta} (H_o T_{op} \sqrt{sin2\beta} - 75)^2 \qquad [stones/wave] \qquad (4.3)$$

In Equation 4.2 and 4.3 the dimensionless wave height is represented by H_o, which is equal to N_s. T_{op} is the dimensionless peak period $T_{op} = T_p \sqrt{g/D_{n50}}$. The ability of the both equations to assess the Longshore Transport is visually represent in Figures 4.1 and 4.2. A clear underestimation can be seen for both formulations. Mulders (2010) already showed an underestimation and altered the coefficient from $0.8 \cdot 10^{-6}$ to $0.8 \cdot 10^{-4}$. In this way Mulders acquired a better fit for berm breakwater data. Still Equation 4.3 underestimates S values by a factor 1000, which is considerably.
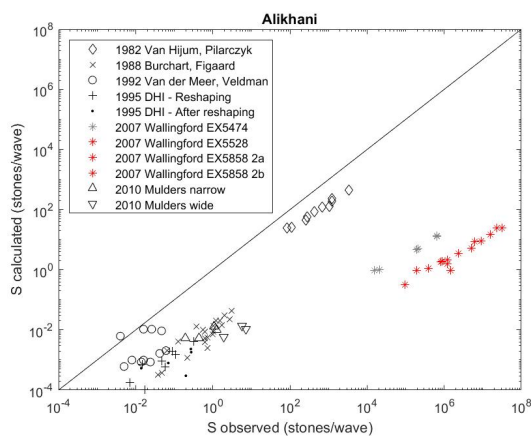
Figure 4.1: Calculated vs. observed LT for the Alikhani relation.
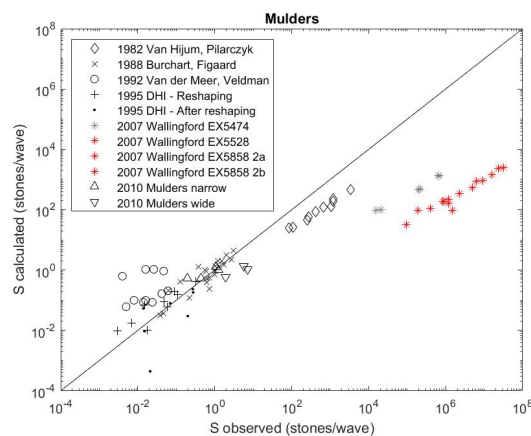
Figure 4.2: Calculated vs. observed LT for the Mulders relation.

The underestimation of these formulas can easily be explained by obtaining the stability numbers of the tests executed by Wallingford, presented in Table 4.3. The scale model tests were done in 2007 in order to gain insight in the behaviour of a DRS. At that time, only the properties of the available quarry stones were known and the design did not include the Block Dam. The reason for the underestimation of berm breakwater formulas is clear as the scale model tests of Wallingford all fall in the region of a rock or gravel beach. A logic result is a better fit of the historical SMT data - which are all berm breakwater tests - to the formulas of Alikhani and Mulders than those of the more recent test of Wallingford.

Test	N_s	Structure Type
EX 5474	27-67	Rock / gravel beach
EX 5828	12-29	Rock / gravel beach
EX 5858 2a	20-51	Rock / gravel beach
EX 5858 2b	20-51	Rock / gravel beach

Table 4.3: Stability numbers of Wallingford tests.

Although the Block Dam in theory reduces the wave height, thereby lowering stability numbers, it is shown berm breakwater relations are not able to compute Longshore Transport rates following from scale model tests executed by HR Wallingford. This again shows what difficulties the presence of the Block Dam at the Dynamic Rock Slope at Maasvlakte 2 brings along when making a choice of non-dimensional LT relation purely based on stability numbers.

4.4. General Longshore Transport model

Clearly a model is needed that is able to estimate Longshore Transport rates for any type of structure. In other words a relation which does not proposes a different relation for a different region of stability number. Tomasicchio et al. (2013) firstly presented a model which is able to assess transport rates for any coarse-grained material, i.e. a wide range of D_{n50}. This so-called General Longshore Transport model was introduced in Section 3.2.

Although the GLT model does not make a distinction between regions of stability number for the final assessment of the LT, it is of interest to show which type of structure is defined by the GLT model for the Wallingford tests. The updated stability numbers are shown in Table 4.4. What can be seen is that the breakwater type of the Wallingford tests are also defined as a gravel to sandy beach for N_s^{**}. This is a similar distinction as for the original stability number N_s, which was presented in Table 4.3.

Test	N_s^{**}	Structure Type
EX 5474	22-53	Gravel beach / Sandy beach
EX 5828	11-19	Gravel beach
EX 5858 2a	19-45	Gravel beach / Sandy beach
EX 5858 2b	17-47	Gravel beach / Sandy beach

Table 4.4: Updated stability numbers and corresponding structure type for the Wallingford tests.

When it comes to computing transport rates, the difference of the GLT model with respect to all other LT relations is the the way the updated stability number is used as input for N_{od} and l_d. The amount of damage N_{od} and the displacement length l_d can, according to the model, be computed for any N_s^{**}. This means any D_{n50} larger than that of sand and any wave height can be used as input parameter for the updated stability number, Equation 4.4. The result is a more generally applicable model which in case of Maasvlakte 2 is desirable considering the influence of the Block Dam on transmitted wave heights and subsequent stability numbers.

$$N_s^{**} = \frac{H_k}{C_k \Delta D_{n50}} \cdot \left(\frac{s_{mo}}{s_{mk}}\right)^{-1/5} \cdot (\cos\beta_o)^{2/5} \tag{4.4}$$

When computing LT rates for the Wallingford tests by use of the GLT model, it is possible to compare these outcomes with observed transport rates. The agreement between experimental data and calculated values for the GLT relation is presented in Figure 4.3. The agreement appears to be significantly better than for the berm breakwater relations of Section 4.3. The estimated values for the GLT relation are within the same order of magnitude, but are still underestimated by the model. Next to the underestimation of the Wallingford tests a remark on the overestimation of calculated transport rates on the berm breakwater data has to be made. This overestimation was equally concluded by Tomasicchio et al. (2016). It appears the GLT relation underestimates LT when transport rates are lower and overestimates LT when transports are higher.
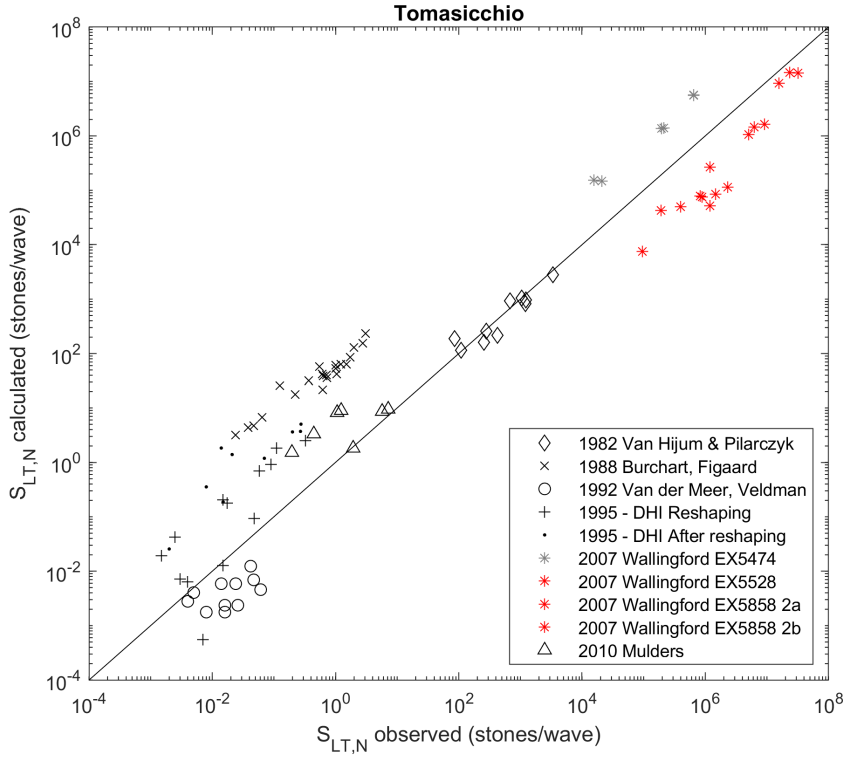
Figure 4.3: Observed S_N vs calculated S_N according to the GLT model.

4.5. Conclusions

So far an assessment was done in order to conclude which non-dimensional LT relation might by suitable to predict LT rates at the DRS next to the dimensional relation of PUMA. For the remainder of this research two LT relations will be investigated. The first one being the specifically calibrated dimensional relation of PUMA (Projectorganisatie Uitbreiding Maasvlakte, 2012):

$$S_{LT,P} = 6.21 \cdot H_{s,t}^{3.6} \cdot \sin(2.00 \cdot \beta_t)^{0.86} \cdot (T_{p,t} - 6.00)^{0.10} \qquad \text{for } S_{LT,P} < 150 kg/s \qquad [kg/s] \qquad (4.5)$$

and the second one being the GLT relation (Tomasicchio et al., 2016):

$$S_{LT,N} = \frac{l_d}{D_{n50}} \cdot \frac{N_{od}}{N} \cdot \sin\beta_{k,b} \qquad\qquad [stones/wave] \qquad (4.6)$$

The choice of the GLT relation is based on the results obtained in this chapter. In short the Block Dam reduces the wave height significantly. Because of this reduction in wave height a Longshore Transport relation which is fully based on the stability number becomes inapplicable, i.e. when a different relation is needed for a different region of stability number, such a relation becomes inapplicable for the specific case of the DRS at Maasvlakte 2.

The GLT relation is able to compute transport rates for any updated stability number, which means no different relation is needed for a different stability number, making it applicable for assessing LT at the DRS of Maasvlakte 2. Because the GLT relation has this property it is of interest to see how it performs in comparison with the PUMA relation for the data of the DRS. Next to this advantage, the GLT relation is a non-dimensional relation, which means this Longshore Transport relation is not specifically calibrated for one situation, as the PUMA relation is for the DRS at Maasvlakte 2. In theory, this makes a non-dimensional relation applicable for the computation of LT for any type of structure and not only for a situation comprising of the characteristics, as found at the DRS of Maasvlakte 2.

5
Wave climate analysis

A reason for the difference in prognosis and observed Longshore Transport rates at the Dynamic Rock Slope of Maasvlakte 2 could be a significant difference in wave climate. To assess if this is the case the wave climate of the period 1979-2005, which was used by PUMA during the design phase of the project, will be compared to the wave data of the last 5 years. This wave data of the recent years will be used as input data for the estimation of Longshore Transport in Chapter 6.

5.1. Area of interest

The DRS at MV2 has a length of approximately 3.5 kilometers. Therefore in the remainder of this research it is important to clearly state which point along the DRS is referred to. Therefore an interest area is set on beforehand.

In the southwestern part of Figure 5.1 the transition from the soft to the hard sea defence can be seen. Over the years sand has been transported into the system of the DRS, meaning behind the BD and on the slope of the DRS. The transportation of this sand is partly due to wind and partly due to waves. Interference of this sand with the cobblestones on the DRS is a problem for PUMA when it comes to their maintenance program. Momentarily PUMA is assessing the consequences of the introduction of sand into the system of the hard sea defence. To avoid complications which follow from this soft to hard sea defence transition, a more easterly area of interest is chosen. The area of interest for the remainder of this thesis research ranges from KP 600 to 1800, as can be seen by the in grey delineated area in Figure 5.1. A second reason for the choice of area of interest is the change in orientation of the DRS along KP 600 to 1800. The bending shape within the area of interest causes a difference in hydraulic forcing along this area, resulting in differences in Longshore Transport. A difference in Longshore Transport in longitudinal direction will cause erosion or accretion along the DRS, therefore it is of interest to investigate how the DRS behaves along this part of the hard sea defence.
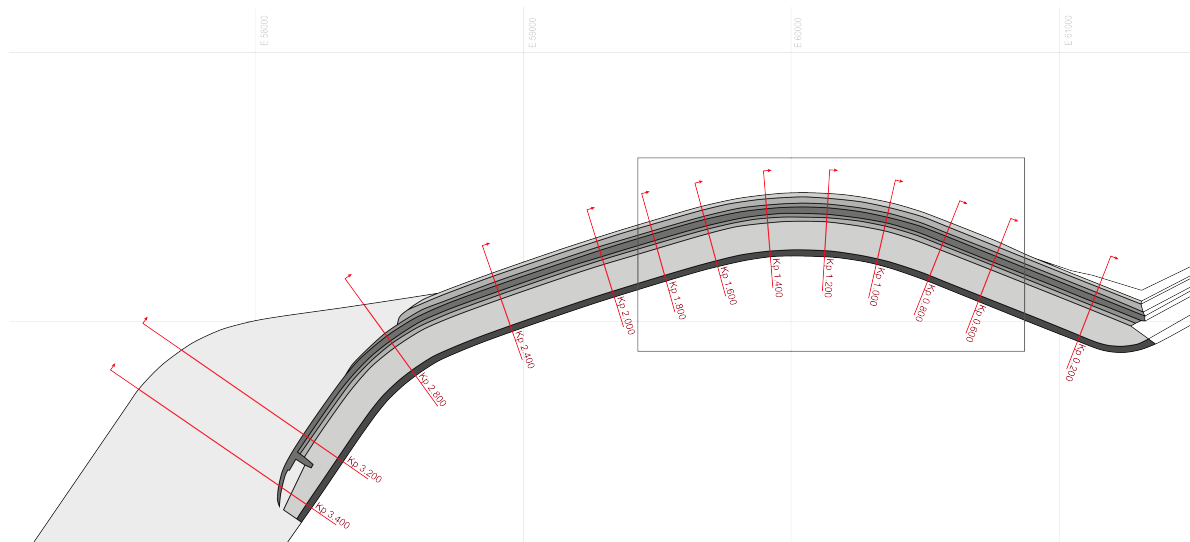
Figure 5.1: Area of interest along the DRS.

5.2. SWAN transformation

During the design phase of Maasvlakte 2 Svasek, commissioned by PUMA, analysed the wave conditions of the period 1979 to 2005. Svasek transformed the historic wave data from the Europlatform to 34 nearshore wave points. Within this study a similar transformation is done.

In order to make a comparison of the wave climates over the different periods, hourly wave and wind data of 1/1/2013 until 1/5/2018 is requested at Rijkswaterstaat and the KNMI. All the measured data was obtained from the Europlatform, approximately 50 km offshore of Maasvlakte 2. The data consists of the following parameters; wave height, wave direction, peak period, wind speed and wind direction. The program SWAN was used to transform these parameters nearshore. The set-up of the SWAN model is discussed more extensively in Appendix D.
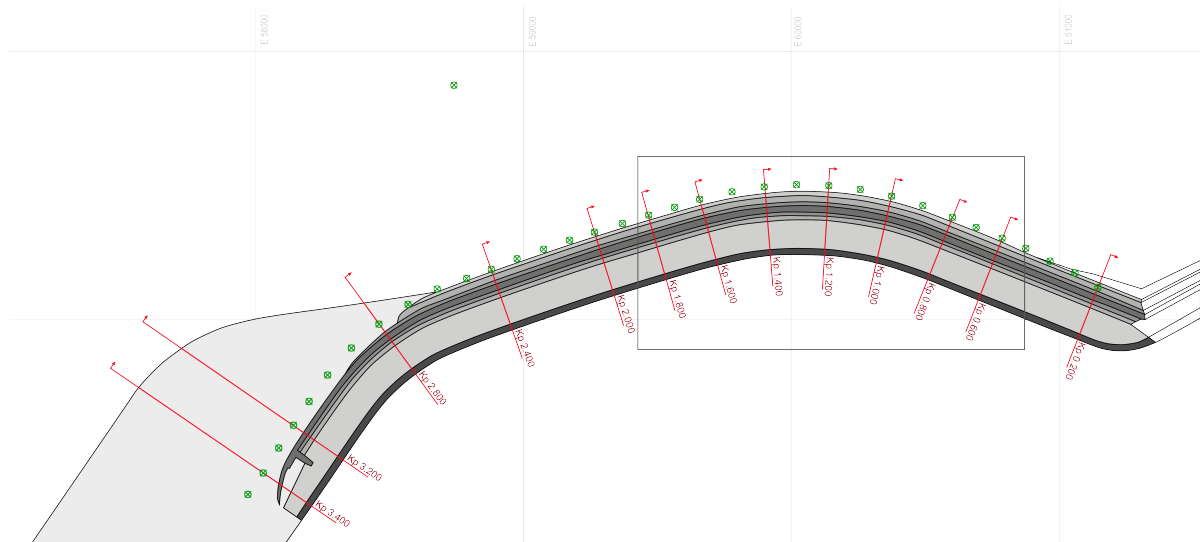
Figure 5.2: Overview of the DRS including 35 wave locations.

The wave data in this study is transformed from the offshore location of the Europlatform to 35 nearshore wave points along the DRS of MV2. The 34 output points are located at the toe of every 100 meters of the DRS. All wave locations are represented by the green dots in Figure 5.2. The coordinates of these output locations are equal to the ones Svasek used in their transformation and can be found in Appendix D. Another point, output point 35 is used to assess the storm events over the period of 2013 to 2018. This point is used as it lies slightly more offshore and is therefore less influenced by the morphological active zone right in front of the DRS, as will be obtained later in this chapter.
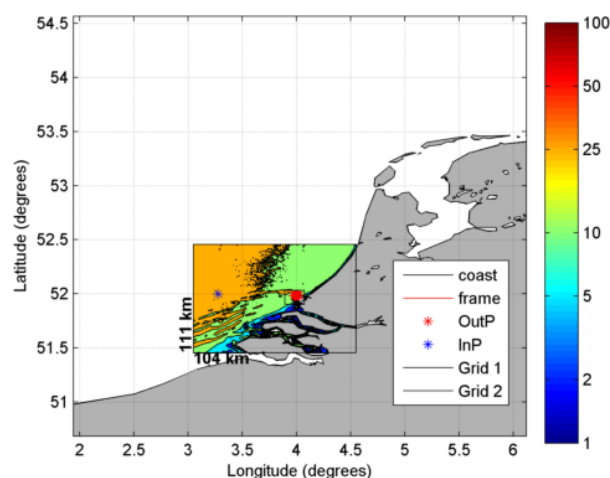
Figure 5.3: SWAN model set-up.

5.3. Comparison of year-round wave conditions at the Europlatform

In this Section the input data for both transformations are compared in order to assess if large differences are obtainable. In other words the historic wave data of Svasek will be compared to that of the period of 2013 until 2018. This is done for the input location of the Europlatform.

When comparing the main wave directions of the Europlatform data for the two different periods, one wave direction seems to occur more frequently over the recent data. This wave direction comes from the southwest, which can be seen in Figures 5.4 and 5.5. All other wave directions are similarly distributed, i.e. waves from a particular direction tend to occur an equal amount of times over the different data sets. Next to the wave directions, the wave heights seem to be similarly distributed over all directions, meaning on average waves are similarly in height. This agreement on wave height distribution can also be concluded when looking at the overall distribution, presented in Table 5.1.
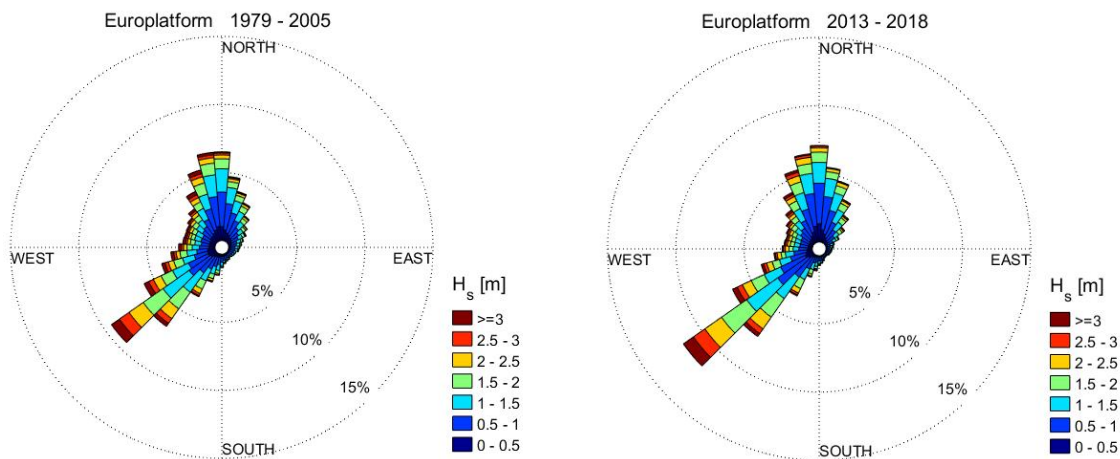
Figure 5.4: Wave rose of Europlatform over the period of 1979-2005. Figure 5.5: Wave rose of Europlatform over the period of 2013-2018.

The historic wave data obtained from Svasek only contained mean wave periods $T_{m-1,0}$. Therefore an alteration of the mean wave period $T_{m-1,0}$ of the historic wave data was necessary in order to make a comparison of peak periods between both data sets. A ratio of $T_p = T_{m-1,0} \cdot 1.112$ is used (CIRIA, CUR, 2007). This ratio is based on the peak enhancement factor γ_p of 3 for a JOHNSWAP spectrum.

When comparing the peak periods of both data sets a similar distribution is obtained as there is for the overall wave height distribution. Therewith it is concluded the input data for the SWAN run at the Europlatform shows similar year-round conditions.

H_s [m]	1979-2005	2013-2018
0.0-0.5	14%	12%
0.5-1.0	31%	33%
1.0-1.5	24%	24%
1.5-2.0	14%	15%
2.0-2.5	8%	9%
2.5-3.0	4%	5%
>3	4%	3%

T_p [s]	1979-2005	2013-2018
0.0-4.0	4%	1%
4.0-5.0	22%	29%
5.0-6.0	30%	24%
6.0-7.0	25%	24%
7.0-8.0	14%	15%
8.0-9.0	4%	4%
9.0-10.0	1%	1%
>10.0	0%	1%

Table 5.1: Distribution of wave heights for both data sets. Table 5.2: Distribution of peak periods for both data sets.

5.4. Nearshore wave data

Now the input data of the Europlatform is validated, the output data at the toe of the DRS can be analyzed. The output data of SWAN over the period of 2013-2018 will be used as input data for the computation of Longshore Transport rates at the DRS over this period, as will be explained in Chapter 6. This procedure was equally followed by PUMA in their LT prognosis, only PUMA used a 26 year wave climate, following from the period 1979 to 2005.

Figures 5.6 and 5.7 show the wave roses for the wave transformations over both periods at the same output location of KP 1400. Tables 5.3 and 5.4 show the distribution of significant wave height and peak period for both data sets respectively. A valid comparison is difficult to make as it is unknown which bathymetry Svasek used in their transformation at the time of design.
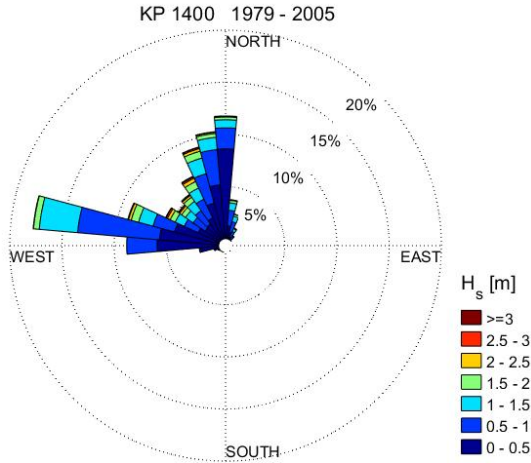
Figure 5.6: Wave rose of KP 1400 over the period of 1979-2005.
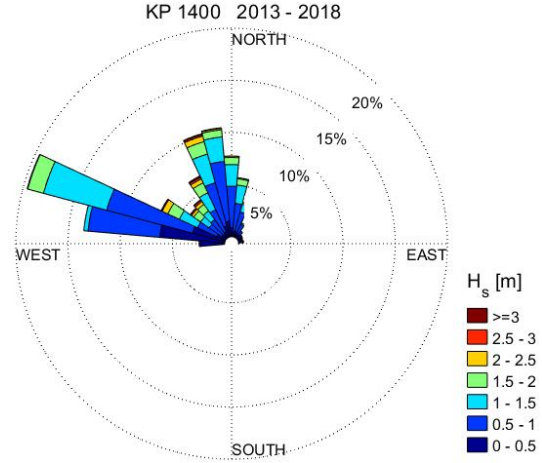
Figure 5.7: Wave rose of KP 1400 over the period of 2013-2018.

Nevertheless when comparing the output of wave data from both SWAN transformations at KP 1400, one obtains certain differences. The largest difference being the narrower wave rose over the more recent period of 2013-2018, which indicates more waves originating from the north to west are refracted when traveling nearshore to the toe of the DRS. Next to this difference in refraction over the data sets differences in distribution of wave heights and peak periods is obtainable from Tables 5.3 and 5.4. First of all the wave height distribution appears to be different for wave heights up to 1.5 meters. The distribution of the higher wave events are relatively similar. Although it is difficult to say where this difference in distribution over the lower wave heights comes from it is expected this difference in wave height distribution will not have a severe effect on the computation of Longshore Transport, as the Block Dam reduces especially the lower waves within a wave field. With respect to the difference in peak period distribution, no reasoned conclusions can be drawn as again a standard ratio is used for the obtainment of the peak periods over the period 1979 to 2005.

H_s [m]	1979-2005	2013-2018
0.0-0.5	42.9%	21.5%
0.5-1.0	32.9%	43.5%
1.0-1.5	15.3%	22.5%
1.5-2.0	5.6%	8.8%
2.0-2.5	2.1%	2.6%
2.5-3.0	0.8%	0.8%
>3	0.4%	0.3%

Table 5.3: Distribution of wave heights for the wave point at KP 1400 and for both data sets.

T_p [s]	1979-2005	2013-2018
0.0-4.0	18.4%	9.5%
4.0-5.0	30.5%	21.3%
5.0-6.0	28.3%	24.4%
6.0-7.0	16.5%	28.1%
7.0-8.0	5.3%	13.0%
8.0-9.0	0.9%	3.0%
9.0-10.0	0.1%	0.5%
>10.0	0.0%	0.2%

Table 5.4: Distribution of peak periods for the wave point at KP 1400 and for both data sets.

As stated, the nearshore wave data PUMA used in their prognosis is difficult to compare with the nearshore wave data presented in this study, as it is unknown which bathymetry Svasek used at the time of design. When

looking at the differences in wave climate, one must conclude a different bathymetry is used by Svasek. The only information on bathymetry that is known from the bathymetry of Svasek, are the local depths at the wave locations, i.e. the local depths at the output points of the 1979-2005 period. Although the exact same coordinates of output points are used in the SWAN transformation of this study, one obtains a difference in local depth. This can be seen when obtaining the exact locations and their consecutive depths in Appendix D.3.1. If the depths of the output points over the period 1979-2005 are compared to the local depths of the output points over the period 2013-2018, one obtains on average a difference of 2 meters in depth over the interest area. This difference in depth is significant and it is difficult to say where this difference in bathymetry comes from. The difference in depth can be simply the result of a different execution of the design. It could be the coordinates of the wave locations in this study do not longer exactly lie at the toe, but already more on the slope of the toe of the DRS. In this case the toe of the DRS would be more extended along the foreshore. This would explain the difference in local depth over the different wave output points.

A more likely cause for the difference in bathymetry, but foremost a cause for the difference in wave climate at the toe of the DRS, could be the alongshore transported sand on the foreshore of MV2. As nourishments have taken place at the Soft Sea Defence to the west of the DRS, sand has been transport along the foreshore of Maasvlakte 2, as can be seen in Figure 5.8. This Figure shows the difference in depth over the years 2014 to 2016. The years of these surveys were used, as these are the most recent survey years which contain the full foreshore of Maasvlakte 2. It can clearly be seen the foreshore of the transition of the sea defence is significantly increased due to the nourishments that have taken place at the soft sea defence. In two years time the increase of foreshore already ranges from half a meter up to 3 to 4 meters. This change in foreshore over the period 2014 to 2016 explains why a difference in the bathymetry Svasek used and the one used in this study results in a significant difference in the nearshore wave data.
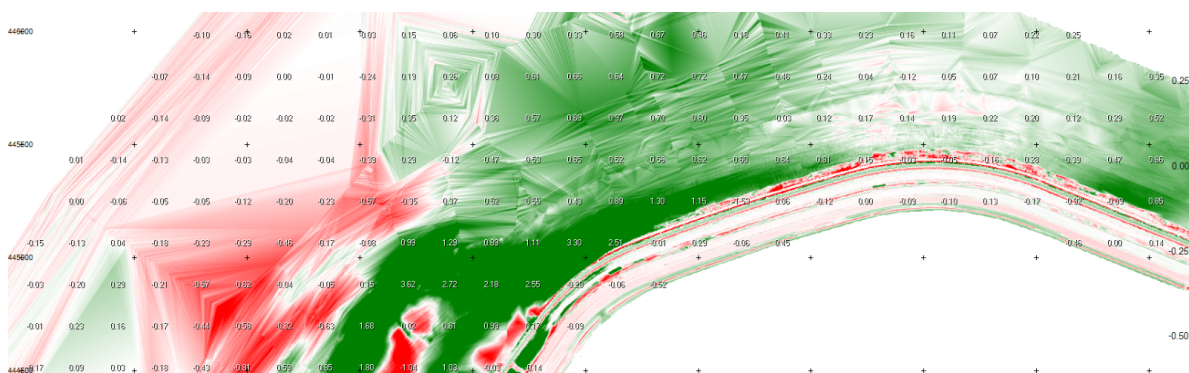
Figure 5.8: Change in depth of the foreshore of Maasvlakte 2 over the period 2014 to 2016. Red areas represent erosion and green areas represent accretion of sand.

5.5. Storm events

Next to the year-round wave conditions the occurred storms over the period 2013 to 2018 are compared to the design storms for which PUMA designed the DRS. Not only will large storms result in high Longshore Transport rates, PUMA also indicated the possible effect of storms on the Block Dam. PUMA expects a severe storm, i.e. a 1:100 year design storm, will rearrange the sub layers of the Block Dam. When this happens the large concrete blocks could settle, resulting in a lower average crest height of the BD. A large settlement of the BD is not yet obtained over the last five years, this is also explainable when assessing the storm events over the last five years.

Tables 5.5 and 5.7 show the observed storms for wave point 35 over the period 2013 to 2018. For the low water level storms, only the five storms with the highest wave height are presented. All low water level storms can be obtained from Appendix D.3.3. PUMA made a distinction between high water level and low water level storms. This distinction is followed here equally. Important to mention is the threshold values which are used to define a storm in the wave data over the last five years. These threshold values are subsequently $H_s > 3.5$ m for low water level storms and $h > 2$ m + NAP for high water level storms.

In order to compare the occurred storms to the design storms, Tables 5.6 and 5.8 show the design storms applied by PUMA. Here the design storms for the middle part of the DRS, indicated by 'HZm', and the eastern part, indicated by 'Hzo', are given as these sections correspond to the interest area used within this study. Appendix B.1.2 gives the design storms for every section of the DRS and for smaller return periods.

Year-Month	H_s max. [m]	$T_{m-1,0}$ max. [s]	Dir_{av} mean [° N]	Water level max. [m+NAP]
2015-7	4.29	8.27	296	1.54
2016-1	4.87	9.22	323	1.81
2017-1	4.15	9.08	307	2.22
2017-2	4.18	8.75	263	1.82

Table 5.5: Occurred low water level storms during 2013-2018.

1:10 yr				
Section	H_s [m]	$T_{m-1,0}$ [s]	Dir_{av} [°N]	Water level [m+NAP]
HZo	5.00	8.9	309	0.41
HZm	5.40	9.1	301	0.40

Table 5.6: Hydraulic design storm conditions at low water excluding SLR (Projectorganisatie Uitbreiding Maasvlakte, 2011a).

When looking at the storm events of the last five years it can be seen no 1:10 year or higher design storm has occurred. This holds both for low water level storms and high water level storms. With respect to storm events it is safe to say only 1:5 year storms have occurred during the period of 2013 to 2018. The absence of a large storm over this period will logically result in lower transport rates.

Year-Month	H_s max. [m]	$T_{m-1,0}$ max. [s]	Dir_{av} mean [° N]	Water level max. [m+NAP]
2013-9	4.09	8.76	327	2.08
2013-12	4.08	9.32	314	3.01
2014-10	4.31	8.68	303	2.77
2015-1	3.54	7.63	273	2.12
2018-1	3.70	7.09	254	2.11

Table 5.7: Occurred high water level storms during 2013-2018.

1:10 yr				
Section	H_s [m]	$T_{m-1,0}$ [s]	Dir_{av} [°N]	Water level [m+NAP]
HZo	5.25	9.1	310	3.10
HZm	5.65	9.2	302	3.10

Table 5.8: Hydraulic design storm conditions at high water with 50 years of SLR (Projectorganisatie Uitbreiding Maasvlakte, 2011a).

5.6. Conclusions

From this chapter it was obtained year-round offshore wave conditions at the Europlatform for the periods 1979 to 2005 and 2013 to 2018 compare sufficiently to be used as input data for the SWAN run.

When comparing nearshore wave data over both periods it was obtained clear differences in nearshore wave climate - following from the SWAN runs - are present. As it is unknown which bathymetry Svasek used, the agreement on wave conditions at the Europlatform show, a difference in bathymetry must be the cause for these differences in nearshore wave climate. Although it is difficult to determine the exact cause of this difference in bathymetry, it is likely the morphodynamic activity on the foreshore of the DRS is a reason for differences in nearshore output data. The transformation in this study is done using the present bathymetry. As explained this is probably the cause for the increase in refraction and the difference in wave height and peak period distribution. Logically this will result in different input data for the calculation of transport rates compared to the period of 1979 to 2005. Nevertheless, in this study the recent bathymetry of the foreshore of Maasvlakte 2 is used. Therefore it is assumed the transformation of this study is more reliable and therewith the nearshore wave data at the toe of the DRS represent the wave climate that has been present over the period 2013 to 2018.

An analysis of the storm events which occurred over the period 2013 to 2018 was carried out. Following from the data over this period, no severe storm event has been present during this period. A severe storm being a 1:10 or higher design storm, which PUMA used in their design. It was concluded only 1:5 year storm event have passed over the period 2013 to 2018.

5.7. Discussion

Within the comparison of wave climates over the periods 1979-2005 and 2013-2018, a standard factor was used to obtain peak periods for the year-round wave conditions over 1979-2005. Therefore the comparison of the peak periods over both periods of time, is not fully valid. This must be kept in mind when drawing conclusions with respect to the peak periods over the different data sets.

With respect to the storm events of the recent wave data it was concluded no severe storms have occurred during 2013 to 2018. A severe storm being one that has the same characteristics as the 1:10 year or higher design storms formulated by PUMA. Although the maximum wave height has been taken from all wave heights during such a storm, these might be even slightly higher at the toe than at the wave point which is used in the analysis. This wave point was taken in order to stay clear of consequences following from the alongshore transported sand along the foreshore of the DRS, only this could result in slightly higher wave heights at the toe of the DRS. It is expected this difference can result in approximately higher wave heights of 10 to 20 cm. This probable increase in wave height is not seen as a reason to assume a higher than 1:5 year storm event has passed over the years 2013 to 2018.

Methodology of calculating transport rates

This chapter describes the methodology which is applied to calculate Longshore Transport rates resulting from the wave data of the period 2013 to 2018. Using all the known parameters regarding the DRS and the Block Dam situated in front of it, an attempt is made to calculate the transport rates that occurred during this period. In this assessment two LT relations will be used to compute Longshore Transport rates.

6.1. Methodology

In order to calculate the Longshore Transport rates due to the wave conditions of the past five years a model has been set-up. This model is able to calculate the transport rate S, for every 100 meters along the DRS of MV2. Along every ray, indicated by KP 600 to KP 1800, the three main forcing parameters wave height, peak period and wave direction are altered due to the influence of the water depth and the interaction with the Block Dam. A schematic overview of the steps within the model is shown in Figure 6.1.

Figure 6.1: Methodology of calculating LT.

The consecutive steps from Figure 6.1 are treated in Sections 6.2 to 6.6. The first step is the assignment of a wave climate to the different rays along the DRS. Secondly the main forcing parameters within this wave climate will be altered due to interaction of the block dam. Also the depth dependence of the wave height and wave angle are taken into account when travelling along a wave ray. The main forcing parameters are computed up until an imaginary breaker-line behind the BD with a corresponding water depth. Next, the parameters $H_{s,t}$, $T_{p,t}$ and β_t are put into the desired Longshore Transport relation to obtain hourly transport rates. Summation of the hourly transport rates over a certain period will result in the total transport of stones over that period.
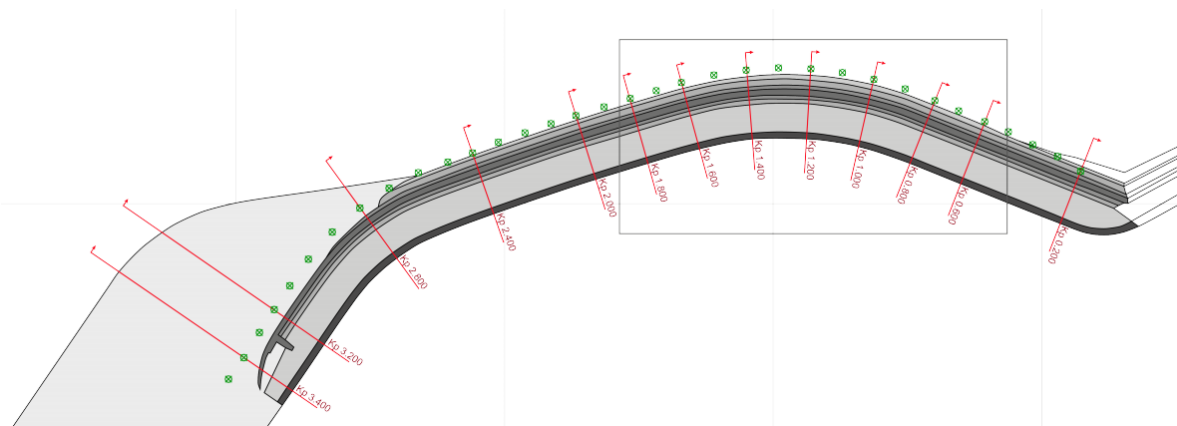
Figure 6.2: Overview of the DRS with sectional rays and corresponding wave output points.

In order to obtain actual erosion or accretion volumes within a certain section along the DRS, gradients in transport over such a section are computed. These calculated gradients are in a later stadium of this thesis compared to observed gradients, which in their turn are obtained from survey data, as will be explained in Chapter 7. The consecutive steps from Figure 6.1 will be explained in more detail in the following sections.

6.2. Wave climate per ray

Every 100 meter of the area of interest of the DRS, presented as KP 0.600 - KP 1.800, is assigned to a wave climate resulting from the SWAN transformation. The output locations of the wave transformation were set to the coordinates corresponding with the toe of every 100 metres of the DRS. These locations can be obtained from Figures 6.2 and 6.3. All nearshore wave locations are indicated with green crossed-out circles.
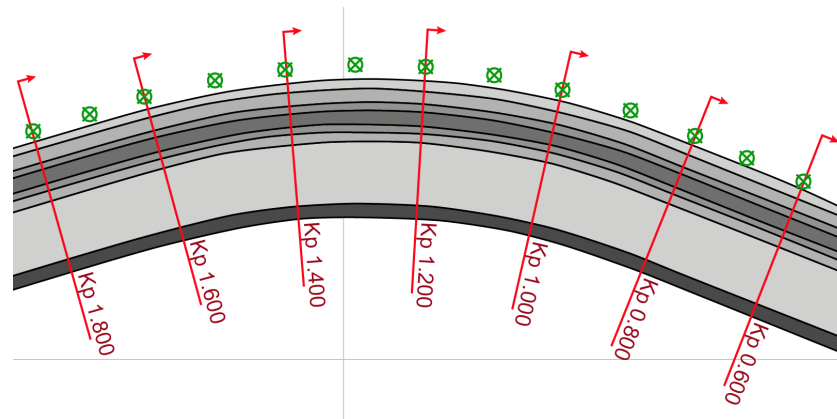
Figure 6.3: Area of interest with wave locations along the toe of the DRS.

6.3. Depth dependence of forcing parameters

One of the most important reason for the alteration of the main forcing parameters is that of the influence of the depth. The local water depth influences the wave height due to shoaling effects. Besides the wave height, the wave angle is equally influenced by the local water depth and waves will refract as the depth becomes more limited. The influence of both phenomena will be treated separately below.
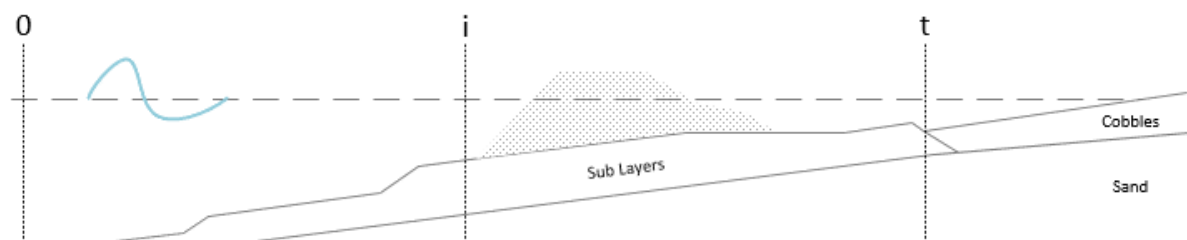
Figure 6.4: Cross-shore distinction of sections.

6.3.1. Shoaling effects

The shoaling of the waves along the different rays will be computed for two consecutive sections in cross-shore direction. The first being the section from the wave-point up until the BD, i.e. the shoaling resulting from difference in depth between d_0 and d_i. In the remainder of the model calculation the local water depth is corrected for the water level at that point in time, in that way tidal influences are taken into account. So for transect 0 the local water level results from $h_0 = d_0 \pm SWL$, where d_0 is the water depth and SWL the tidal level at that point in time. The second section over which the water depth decreases is the section over the BD, i.e. the shoaling that results from the water level difference between h_i and h_t. Over this section the shoaling is indirectly taken into account by the wave transmission equation of PUMA, which describes the transmission of the wave height as a result of the interaction with the Block Dam, as explained in Section 6.4. Below the computation of the shoaling factor over the first section will be explained.

The water level at the wave point is taken as the offshore water level, h_0. This depth is approximately 16 meters. To estimate the wave height at a point just in front of the Block Dam, linear wave theory is used. The depth just in front of the Block Dam is represented by h_i. Now the shoaling factor K_s is computed, based on the different group celerity's.

$$K_s = \sqrt{\frac{c_{g,i}}{c_{g,0}}} \tag{6.1}$$

In order to determine the different group celerity's the wavelength needs to be determined at the different water depths. This is done by iteration.

$$L = L_0 \cdot tanh \cdot \left(\frac{2\pi \cdot h}{L}\right) \quad \text{where} \quad L_0 = \frac{g \cdot T_{p,0}}{2\pi} \tag{6.2}$$

The wave length results in the computation of the group celerity c_g through Equations 6.3-6.4.

$$c_g = n \cdot c \tag{6.3}$$

where

$$c = \sqrt{g/k} \cdot tanh(kh) \quad \text{and} \quad n = \frac{1}{2}\left(1 + \frac{2kh}{sinh2kh}\right) \tag{6.4}$$

Now the shoaling factors for the two sections for every hourly wave height can be computed. Next the wave height is multiplied by this shoaling factor to give the wave height in front of the BD, in the treated case resulting in $H_{s,i}$.

$$H_{s,i} = K_s \cdot H_{s,0} \tag{6.5}$$

When waves get to steep, they will break. Therefore after the multiplication of the shoaling factor, waves that are too steep and will break are capped with a maximum wave height. This is done by means of the breaker index, given by Equation 6.6 (McCowan, 1894). When the breaker index exceeds 0.78, the corresponding wave height will become the maximum possible wave height at that depth, i.e. $H_{s,t}^{max} = 0.78 \cdot h_t$. In this way the wave energy of this broken wave is still taken into account when calculating transport rates, as this wave energy will still induce Longshore Transport.

$$\gamma_b = \frac{H_{s,t}}{h_t} = 0.78 \tag{6.6}$$
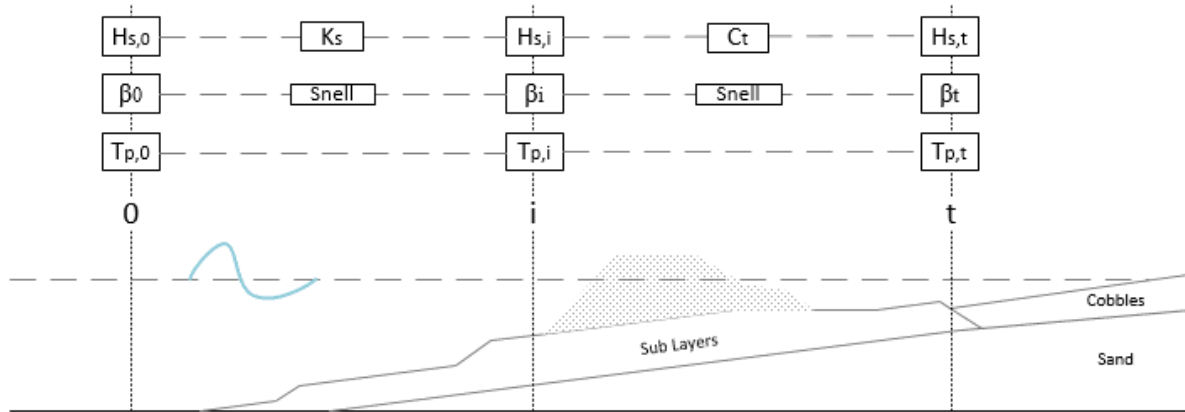
Figure 6.5: Alteration of main forcing parameters to imaginary line behind the BD due to limiting depth.

6.3.2. Refraction
Similar to the wave height, the wave angle will be influenced by the limiting depth. According to linear wave theory waves tend to become more shore normal oriented when the depth decreases. This phenomenon is called refraction and will be taken into account by applying Snell's law. Within this relation the ratio of the wave angle over the local depth stays constant. Equation 6.7 shows this relation for the first section.

$$\frac{sin\beta_0}{\sqrt{c_0}} = \frac{sin\beta_i}{\sqrt{c_i}} \tag{6.7}$$
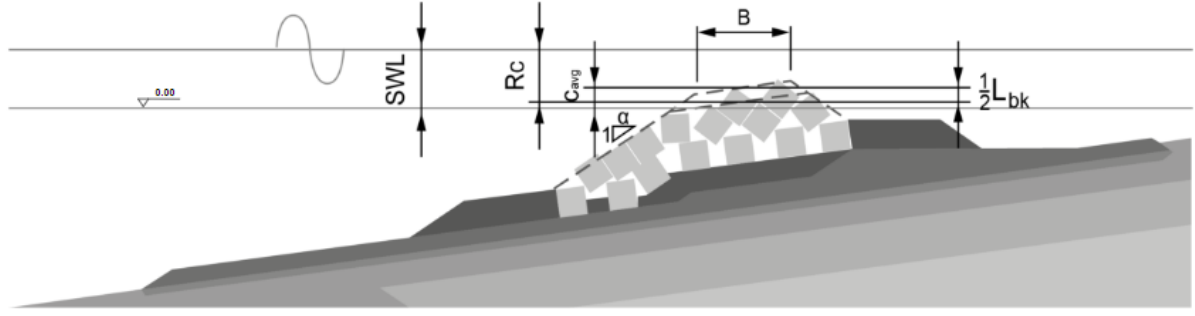
Figure 6.6: Block Dam with corresponding parameters.

6.4. Block Dam transmission

When travelling nearshore the forcing parameters will encounter the Block Dam. The interaction with the BD is taking into account following the same approach of PUMA, as explained in Appendix B. The alteration of different parameters due to the BD with respect to the different forcing parameters will be discussed separately below.

6.4.1. Transmitted wave height $H_{s,t}$.

The most important alteration is that of H_s. For this a C_t needs to be computed through Equation 6.8. This equation was specifically calibrated for the BD of Maasvlakte 2 (Projectorganisatie Uitbreiding Maasvlakte, 2009).

$$C_t = \left(-0.34294 \frac{R_c}{H_{s,i}} + \left(0.47609 \cdot \frac{B}{H_{s,i}} \right)^{-0.27492} \cdot (1 - e^{-0.5\xi_p}) \cdot 0.64 \right) \cos^{0.10007} \beta_i \qquad 0.075 < C_t < 0.8 \qquad (6.8)$$

where

$$\xi_p = \tan\alpha \left(\frac{H_{s,i}}{L_0} \right)^{0,5} \qquad (6.9)$$

$$R_c = c_{avg} - \text{SWL} - 0.5 \cdot L_{BK} - z_{BK} \qquad (6.10)$$

All parameters that represent characteristics of the Block Dam are presented in Figure 6.6. In Equation 6.10 L_{BK} represents the rib length of the concrete cubes of the BD, which is taken as a constant of 2.54 m. SWL represents the still water level. As input for SWL the hourly water levels are used. Furthermore, the settlement of the BD is represented by z_{BK}. Yearly surveys of the settlement of the BD are executed by PUMA. The observed settlements per year are taken into account and put into the calculation model. The freeboard R_c is influenced mostly by the average crest height of the BD, represented by c_{avg}. The average crest height and the yearly average settlements of the BD for the interest area of KP 600 to KP 1800 are given in Table 6.1.

c_{avg}	z_{bk}				
2013	2013-2014	2014-2015	2015-2016	2016-2017	2017-2018
3.26 m + NAP	0.7 cm	2.0 cm	4.2 cm	2.9 cm	0.3 cm

Table 6.1: Average crest height and yearly settlements of the BD along the interest area.

Within the prognosis of PUMA the average design BD height after 50 years of 2.0 m was taken. In the calculation model the actual height of the block dam is used as input for c_{avg}. The height of the Block Dam is highly irregular in longshore direction as the block placement differed equally. Therefore an average crest height is taken over the interest area of KP 600 to 1800. The same is done for the yearly settlement z_{BK}. No major settlements of the BD have taken place over the past five years. The overall settlement is approximately 10 cm over the past five years.

When all parameters are put into the transmission relation, C_t can be obtained. Next the transmitted wave height is computed through:

$$H_{s,t} = C_t \cdot H_{s,i} \qquad (6.11)$$

As the BD is situated at an angle, again shoaling needs to be taken into account, only now this shoaling is incorporated within C_t from Equation 6.8. The computed $H_{s,t}$ can subsequently be used - in combination with other transmitted parameters - as input for one of the two Longshore Transport relations.
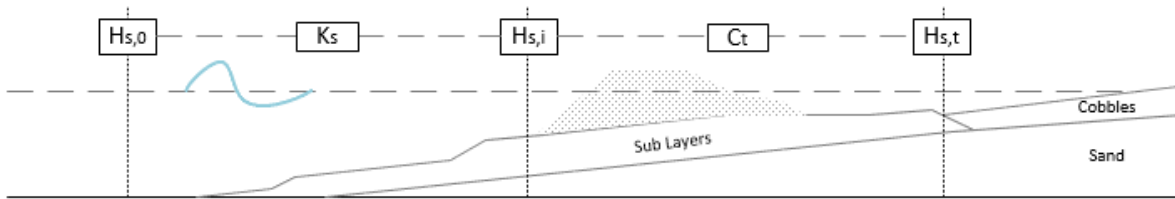
Figure 6.7: Alteration of the wave height due to the the limiting depth and the interaction with the BD.

Intermezzo: Dismissing westerly Longshore Transport

In Chapter 5 it was observed practically all waves come from the north to northwest. When looking at the wave data at the toe of KP 1200 it is seen only 16 % of the waves originate from the north to north east. A wave climate which includes mostly easterly directed waves will logically result in easterly directed Longshore Transport, which is dominant over westerly transport. Along the interest area KP 1800 to KP 600 of Maasvlakte 2, westerly directed LT will from this point onward be dismissed from the computation.
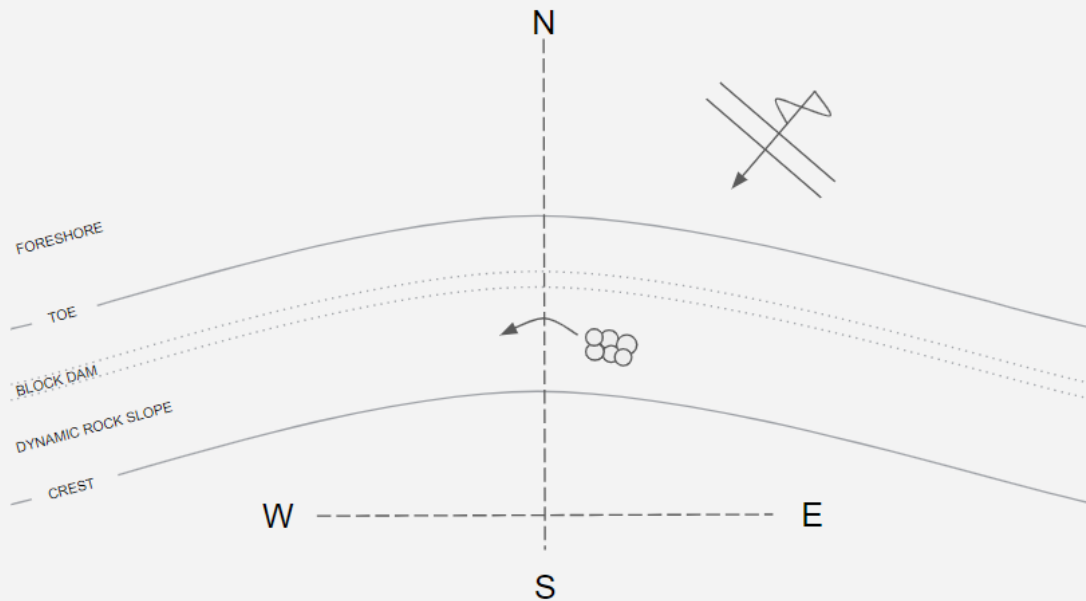
Figure 6.8: Waves coming from the north to east resulting in westerly directed LT.

The basis for this conclusion is not only the dominant wave directions, but also the computed transmitted wave heights following from these westerly directed waves. The transmitted wave height being the average wave height $H_{s,t}$ that results from computation using the method described in Section 6.4. For the computation of the average of $H_{s,t}$ over the five years of wave data, again the wave characteristics of KP1200 are taken. When averaging the transmitted wave heights that come from the east a $H_{s,t}$ of 0.049 m can be observed. This is significantly lower than $3 \cdot D_{n50} = 3 \cdot 0.065 = 0.195$ m which is assumed to be the minimal forcing to move a stone.

6.4.2. Transmitted peak period T$_{p,t}$.

During the tests for the calibration of the wave transmission relation - which resulted in Equation 6.8 - the peak period was measured equally. It followed from these tests that a significant change in spectrum was obtained due to the wave transmission through the BD (Projectorganisatie Uitbreiding Maasvlakte, 2009). Despite this change in spectrum, no significant change in peak period was observed when comparing peak periods measured in front and behind the BD. This observation is presented in Figure 6.9. Therefore the peak period is assumed to stay the same during wave transmission through the BD . Within the calculation of the model this assumption is equally followed, so $T_{p,0} = T_{p,t}$.
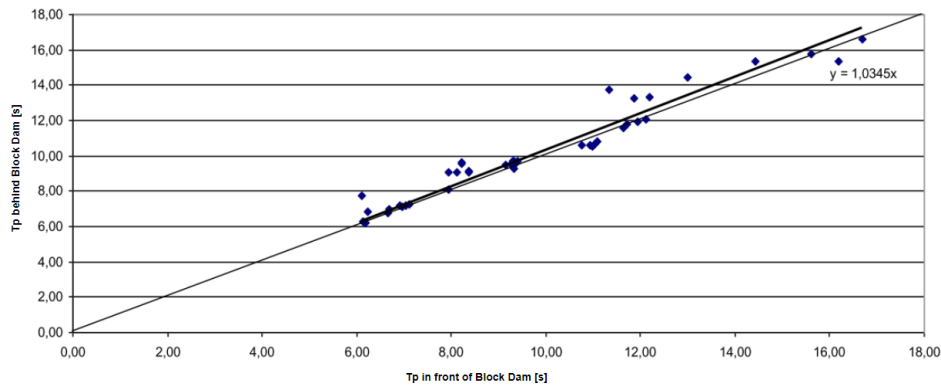
Figure 6.9: Results from scale model tests on peak period alteration due to transmission through the BD. (Projectorganisatie Uitbreiding Maasvlakte, 2009).

6.4.3. Transmitted shore normal wave angle β_t.

PUMA made an assessment on the rotation of the wave angle during interaction of incoming waves with the BD. Two assumptions were made as the actual effect of the BD on the wave angle was not measurable in scale model tests. The first assumption being that waves are assumed to get 20% less oblique when travelling through the block dam. This would be with equal depth in front and behind the block dam. The second assumption was the alteration of the wave angle by means of Snell's law, Equation 6.7. PUMA did not clearly state if both assumptions were used separately or in sequence. The calculation model therefore only accounts for the refraction due to the limiting water depth and disregards the assumption of a 20 % wave angle reduction due to the BD.
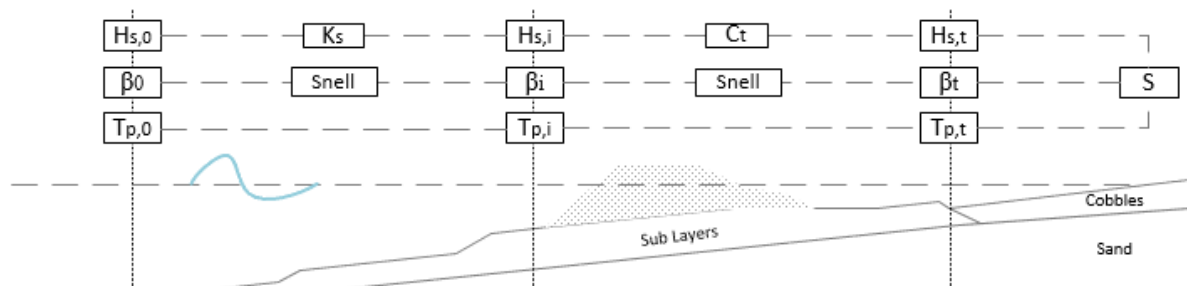
Figure 6.10: Altered parameters used as input for the desired transport equation.

At this point all forcing parameters within the model are transmitted to an imaginary line behind the Block Dam. The transmitted wave characteristics $H_{s,t}$, $T_{p,t}$ and β_t will be used as input parameters for the longhore transport relation of choosing, as can be seen in Figure 6.10. In the following sections both LT relations and their usage in the calculation model are discussed.

6.5. Longshore Transport relation

The following step in the calculation model is to use the three main forcing parameters as input for the pre-ferred Longshore Transport relation. As explained in Chapter 4 two formulas will be assessed within this re-search. The first being the dimensional relation calibrated by PUMA. The second being the non-dimensional GLT relation of Tomasicchio.

6.5.1. PUMA's Longshore Transport relation

First the relation PUMA calibrated will be discussed. The dimensional equation PUMA calibrated and used in their prognosis is the following (Projectorganisatie Uitbreiding Maasvlakte, 2012):

$$S_{LT,P} = 6.21 \cdot H_{s,t}^{3.6} \cdot \sin(2.00 \cdot \beta_t)^{0.86} \cdot (T_{p,t} - 6.00)^{0.10} \qquad \text{for } S_{LT,P} < 150 kg/s \qquad [kg/s] \qquad (6.12)$$

The relation of PUMA is dimensional and was specifically calibrated for the DRS at Maasvlakte 2. This means the PUMA relation is only applicable for the stone size used to construct the DRS. This stone size is generally represented by the D_{n50} and for the quarry rock used on the DRS of MV2 amounts to 65 mm. Because the PUMA relation uses this dimensional approach, computing the transport rates is simply a matter of providing the relation with the three forcing parameters $H_{s,t}$, β_t and $T_{p,t}$.

Within the calculation the hourly forcing parameters are used to calculate the transport along a ray in kg/h, by use of Equation 6.12. Subsequently these hourly transport rates are summed over the required period. To acquire the volumes in m^3 the ratio of 1620 tonnes per cubic meter is used. This weight to volume ratio was given by PUMA. Now the model produces transport of stones over a certain period in volumes. In other words the output of the model is the amount of stones in volumes that will pass that ray over a certain period of time. This is schematically represented in Figure 6.11. The amount of Longshore Transport is calculated for every 100 meters along the area of interest.
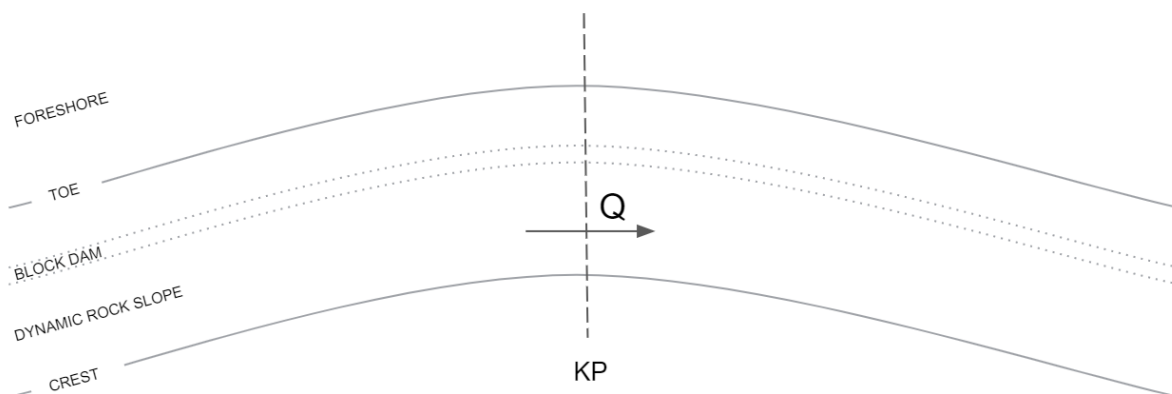
Figure 6.11: Schematic representation of Longshore Transport passing a ray along the DRS.

6.5.2. General Longshore Transport relation

Next to the PUMA relation, the GLT relation of Tomasicchio is used to assess transport rates. As the GLT relation is a non-dimensional relation, the stone size is taken into account when calculating transport rates. Consequently this Longshore Transport relation would theoretically be applicable for any type of dynamic structure. The approach of Tomasicchio is based on scale model tests and contains multiple parameters which are set to theoretical values, easily obtainable in a model situation. Applying the GLT relation in the calculation model asks for multiple assumptions. These assumptions are discussed below.

The wave characteristics along a ray are used as input for the GLT relation. The dependence of Equations 6.13-6.18 on the wave characteristics is represented by the flow chart in Figure 6.12. This depence was equally presented by Tomasicchio et al. (2013).
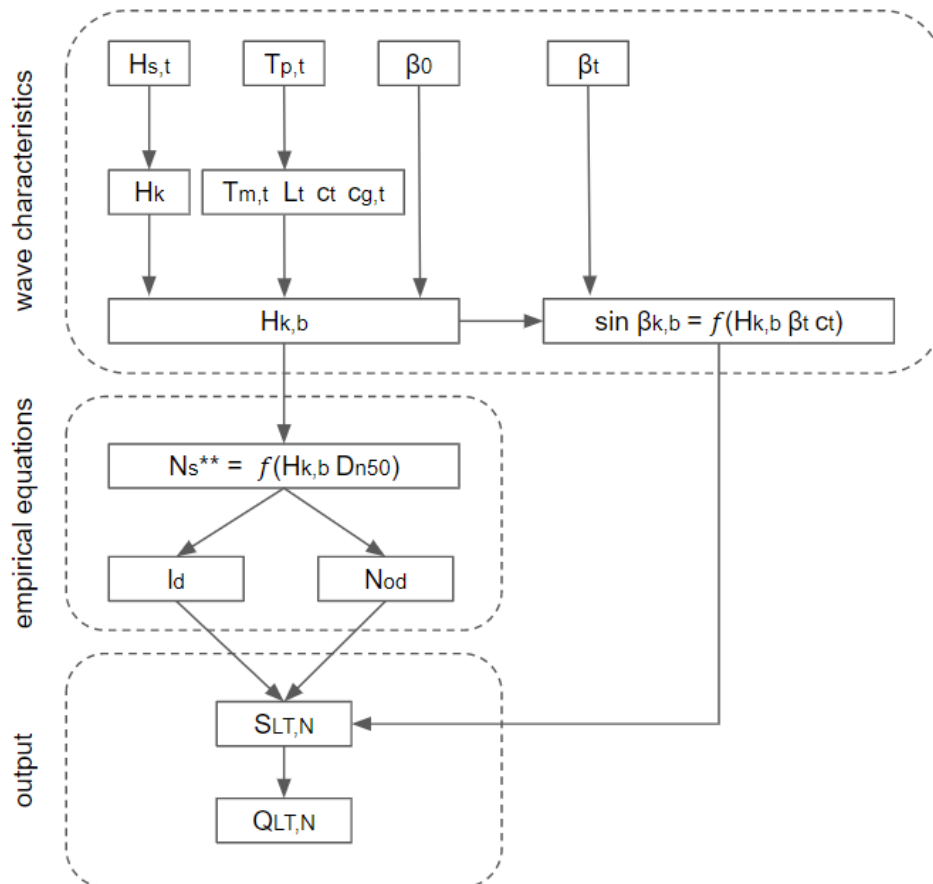
Figure 6.12: Dependence of wave characteristics to the equations within the GLT relation.

First the wave height is altered to obtain the wave height at breaking.

$$H_{k,b} = \left(H_k^2 c_{g,t} \cos\beta_t \sqrt{\gamma_{b,T}/g} \right)^{2/5} \tag{6.13}$$

In this equation the characteristic wave height is found through $H_k = C_k \cdot H_{s,t}$. In this calculation $C_k = 1.55$ is used. According to Lamberti and Tomasicchio (1997) H_k is then equal to $H_{1/50}$. Furthermore $\gamma_{b,T}$ represents the breaker index used by Tomasicchio et al. (2013) and is set to 1.42. Next, the wave height at breaking is used to compute the influence of wave incidence on the Longshore Transport in Equation 6.17.

$$\sin\beta_{k,b} = \frac{c_{k,b}}{c_t}\sin\beta_t = \frac{\sqrt{gH_{k,b}/\gamma_{b,T}}}{c_t}\sin\beta_t \tag{6.14}$$

The wave characteristics are then used to determine the updated stability number. This updated stability number N_s^{**} is not only dependent on wave height, specific density and stone size - like the commonly used

stability number - but also on wave steepness and offshore wave angle. The offshore wave steepness is computed through $s_{m,0} = H_{s,t}/L_0$ and the characteristic wave steepness $s_{m,k}$ is set to 0.03.

$$N_s^{**} = \frac{H_{s,t}}{\Delta D_{n50}} \cdot \left(\frac{s_{m,0}}{s_{m,k}}\right)^{-1/5} \cdot (\cos\beta_0)^{2/5} \tag{6.15}$$

The updated stability number is subsequently used to obtain the displacement length l_d and the number of displaced particles N_{od}, through Equation 6.16. In the calculation model N_{od} for $N_s^{**} \leq 23$ is used, which produces the displacement of coarse-grained material, i.e. up to sand particles.

$$l_d = \frac{(1.4N_s^{**} - 1.3)}{tanh^2(k_t h_t)} D_{n50} \qquad\qquad N_{od} = 20N_s^{**}(N_s^{**} - 2)^2 \qquad \text{for} \quad N_s^{**} \leq 23 \tag{6.16}$$

Now the actual transport rate over a ray can be obtained through Equation 6.17. The Longshore Transport rate is represented in stones per wave in this equation. N represents the amount of waves that approximately arrived at the DRS over a certain amount of time. As the wave data used in the calculation method is hourly, N is obtained through $N = 3600/T_{p,t}$.

$$S_{LT,N} = \frac{l_d}{D_{n50}} \cdot \frac{N_{od}}{N} \cdot \sin\beta_{k,b} \qquad [stones/wave] \tag{6.17}$$

The Longshore Transport rate $S_{LT,N}$ is related to the mass transport in $[m^3/s]$ through Equation 6.18. Here n is the porosity of the transported material. For the stone size, the D_{n50} applied at the DRS is taken, which amounts to 65 mm.

$$Q_{LT,N} = \frac{S_{LT,N}D_{n50}^3}{(1-n)T_{m,t}} \qquad [m^3/s] \tag{6.18}$$

Now the transport in cubic meters per second is known and the calculation model translates this to hourly transports. The hourly transports are then summed over a certain period in time to obtain yearly transport of stones passing that ray along the DRS. This procedure is equally followed for the computation of Longshore Transport according to the PUMA relation.

Intermezzo: Porosity of rock material at Maasvlakte 2

For the translation from transport rates to transport volumes within the GLT relation, the porosity of the rock material at Maasvlakte 2 needs to be obtained. Equation 6.19 gives the porosity based on the void ratio according to The Rock Manual (CIRIA, CUR, 2007).

$$n = \frac{1}{1+e} \tag{6.19}$$

In which e is the void ratio and can be obtained through:

$$e = \frac{1}{90}(e_o)\arctan(0.645n_{RRD}) \tag{6.20}$$

In Equation 6.20 e_o ranges from 0.92 to 0.96 for typical mechanically crushed fragments, where 0.96 tends more toward flat stones and 0.92 more to round pebbles. Therefore n is computed for $e_o = 0.96$, as the rock applied at the DRS is more angular shaped than being round pebbles.

The grading of the material is used to establish n_{RRD}. The grading of the rock at MV2 is relatively wide, 20/135 mm, with respect to standard gradings. Therefore the ideal n_{RRD} is taken for a standard wide and coarse grading, this grading being 45/180 mm. With this n_{RRD} of 2.41, a porosity of 0.379 is found for the rock on the DRS at Maasvlakte 2.

6.6. Volume changes

In the previous sections the steps that were taken in order to compute the transport rates were discussed. At this point the calculation model takes a last step; computing the transport gradients over a certain section along the DRS.

So far the calculation model computes the transport of stones over a certain period in time for every 100 meters along the interest area. In other words, the amount of stones in m^3 per period of time that are transported over an imaginary cross-sectional line. The passing of the amount Q in m^3 per period of time over this imaginary line is schematically presented in Figure 6.13.
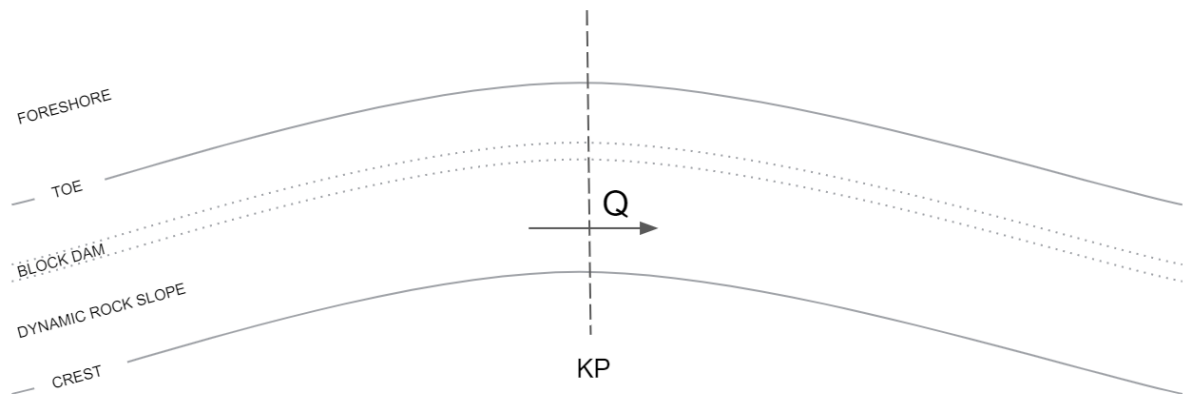
Figure 6.13: Schematic representation of transport in volumes over a cross-sectional line along the DRS.

If the transport rate at a certain KP is lower than the transport rate at another KP, e.g. $Q_1 < Q_2$, the volume in the control section will decrease, resulting in erosion. Vice versa; $Q_1 > Q_2$, would result in accretion over that section. Figure 6.14 gives a schematisation of erosion over a 100 meter wide section. The calculation model will compute these gradients in Longshore Transport over every 100 meter wide section along the interest area. The output volumes in m^3 are the erosion or accretion volumes which are suitable for comparison with the volumes retrieved from the yearly surveys. The survey volumes will act as validation in order to assess the ability of the two LT relations to predict Longshore Transport gradients, i.e. volume changes over a certain section along the DRS, as will be explained in Chapter 7.
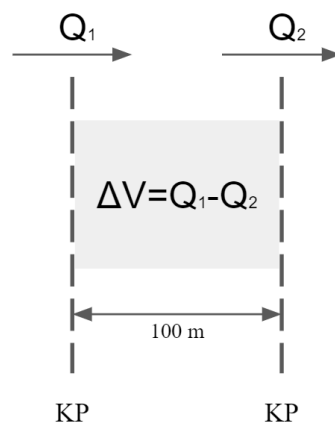
Figure 6.14: Schematic representation of gradients in LT.

6.7. Calculation model applied on historic data

In order to assess if a similar approach of calculation is applied in the calculation model of this research as PUMA did in their prognosis, the data used by PUMA was used as input for the calculation model. The wave data PUMA used in their prognosis was the wave climate over the period of 1979-2005. The historic wave data over this period was obtained from Svasek. This data was used by PUMA to make a prognosis on the yearly average Longshore Transport. Figure 6.15 shows these computed transport rates. The light grey lines indicate the transport over the different years and the red line is the average over these years. PUMA set the BD to a height which they expected after 50 years, which amounts to 2 m + NAP. Also a sea level rise of 35 cm was taken into account.
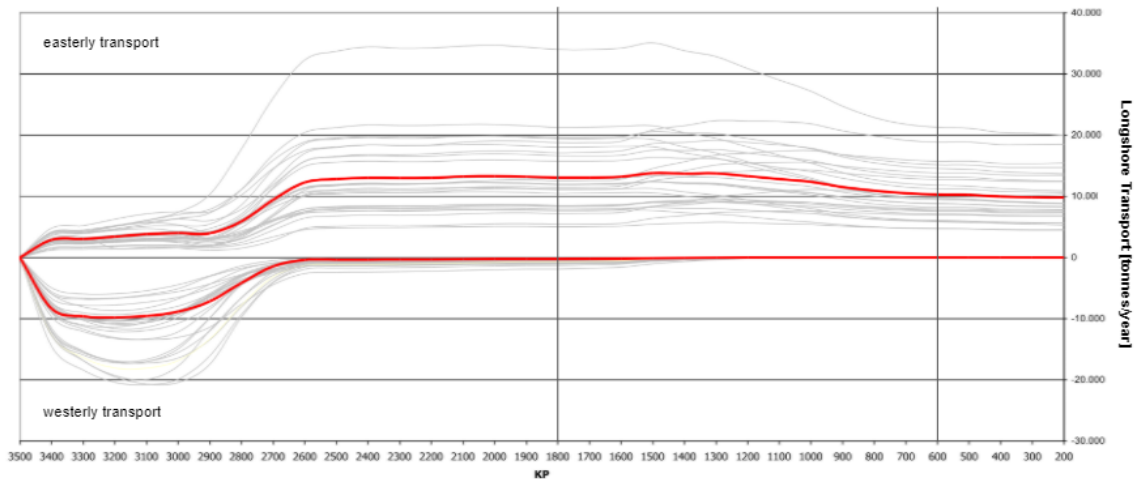
Figure 6.15: Prognosis of bruto Longshore Transport by PUMA, based on the wave climate of 1979-2005 (Projectorganisatie Uitbreiding Maasvlakte, 2012). BD at 2 m + NAP and 0.35 m SLR.

The historic wave data over the period 1979-2005 are used as input for the calculation model of this research and transport rates are computed. The output of the model is shown in Figure 6.16. For the computation both the height of the BD and sea level rise were taken into account equally as PUMA did in their prognosis. When comparing both figures it is possible to conclude the model calculates transport in the same order of magnitude. In the interest area of KP 600 to KP 1800, the transport rates even compare considerably well. Deviating transport rates can originate from differing peak periods. The calculation model uses hourly peak periods as input for the Longshore Transport relation. The historic data only consisted of mean wave periods $T_{m-1,0}$. Therefore a standard ratio of $T_p = T_{m-1,0} \cdot 1.112$ was taken in order to obtain hourly peak periods (CIRIA, CUR, 2007). Also the westerly directed transport, although being very small, is not subtracted in the calculation model.
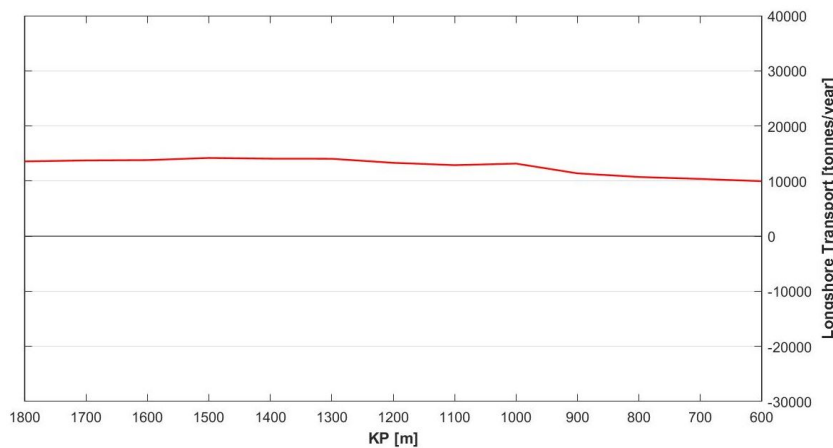
Figure 6.16: Calculated easterly directed Longshore Transport rates by the calculation model using the wave climate of 1979-2005 over the interest area KP 1800 to KP 600. BD at 2 m + NAP and 0.35 m SLR

6.8. Discussion

Multiple steps are taken to finally obtain the forcing input parameters behind the Block Dam, which are used as input for the LT relations. In general this results in large uncertainties in the final obtainment of the Longshore Transport rates. Most uncertainties in the obtainment of the forcing parameters behind the BD arise because of the presence of this BD. With respect to the BD the following issues result in these uncertainties:

- The wave transmission relation of PUMA, which was used to compute the wave transmission through the BD, generates large uncertainties in the wave heights present behind the BD.

- The average crest height c_{avg}, being the main influence on the outcomes of the transmission relation, is averaged over the interest area. Locally this can result in a lower crest height and changes in LT.

- The effect on wave obliquity by the BD is not validated by PUMA. Therefore it is difficult to incorporate the effect of the BD on this parameter into the calculation model.

- The influence of set-up behind the BD is not taken into account within this research.

Results PUMA relation

Using the methodology described in Chapter 6 the calculation method computes Longshore Transport for both the PUMA and GLT relations. This chapter will discuss all the results following from computations using the PUMA relation. In order to maintain an overview of the consecutive parts within this chapter, a short summary is given:

- The first part of this chapter, Section 7.1, describes the differences in computed transport rates over the period 1979-2005 - which PUMA used for their prognosis - and the computed transport rates over the period of 2013-2018, as a result of the wave data over these periods.

- The second part of this chapter, Section 7.2, covers the effect of different parameters on the output of computed transport rates for the PUMA relation.

- The last part of this chapter, Sections 7.3-7.5, assesses the validation of the PUMA relation. In order to validate if the PUMA relation is able to predict the Longshore Transport gradients which occurred over the period 2013-2018, erosion and accretion volumes are obtained through survey imaging and compared to predictions the PUMA formula generates over this corresponding period.

7.1. Prognosis PUMA

Now the calculation model is set-up it is possible to assess where the differences in computed transport rates, as a result of the wave climate of 2013 to 2018, with respect to the prognosis of PUMA come from. The prognosis of PUMA was based on the wave climate of 1979 to 2005. As explained in Appendix B, PUMA made a LT prediction based on the situation they expected to be present 50 years after construction. The two parameters PUMA changed were the height of the Block Dam, which was set to 2 meter + NAP, and the inclusion of Sea Level Rise (henceforth also referred to as "SLR") of 0.35 meter. The computations following from this situation are presented in Figure 7.1.
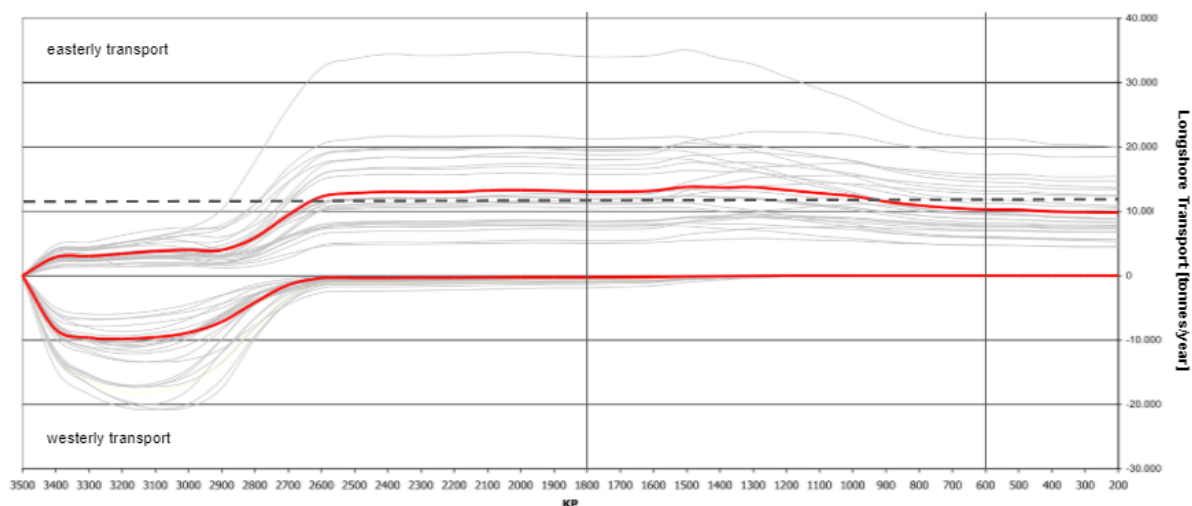
Figure 7.1: Longshore Transport prognosis based on the wave data of 1979-2005 (Projectorganisatie Uitbreiding Maasvlakte, 2012). BD at 2 m + NAP and 0.35 m SLR.

Obviously the computations executed in the prognosis made use of the specifically calibrated LT formula of
PUMA, in this thesis referred to as the PUMA relation. PUMA used the situation presented in Figure 7.1 as a
basis in order to determine the loss of stone over the 50 years following construction. Over the interest area
of KP 1800 to KP 600 an approximately average transport of 12.000 tonnes per year was computed, indicated
by the dashed line in Figure 7.1.

	Prognosis PUMA	This research
LT relation	PUMA	PUMA
Wave climate	1979-2005	2013-2018
SLR	√	√
c_{avg} BD	2.0 m + NAP	2.0 m + NAP

Table 7.1: Input parameters for the comparison of two situations.

When the same situation is taken as used by PUMA in their prognosis, the difference in computed LT result-
ing from the difference in wave climates can be observed. This means setting the BD height at 2 m + NAP and
including a SLR of 0.35 m. Now the only difference in input for the computation of LT rates is the wave climate
on which the computed transport rates are based. As multiple situations comprising of different character-
istics will be compared in the remainder of this report, Table 7.1 will be presented every time a parameter in
a certain situation is altered. For now, solely the difference in wave climate is the variable parameter. This is
done in order to compare computed transport rates over the period 2013-2018 with the prognosis of PUMA.
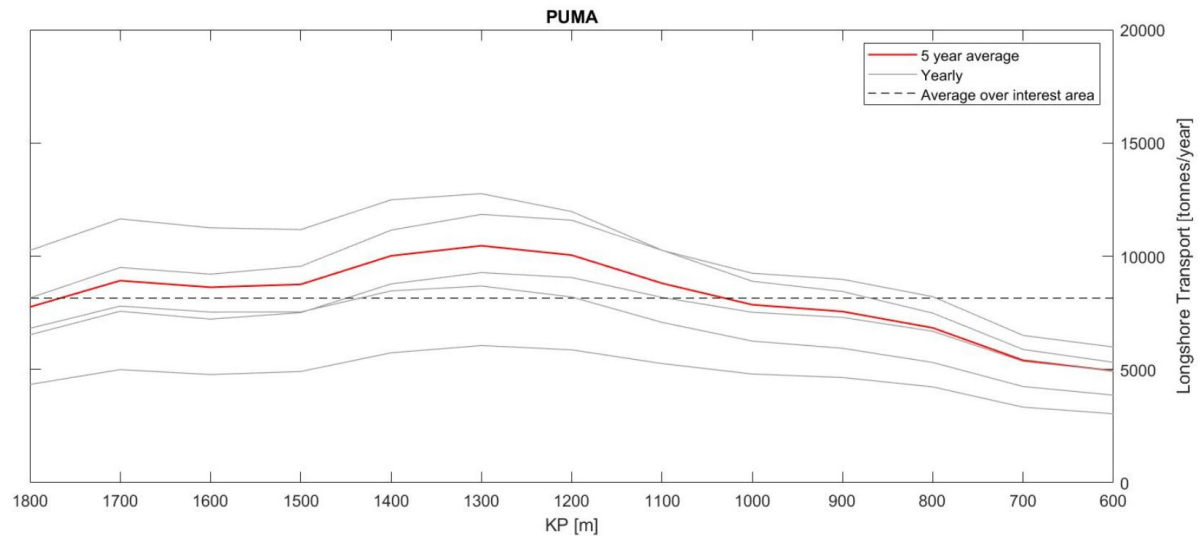
Figure 7.2: Longshore Transport computation based on the wave data of 2013-2018 using the PUMA relation.
BD at 2 m + NAP and 0.35 m SLR.

The output of LT rates for the PUMA relation resulting from the period 2013-2018 are given in Figure 7.2.
What can be obtained from the computed transport rates are a significant lower amount of computed trans-
port rates over the interest area KP 1800 - KP 600. Over this area, the average amount of easterly directed
transport is 8.200 tonnes/y. This is approximately 32% less transport than PUMA predicted using the wave
climate of 1979 to 2005, as can be seen in Table 7.2. This lower amount of computed transport indicates that
the wave conditions over the period 2013-2018 were relatively mild. This milder wave climate is logically the
result of less severe occurred storms over this period, as it was already observed in Chapter 5 only 1:5 year
storms were present during the period of 2013 to 2018.

Average computed LT over 1979-2005	12.000	tonnes/y
Average computed LT over 2013-2018	8.200	tonnes/y
Difference	32%	

Table 7.2: Average LT following from the PUMA relation resulting from the wave climates over the different periods.

7.1.1. Longshore Transport due to storm events

In order to show storm events have a major effect on the computation of Longshore Transport, here the Longshore Transport following from the PUMA relation of KP 1200 is analysed. Figure 7.3 shows the part of Longshore Transport that is the result of a wave height H_s larger than 2.0 meters. The wave heights are taken at the wave point of KP 1200, so in front of the Block Dam. What can be seen is that 69% of the Longshore Transport that is computed for KP 1200 over the period 2013 to 2018, resulted from wave heights higher than 2.0 meters. In Chapter 5 it was obtained wave heights higher than 2.0 meters only occur approximately 3.7% of the time. For this reason waves which are higher than 2.0 meters, are seen as a storm event. Concluding, storm events containing waves that occur only 3.7% of the time over the period 2013 to 2018 account for 69% of the Longshore Transport computed over the period 2013 to 2018, according to the PUMA relation.
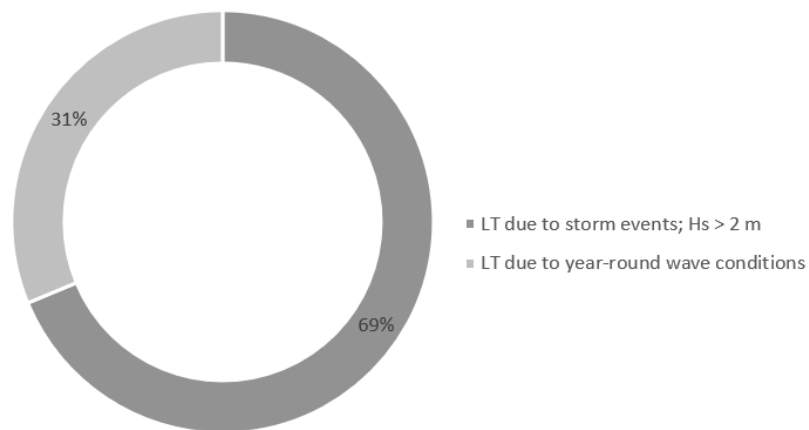
Figure 7.3: Longshore Transport according to the PUMA relation for different events.

Next to the less severe storms that occurred over the period of 2013-2018, it was seen in Chapter 5 that the nearshore transformed wave climate over the period 2013-2018 had a different distribution of waves over the different directions than the nearshore wave climate over the period of 1979-2005. As stated this is probably the result of a different bathymetry along the foreshore of the DRS. This difference in wave angle is included within the wave climates used in this assessment, therefore this difference in wave incidence must be seen as a partial reason for the lower computed transport rates over the recent period of 2013 to 2018. As it is unknown which bathymetry Svasek used in their SWAN transformation, it is not possible to quantify what the difference in computed LT is solely due to this difference in wave incidence. Only because storm events apparently have a major effect on the computation of Longshore Transport over the period 2013 to 2018, it is assumed storm events are the normative reason for the differences in wave climate - and thereby difference in Longshore transport - over the period 2013 to 2018.

7.2. Influence governing parameters

A large number of parameters influence the transport at the DRS of Maasvlakte 2, as was observed in Chapter 6. Therefore it is of interest to quantify this difference in order to create insight in the performance of the LT relations. In order to establish which influence different parameters have on the output of transport rates resulting from a LT relation, a reference situation is needed. This reference situation represents the computed transport rates for the period of 2013-2018 resulting from the PUMA relation.

7.2.1. Reference situation

To quantify what influence different parameters have on the computed transport rates, a reference situation is set. The reference situation will be referred to as the base case. This base case represents the Longshore Transport that actually occurred during the last five years according to the PUMA relation.

	Base case
LT relation	PUMA
Wave climate	2013-2018
SLR	×
c_{avg} BD	2013-2018

Table 7.3: Input parameters for the base case.

The computed transport rates of the base case is the average of the transport rates over the first 5 years after construction, i.e. the period of 2013 to 2018. Next to the occurred wave climate during this period, all other parameters that influence LT at the DRS of Maasvlakte 2 are set to the situation of the last 5 years, as is presented in Table 7.3. The output of Longshore Transport for the base case is presented in Figure 7.4.
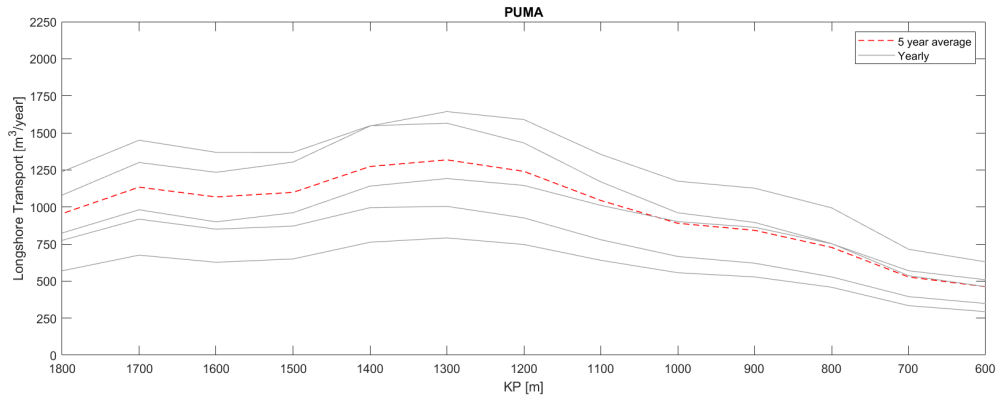
Figure 7.4: Computed LT according to the PUMA relation for the base case over the interest area KP 1800 to KP 600.

In order to compare different cases, the average of LT in space is taken, i.e. the computed LT rates are averaged over the section KP 1800 to KP 600. For the PUMA relation the average of computed Longshore Transport over the interest area resulting from the wave climate of 2013 to 2015 amounts to 968 m^3/y, as can be obtained from Table 7.4

[m^3/y]	Base case
PUMA	968

Table 7.4: Average computed LT over the past 5 years for the PUMA relation.

7.2.2. Influence Block Dam
A major influence on the cobble transport at Maasvlakte 2 is the influence of the Block Dam in front of the DRS. This BD alters mostly the wave height and wave angle as was obtained in Chapter 6. The peak period of the incoming waves appears to be the same in front and behind the BD. Therefore only the effect of the BD on wave height and wave angle are discussed here.

Average crest height
The average crest height of the BD is the input parameter which influences the transmitted wave height mostly. Therefore multiple runs of the calculation model are executed with a lowered crest height as deviating input parameter. Al other parameters are kept constant with respect to the reference situation. Three situations are treated; a lowered average crest height of -0.1 m, -0.25 m and -0.4 m, as is represented in Table 7.5. What can be obtained is the large increase in Longshore Transport when altering the average crest height. The situation of a lowered crest height of -0.1 m is interesting because PUMA expects such a settlement of the BD could occur during a large storm event, i.e. a storm event of 1:100 years or higher. According to the PUMA relation a settlement of the average crest height of the BD of 0.1 m would already result in 15 % increase in transport.

[m³/y]	Base case	-0.1 m	Increase LT	-0.25 m	Increase LT	-0.4 m	Increase LT
PUMA	968	1137	+15%	1444	+49%	2279	+89%

Table 7.5: Results of computed LT rates for a lowered crest height of the BD.

The placement of the BD after construction was approximately 0.4 meter higher than in the design. Therefore it is of interest to look at the transport rates which theoretically would have occurred, was the design followed precisely. The transports would approximately be 89 % higher, meaning almost a doubling in transport.

Refraction
Next to the wave height reduction, the BD alters the wave angle. PUMA made an approximation of the reduced wave angle of 20% based on visual observations during Scale Model Tests. This reduction in wave angle was never quantified by actual measurements during these tests. The influence of this reduction in wave angle constitutes an approximate decrease of transport rates of 15%.

[m³/y]	Base case	20% refraction	Decrease LT
PUMA	968	823	-15%

Table 7.6: Results of computed LT rates for a reduced wave angle due to the BD of 20%.

7.2.3. Influence storm events
As discussed in Section 7.1 a difference in LT can be the result of a difference in occurred storm events over that period. What also was concluded in Chapter 5, was that a 1:10 year design storm did not occur during the period of 2013-2018. In order to see the effect of a single storm event on computed transport rates, a 1:100 year design storm was put into the calculation model. The exact parameters for the input of the 1:100 year design storm are given in Appendix B. A design storm is put into the calculation for both high and low water levels. Also the design storm for the middle section of the hard sea defence is taken, as this is the slightly higher storm that would occur within the area of interest, according to the PUMA design. For the duration of the storm an approximate of 24 hours is used.

[m³/y]	Base case	LWL Storm	Increase LT	HWL Storm	Increase LT
PUMA	968	1678	+73%	1910	+97%

Table 7.7: Results of computed LT rates as a result of a 1:100 design storm.

What can be seen when the 1:100 year design storm is put into the wave climate, is the severe increase of computed transport rates. This is obtainable from Table 7.7. Logically one would expect such a storm event would result in large transport rates, only now this is also confirmed by the output of both LT relations. With respect to future maintenance it important to be aware such a single storm event can result in large transport rates and therefore large amounts of erosion along the DRS.

7.2.4. Influence sea level rise

In Section 7.1 it was observed PUMA incorporated a sea level rise of + 0.35 m for the situation of 50 years after construction. To see what the sole influence of sea level rise is on the computed transport rates an increase of + 0.35 m of the water level is put into the model and the output is presented in Table 8.7. One observes an increase of 82% in Longshore Transport solely due to a water level increase of 35 cm.

[m3/y]	Base case	+ 0.35 m SLR	Increase LT
PUMA	968	1757	+82%

Table 7.8: Results of computed LT rates as a result of 0.35 m sea level rise.

7.3. Validation of the PUMA relation

Up until this point in this chapter, only assessments on computed LT rates were carried out. For the following sections, i.e. Sections 7.3-7.5, a validation of the PUMA relation will be carried out. New Longshore Transport data of the DRS at Maasvlakte 2 will be introduced. Erosion and accretion volumes along the DRS will be extracted from yearly surveys. The first part of this section will give an explanation on how the yearly transport volumes are retrieved from the corresponding surveys.

The second part of this chapter will present the results on comparing the calculated and observed transport gradients. Through this comparison the ability of the PUMA relations to predict erosion or accretion along the DRS of Maasvlakte 2 will be examined.

7.3.1. Usability of survey data

As the hard sea defence at Maasvlakte 2 is a dynamic structure, maintenance of the DRS requires surveys. These surveys are used by PUMA to assess whether the stone layer of the DRS is maintaining its required thickness. The surveys at Maasvlakte 2 are executed by a LIDAR which is mounted on a small airplane that scans the highest point of an area, therewith creating a surface model. The most accurate surface models, which are used for this research, have a cell size of 0.5x0.5 m, meaning these surface models have an accuracy up to half a meter. In theory it is possible to obtain both transport rates and gradients in transport from these surveys, as will be explained in the following sections.

Over the years many surveys are executed, not only for the hard sea defence of Maasvlakte 2, but also to assess the behavior of the Soft Sea Defence, which is situated to the southwest of the DRS. Multiple aspects of the DRS are surveyed, think of the height of the BD, the settlement of the full hard sea defence and the profile development of the rock slope. This has resulted in a rather extensive database of surface models. Therefore it is important to establish which surface models are usable for the validation of Longshore Transport rates. The usable surveys with corresponding remarks to the foregoing period are given in Table 7.9. When looking at the periods in time between every usable survey, it can be concluded every usable survey has a recurrent period of 10 months or more. Only the period between survey 8/2017 and 4/2018 is half a year.

Year	Month	Action	Usable	Remarks
2013	1	Survey	Yes	
2014	4	Survey	Yes	Period of subsequent surveys longer than one year
2015	4	Survey	Yes	
2016	4	Survey	Yes	
2016	9	NOURISHMENT		Unusable period due to nourishment
2016	10	Survey	Yes	
2017	4	Survey	No	Inaccurate survey
2017	8	Survey	Yes	Period of subsequent surveys shorter than one year
2018	4	Survey	Yes	Period of subsequent surveys half a year

Table 7.9: Time line of usable survey data.

7.3.2. Extracting data from surveys

Now the usable surveys are known, it is possible to analyze transport behavior along the DRS. From the survey imaging it is possible to obtain cross sections for every 0.5 m along the DRS. An example of such a cross section is shown in Figure 7.5. In theory it is possible to retrieve information in two different ways from these cross sections, both of which will be explained separately in the following sections. The first approach would be to assess the actual transport rates. The second approach would be to solely obtain the displaced volumes of stone along the DRS.
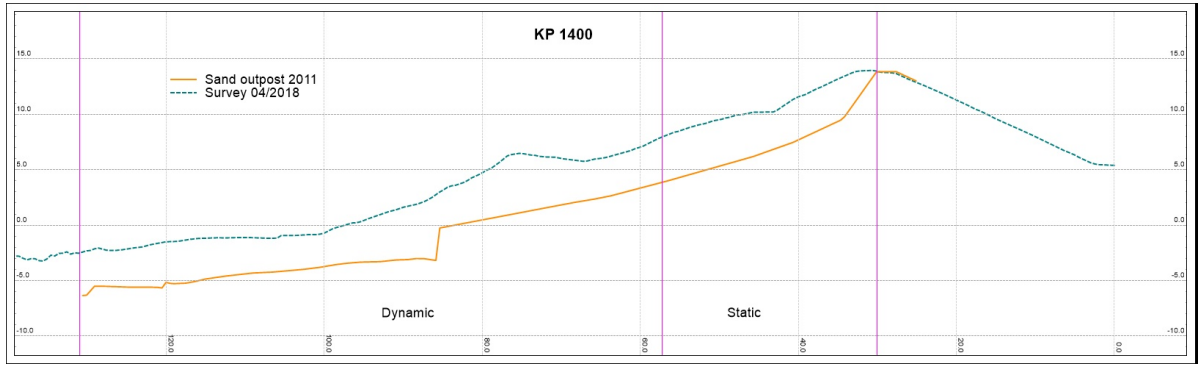
Figure 7.5: Example of a cross section resulting from survey imaging of the DRS at KP 1400.

Obtaining transport rates through volume balance

Would one want to obtain transport rates from survey imaging, a volume balance must be obtained over the consecutive years. In literature, actual transport rates are defined as stones or volumes per unit time that pass an imaginary cross shore line. In order to obtain such transports from the surveys executed at the DRS, a volume balance must be obtained. If no stones would leave the system - which in theory would occur at Maasvlakte 2 due to the Block Dam - a volume balance over consecutive years should be present. If this volume balance is present it is possible to acquire Longshore Transport rates in m^3/s along a cross sectional line. If this cross sectional line is represented by i, the volume ranging from 0 to i, represented by V_1, is computed by taking the summation of these cross sectional areas. A similar approach can be used to obtain V_2. In Figure 7.6, V_1 would be the volume to the left of the cross-sectional line at i and V_2 would be the volume to the right of this line.

$$V_1 = \sum_0^i A \qquad V_2 = \sum_i^n A \tag{7.1}$$

$$\Delta V_1 = V_1^{y1} - V_1^{y2} \tag{7.2}$$

$$Q_1 = \frac{\Delta V_1}{\Delta t} \tag{7.3}$$

In theory one could obtain transport rates by comparing volumes over a certain section with respect to the previous year. Now the difference in V_1 for two consecutive years $y1$ and $y2$, i.e. Equation 7.2, will result in transport of stones over the cross sectional line i during that period of time. The amount of transport Q_1 would then be obtained through Equation 7.3.
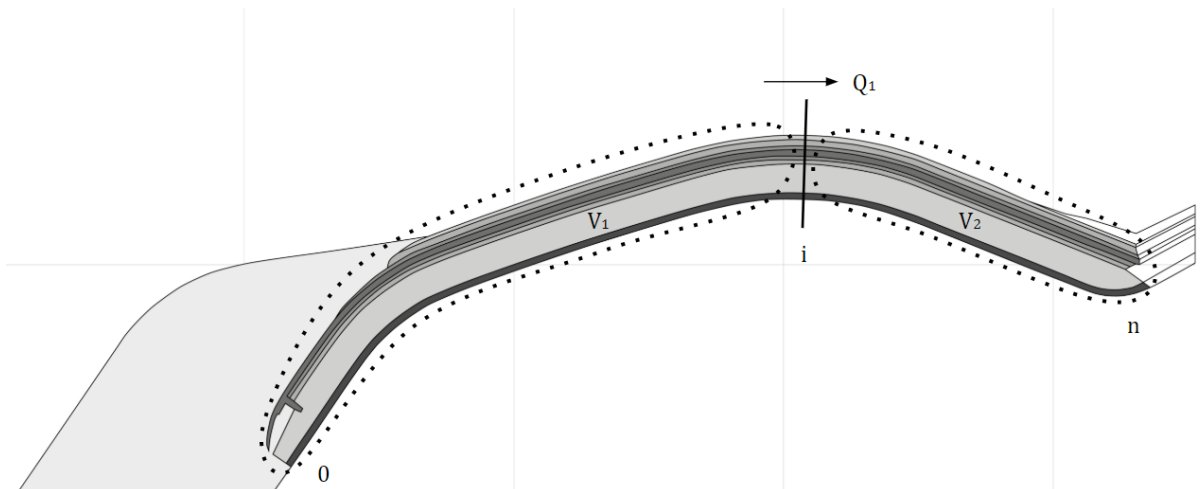
Figure 7.6: Topview of the DRS at MV2 with division of sections in order to obtain transport rates.

The inaccuracies of the surveys at the boundaries 0 and i are the reason why a volume balance is not obtainable through the survey imaging. Transport of sand into the system at the southwestern part of the DRS corrupts the cross shore profile measurements retrieved from survey images. Also the survey images seem not to fully cover the eastern boundary. One would expect to see a growing amount of stones at this eastern boundary, as dominant wave directions are directed easterly. Only as most of the survey imaging is not showing this increase, one must conclude that the survey imaging is inaccurate at the boundaries.

Obtaining displaced volumes
As no volume balance was obtained, the survey imaging was simply used to extract displaced volumes along the DRS. This means an equal approach is used as for the obtainment of the transport rates, only now the displaced volumes per section of a 100 meters along the DRS do not represent actual transport rates. Again a cross shore profile of every 0.5 meter along the DRS is taken, only now the difference in volumes over consecutive years is only obtained per section of a 100 meters along the DRS. In doing so, the volumes that are obtained from the surveys represent the amount of stones which a certain section of a 100 meters lost or gained over that survey period, i.e. accretion or erosion of stones over this section. From this point forward these observed values of accretion or erosion will be used as a reference in order to validate a Longshore Transport relation. Observed volumes of accretion or erosion are the result of a difference in transport over that section of the DRS, as was explained in Section 6.6.

7.3.3. Displaced volumes along the DRS
To obtain volumes of erosion or accretion along the DRS, yearly differences in cross shore profiles are evaluated. A cross shore profile of one year is evaluated with respect to that of the previous year. In doing so the surveys need to be corrected for yearly settlements. PUMA encountered difficulties in establishing the precise settlements at the DRS (Projectorganisatie Uitbreiding Maasvlakte, 2016). PUMA reported that the settlements based on the fly map were most trustworthy, therefore the settlements observed through this technique will be taken here. The different settlements over the years are presented in Table 7.10. An average is taken of the interest area of KP 1800 to 600. PUMA only assessed settlements through the fly map technique for the years of 2013 to 2015. Therefore the settlement over the year 2014-2015 is taken as governing for the following years. The settlement for a period of 386 days, i.e. the period between the fly maps of 2014 to 2015, had an average of 3.7 cm (Projectorganisatie Uitbreiding Maasvlakte, 2015). Now this average settlement is normalized to the periods in time between the surveys of 2014 to 2018.

Period	Settlement [cm]
2013-2014	6.3
2014-2015	3.6
2015-2016	3.5
2016-2017	3.0
2017-2018	2.1

Table 7.10: Average settlements of the DRS along the interest are KP 600 to 1800.

After correcting the different surveys for yearly settlements, transported volumes per section of the DRS can be attained. These accretion or erosion volumes can in a later stadium be compared to calculated gradients in transport over a similar section. Table 7.11 shows the gradients in transport for every section of a 100 metres within the interest area, after the correction for settlements. A negative gradient in transport results in accretion and a positive gradient in erosion. Therefore the addition of stones within a section of 100 meters is indicated in green and as a negative figure. Erosion is indicated in red, which is a result of a positive gradient, i.e. there has been more transport out of the section than has entered.

Whether a section of a 100 meters experiences erosion or accretion can differ significantly per 100 meters. Nevertheless there is a trend to be observed from Table 7.11. Around KP 1300 to 1400 a shift from erosion to accretion seems to be present. This is logically the result of the orientation of the DRS. The part ranging from KP 1800 to KP 1300 has approximately the same orientation with respect to the incoming waves, resulting in an equal amount of Longshore Transport. Nevertheless there is a slight change in orientation, resulting in small amounts of erosion. In the lee side of the bend, approximately the sections KP 1300 to 600, clear accretion of stones is obtained. Obviously the lower wave attack over this part of the DRS, as it lies in the lee

Year	2013	2014	2015	2016	2016	2016	2017	2018
Month	1	4	4	4	9	10	8	4
Section		m^3	m^3	m^3			m^3	m^3
1700-1800		138	84	-231	N		-15	108
1600-1700		-18	68	-214	O		86	192
1500-1600		19	190	-475	U		197	108
1400-1500		-88	230	-529	R		177	54
1300-1400		-74	-517	-81	I		20	19
1200-1300		-312	-504	49	S		-72	-95
1100-1200		-433	-433	-141	H		-35	-215
1000-1100		-328	-419	-59	M		-97	-202
900-1000		-532	-384	-285	E		-104	-169
800-900		-481	-387	-234	N		-55	-102
700-800		-300	-301	-66	T		15	-4
600-700		-426	-197	-178			-107	-34

Table 7.11: Observed transported volumes of stone per 100 m sections along the DRS. Erosion indicated as a positive gradient and accretion indicated as a negative gradient.

of the bend, is the cause for this accretion. It is also observed that the survey years 2013 to 2016 show higher amounts of accretion than the years 2016 to 2018. This can be the result of the time in between consecutive surveys, i.e. the survey periods over the years 2013 to 2016 are longer than that of the periods of 2016 to 2018.

Over the years 2015 to 2016 the trend of erosion over KP 1800 to KP1300 is not obtainable. There mostly accretion can be observed. This accretion can be the result of stones being transported from the section KP 3500 to KP 1800, outside of the interest area, as the data shows erosion over this section. Although this could be an explanation for this deviating trend over the year 2015-2016, the volumes resulting from this year appear to be unreliable and will no longer be used as a reference. The remaining transported volumes which will be used as a reference, resulting from Table 7.11, are visually represented in Figure 7.7. The average amount of transported volumes per 100 meters along the interest area is 197 m^3/y in absolute terms. Here the periods of time over which the observed gradients in transport are retrieved is taken into account.
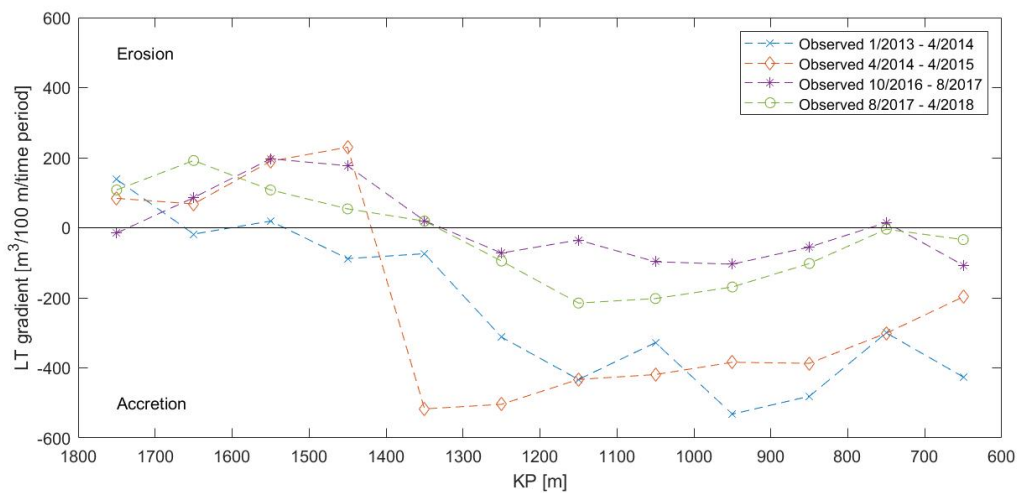
Figure 7.7: Observed gradients in transport per section of 100 metres along the DRS.

7.4. Comparing calculated and observed transport gradients

In Section 7.3.2 it was explained computed transport rates can not be compared to observed transport rates. The survey data is not accurate enough to extract actual transport rates from the imaging. Therefore calculated and observed gradients in transport over a 100 meter section are compared, as these gradients in transport are obtainable from the yearly surveys. As a reminder it needs to be stated that when using the term transport gradient, this is nothing more than a displaced volume of stone, i.e. erosion or accretion along the DRS. In the next section, firstly the computed transport rates over the consecutive survey periods, resulting from computation using the PUMA relation, are presented. Thereafter computed gradients over these periods are compared to the observed gradients, which were retrieved from the survey imaging.

7.4.1. Computed transport rates over a survey period

In order to obtain the transport gradients over the different survey periods, the transport rates for these consecutive periods need to be calculated. To do so the calculation model is used to compute the transport rates over the usable survey periods obtained from Section 7.3.3. As explained, these transport rates are then used to obtain the gradients in transport over every 100 meters along the interest area of the DRS. Important to notice is that for the computation of the transport rates over the survey periods, all parameters are set to the conditions as they were during that survey period. Figure 8.2 shows the output of computed transport rates for the PUMA relation over the four survey periods.

From the computed transport rates one can see that over the section KP 1800 to KP 1300 the differences in transport rates in longitudinal direction are minimal. This will result in minor gradients in transport and thus small volumes of erosion. On the other hand the transport rates drop significantly in the lee side of the bend, i.e. KP 1300 to KP 600. In theory this will result in accretion of stones over these sections.
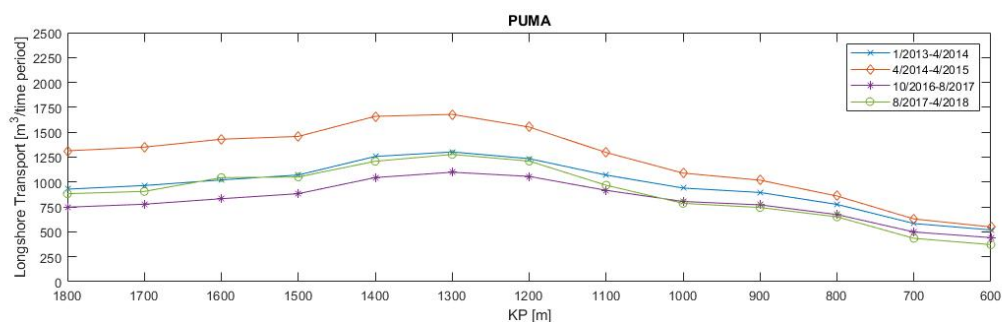
Figure 7.8: Calculated Longshore Transport rates for the PUMA relation over the different survey periods.

What also can be obtained, is the difference in computed transport over a longer period of time. A longer period of time in between two surveys logically results in more hydraulic attack on the slope of the DRS and consequently higher transport rates. The higher amount of hydraulic attack for a longer period of time would in theory be more pronounced over the area KP 1800 to KP 1300 as this area covers the head of the bend. The lee side of the bend, KP 1300 to KP 600 of the interest area, is more protected from the easterly waves. This difference in hydraulic attack can be seen from the computed transport rates as the difference in computed transport rates for different periods of time are more pronounced over the so-called head of the bend than over the lee side of the bend.

7.4.2. Calculated versus observed gradients

In order to validate if the PUMA relation is able to predict erosion or accretion along the DRS at Maasvlakte 2, gradients in calculated transport are compared to the observed erosion or accretion volumes. As explained a gradient in transport over a certain section is a difference in incoming and outgoing amount of stones, resulting in erosion or accretion within this section.

The computed gradients in LT for the PUMA relation are shown in Figure 8.4. As was already observed looking at the transport rates, erosion is computed by the PUMA relation over KP 1800 to KP 1300. On the other hand accretion is computed over KP 1300 to KP 600 of the interest area.
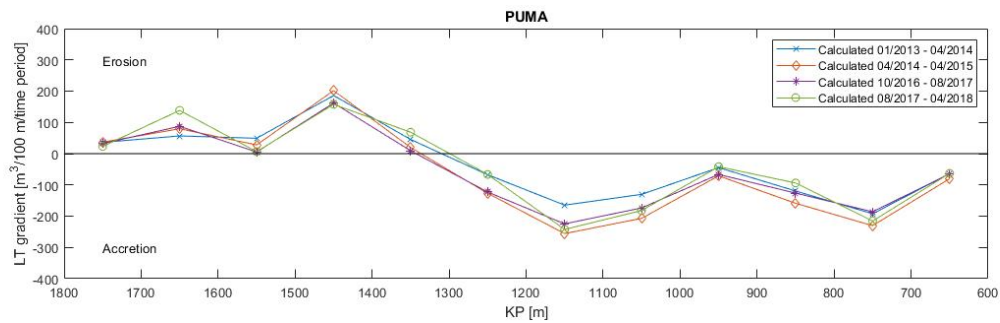
Figure 7.9: Calculated gradients in LT for the PUMA relation.

As was observed from the output of the transport rates, differences in amounts of LT were present over different survey periods. Higher amounts of transport rates would logically result in larger gradients. This difference is noticeable in the output of the gradients, only differences are not very pronounced. This can be the result of small differences in longitudinal direction within the computation of LT gradients. Now, the largest difference over a section of 100 meters is the orientation of the DRS with respect to the incoming waves. Apart from the difference in orientation there are a lot more differing characteristics in longitudinal direction of the DRS, think of a variable BD height, local settlements and a change in water depth behind the BD due to the displacement of cobbles, as it remains to be a dynamic structure. These characteristics can result in local erosion or accretion and are not taken into account in the calculation model.

Now the computed gradients in transport are presented, it is possible to compare these computed gradients in transport for the PUMA relation to the actual occurred transported volumes over the corresponding survey period. In Appendix E the comparison of computed and observed gradients in transport of all survey years are separately presented. For sake of clarity here only the trend in gradients over the different survey years are presented in Figure 7.10.

The agreement on the shift from erosion to accretion along the interest area can be obtained from Figure 7.10. It appears the orientation of the DRS would in theory result in a shift from erosion to accretion around KP 1300. However the observed gradients in transport show a more random shift over the different years. The one year accretion is already present over the section KP 1500 to KP 1400 and the other year accretion starts to occur over the section KP 1300 to KP 1200. This shows that in reality the reason for a stone to be deposited at one place or another along the DRS, is depending on more than only the three forcing parameters used in the PUMA relation, namely wave height, peak period and wave angle.
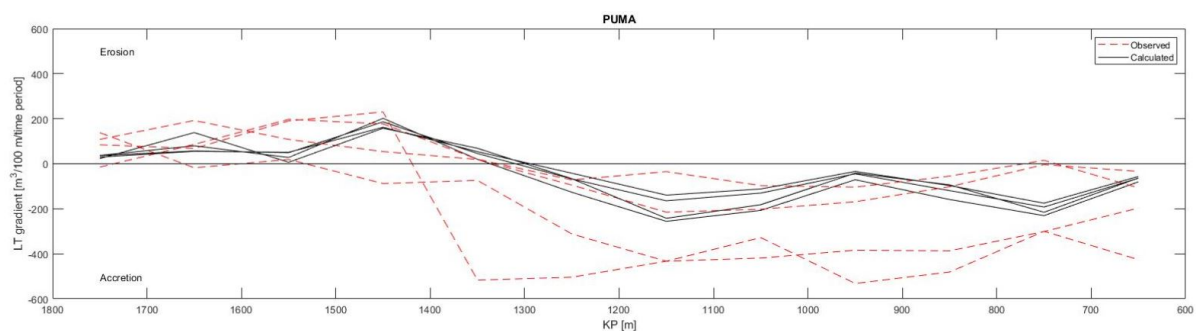
Figure 7.10: Trend in gradients for the PUMA relation.

Figure 7.11 shows the comparison of the computed gradients resulting from the PUMA relation with respect to the observed gradients for the most recent survey period of 10/2017 to 08/2018. This survey period is the shortest out of the four survey periods, making this survey the most reliable. The agreement on whether a section will experience erosion or accretion is one of the best for this survey year, compared to other survey

years.
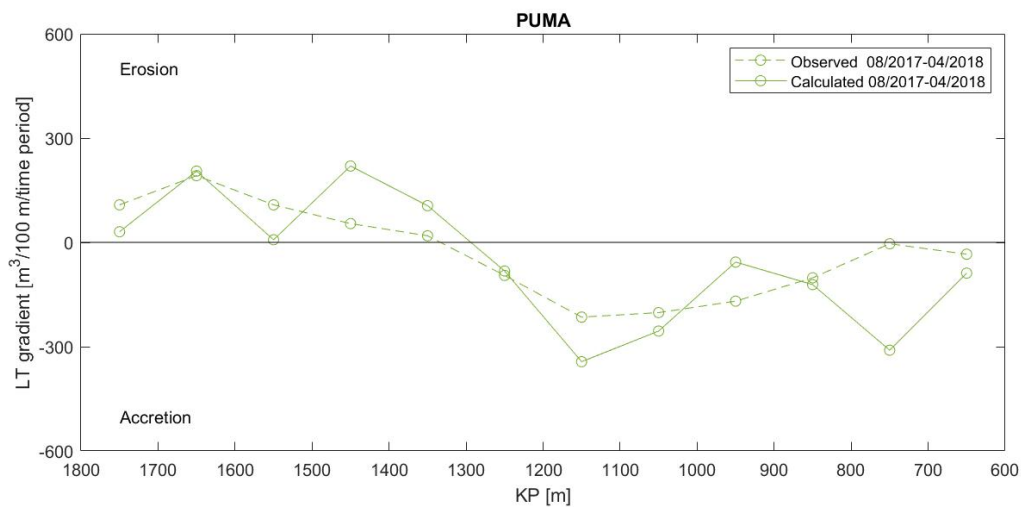
Figure 7.11: Calculated and observed LT gradients over 2017 to 2018 for the PUMA relation.

What can be obtained from the comparison of computed and observed LT gradients of the 2017-2018 survey period, is the general agreement in shift from erosion to accretion along the interest area. The PUMA relation performs well in predicting the volumes of erosion and accretion along the interest area. Keep in mind that for the computed gradients in Figure 7.11 all parameters are set to as they were during this period. Therefore it must be concluded the PUMA relation performs well in predicting Longshore Transport along the DRS. As explained in the foregoing sections of this chapter, circumstantial differences are more likely the cause for the differences in observed transport rates and the calculated transport rates following from the prognosis of PUMA, think of the milder wave climate and a higher placement of the Block Dam.

7.5. Accuracy PUMA relation

Here the ability of the PUMA relation to compute gradients in Longshore Transport along the DRS is quantified. In order to quantify the accuracy of the PUMA relation, observed displaced volumes over a section of a 100 metres are compared to the computed gradients in transport.

As explained a negative gradient in transport results to accretion and a positive gradient in transport to erosion. In order to compare all gradients in transport, these values are used in absolute terms. Along the interest area it was seen there is a shift from erosion to accretion present along the interest area. When comparing computed and observed gradients, the situation can occur were a negative gradient is observed and a positive gradient is computed, or the other way around. In order to take these gradients into account the negative gradient will be taken as a positive gradient and the absolute difference will be added to this positive gradient. In this way the difference between calculated and observed gradients can still be assessed for every computed gradient.

Figure 7.12 shows the calculated versus the observed gradients for the PUMA relation. It appears the accuracy of the PUMA relation is in the order of a factor 2. This means a calculated gradient can be twice as large or two times as small as the observed gradient in transport.
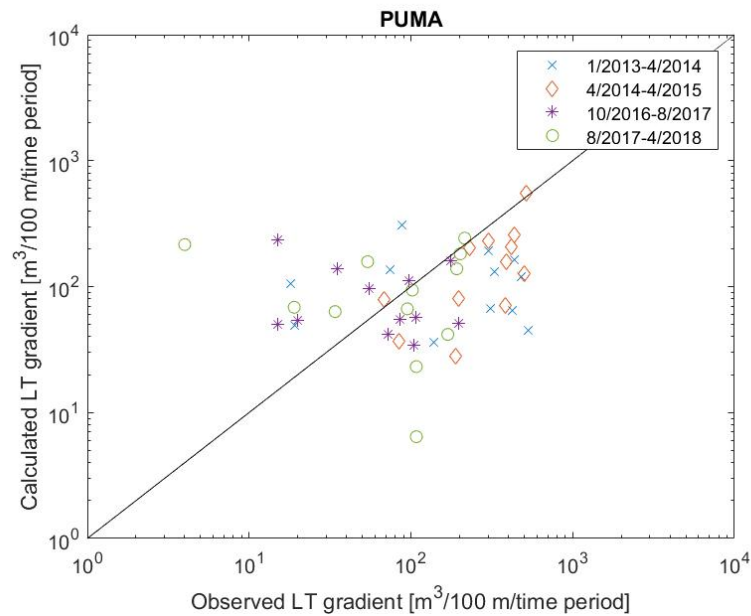
Figure 7.12: Calculated vs. observed gradients in LT for the PUMA relation.

7.6. Conclusions

When comparing the prognosis of PUMA to the computed transport rates over the period of 2013 to 2018, it was seen that the first reason for the lower amount of computed transport rates over this period are differences in wave climate. For the period of 2013 to 2018 the PUMA relation on average computes 32% less transport than the prognosis of PUMA, for which the wave climate of 1979 to 2005 was used. As was already concluded in Chapter 5, the reason for this difference in wave climate is partly due to the less severe storm which occurred over the period of 2013 to 2018. The large influence of storms, containing wave heights higher than 2 meters, on the computation of Longshore Transport showed a milder wave climate is the most probable cause for the lower transport rates over the period 2013 to 2018. The influence of severe storms was also seen for the hypothetical situation of a 1:100 year design storm occurring. By including such a storm into the wave climate, it was seen such a storm would in theory result in an approximate 75% to 100% increase in Longshore Transport.

Next to the milder wave climate over the period 2013 to 2018, differences in foreshore are likely the cause of changes in wave climate for the different periods, as was concluded in Chapter 5. Quantifying the contribution of this difference in output of Longshore Transport, with respect to the contribution of the milder wave climate, was impossible as these differences are incorporated within the wave climate following from the SWAN run. As the impact of storm events on the computation of Longshore Transport is that severe, it is assumed within this thesis that storm events are the governing reason for the difference in wave climate - and thereby the lower computation of Longshore Transport over the period 2013 to 2018 - and not the difference in wave angle.

The second reason for the lower transport rates over the period 2013 to 2018 is the average crest height of the Block Dam in front the Dynamic Rock Slope. On average the crest height of the Block Dam was placed 0.4 meters higher over the interest area than it should have been, was the design followed more accurately. From calculations it follows that the higher placement of the crest height of the BD resulted in half the amount of transport that occurred during 2013 to 2018. In other words, would the design be followed exactly, the amount of transport would approximately be double the amount of transport which is obtained currently.

The last part of this chapter covered the validation of the PUMA relation. A comparison was made between computed erosion and accretion volumes along the DRS over the period 2013 to 2018 following from the PUMA relation and observed displaced volumes over the same period, following from survey imaging. In short the inaccuracies at the outer areas of the DRS resulted in the impossibility of using the surveys for validation of transport rates. Therefore the erosion or accretion of stones per 100 meters were retrieved and are used as a reference for the gradients in transport which actually occurred along the DRS over the period 2013 to 2018. When comparing the occurred erosion and accretion along the DRS with the Longshore Transport computations following from the PUMA relation, it was seen the PUMA relation performs well in predicting the sections over which erosion and accretion occur. Also the magnitude of these displaced volumes of accretion and erosion agreed generally well, only the scatter for different survey periods was large. The accuracy of the PUMA relation appeared to be in the order of ±2 orders of magnitude, meaning a computed gradient in transport can be twice as large or two times as small as the occurred gradient over a particular section of a 100 meters along the DRS.

The validation of the PUMA relation showed that the prediction of erosion and accretion following from the PUMA relation over the period 2013 to 2018 generally resulted in a good fit with the actual occurred erosion and accretion along the interest area. The lower transports over this period are therefore more so the result of the circumstances over the period of 2013 to 2018 than the predictive abilities of the PUMA relation, i.e. the presence of a difference in wave climate and the higher placement of the Block Dam are the cause for the lower observed transport rates over the period 2013 to 2018 and not the computation of Longshore Transport following from the PUMA relation.

7.7. Discussion

The division of parts within this Chapter is equally followed within this discussion. The three consecutive sections are treated below.

Prognosis PUMA

A minor remark must be made on the average of LT which was computed within the prognosis of PUMA. The average computed LT over the interest area for the PUMA prognosis was obtained visually from Figure 7.1. Although it is clearly seen this is an approximate of 12.000 tonnes/year, this number is not exact. This can result in small differences in the comparison of the computed LT for both wave climates. It is expected this approximation is within a range of ±250 tonnes/years, which is only 2% of 12.000 tonnes/year.

Influence governing parameters

With respect to the sensitivity analysis on the computation of Longshore Transport rates for differing parameters, it must be stated that the effect of the different parameters is solely based on calculations. This means only hypothetical situations are assessed, as there are no scale model test results or field measurements available to back these calculations.

Validation of PUMA relation

The presented data on displaced volumes in this chapter are used as a reference for the actual transports occurred at the DRS over the past five years. When doing so, it is important to keep in mind the inaccuracies which arose during the extraction of data from the survey imaging. The displaced volumes along the DRS were corrected for yearly settlements. Although these yearly settlements are in the order of centimeters, the impact on extracted volumes over such a large surface area as that of the DRS is quite significant. A deviation in settlement of 1 *cm* over a year can lead to a difference of ±75 m^3/y in transported amount of stones per section of a 100 meters along the DRS. This means a deviation of ±38% of the observed average transported volumes per 100 meters.

Results General Longshore Transport relation

Next to the predictions the PUMA relation generates, the transport rates computed by the General Longshore Transport (GLT) relation can be assessed. This chapter discusses the results concerning the computation of transport rates following from the GLT relation. In general this chapter is built up out of two parts:

- The first part of this chapter, Sections 8.1 and 8.2, covers the theoretical performance of the GLT relation in comparison to the PUMA relation. Here solely theoretical computed transport rates are discussed.

- The second part of this chapter comprises over Sections 8.3 and 8.4. Similar to the validation of the PUMA relation, calculated gradients in transport following from the GLT relation are compared to observed gradients in transport.

8.1. Theoretical performance of the GLT relation

The computed LT rates for both LT relations can be compared in order to assess the difference in computed transport rates. Important to notice is that the computed transport rates are following from computations using all the input parameters as they occurred during the last 5 years, which can be observed from Table 8.1. This means the average BD height is set to 3.26 m + NAP including the yearly settlement, as explained in Chapter 6. Also the wave climate of 2013 to 2018 is used, containing the hourly forcing parameters H_s, T_p, β and water level.

Figure 8.1 shows the computed transport rates over the interest area KP 1800 to KP 600 for both the PUMA and the GLT relation. The grey lines show the yearly transport rates for both relations and the dashed red line is the average over the 5 years.

What can be obtained from the computed transport is that both relations predict similar amounts of transport per KP over the years. The GLT relation computes slightly lower transport rates with respect to the PUMA relation. This agreement on computed transport rates is remarkable as this means the non-dimensional GLT relation of Tomasicchio performs equally in predicting Longshore Transport rates at the DRS as the dimensional formula of PUMA, which was specifically calibrated for the DRS at Maasvlakte 2.

	Base case
LT relation	GLT
Wave climate	2013-2018
SLR	×
c_{avg} BD	2013-2018

Table 8.1: Input parameters for the computation of transport rates over the period 2013 to 2018.

The theoretical performance of the GLT relation at a breakwater with characteristics of a Dynamic Rock Slope was already assessed through analysing the data resulting from the scale model tests of Wallingford. This was discussed in Chapter 4. There it was observed that for scale model tests the GLT relation was able to predict LT for a DRS, although being it with an underestimation. The LT rates computed by the GLT relation as a result of wave data now show the GLT relation is also applicable on the DRS at Maasvlakte 2.

Although there is a general agreement between the both relations in computing transport rates at the DRS of MV2, there is a difference obtainable. When averaging the computed transports over the interest area,
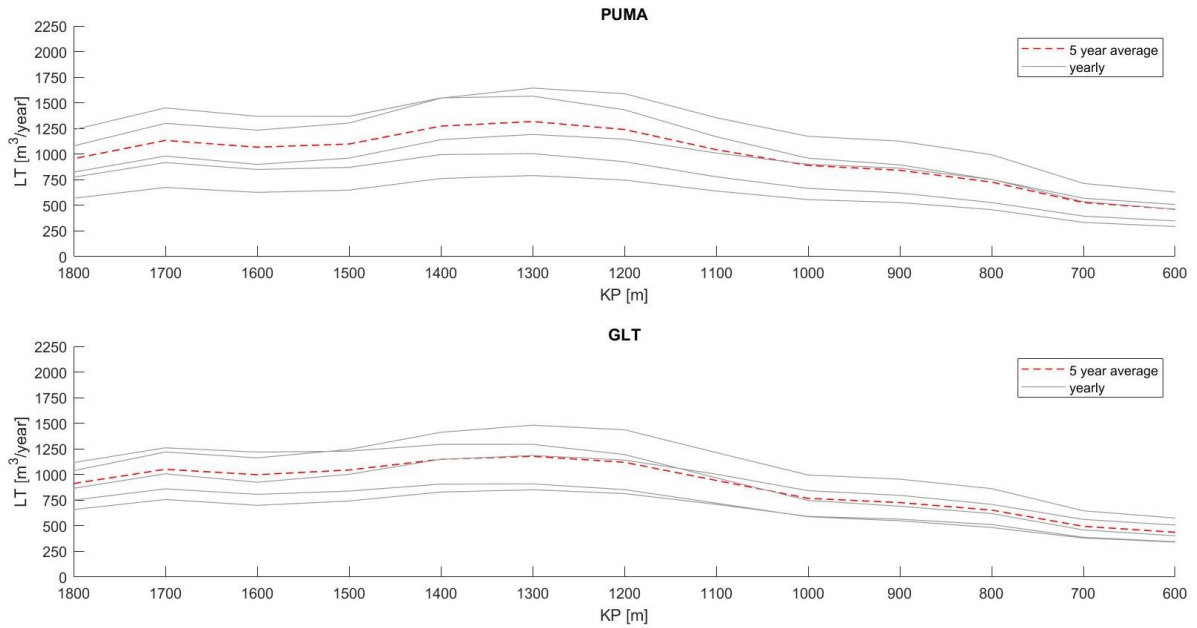
Figure 8.1: Calculated LT along the DRS for the PUMA and GLT relation.

the PUMA relation gives an average transport of 968 m^3/y. The GLT relation in its turn computes an average transport of 863 m^3/y, as can be obtained from Table 8.2. The GLT tends to compute lower transports than the PUMA relation. The approximate difference between the two relations in their prediction of LT rates over the period of 2013 to 2018 comes down to 9%.

PUMA	968	m^3/y
GLT	883	m^3/y
Difference	-9%	

Table 8.2: Average computed LT over the past 5 years for the PUMA and GLT relation.

8.2. Influence governing parameters on GLT relation

Similar to the PUMA relation in Chapter 7, it is possible to quantify the influence of different parameters on the computation of Longshore Transport following from the GLT relation. Again a reference situation is needed. This reference situation represents the computed transport rates for the period of 2013-2018 resulting from both LT relations, as they are presented in Section 8.1. This reference situation is called the base case, as was done before, and is again presented in Table 8.3. This base case represents the Longshore Transport that actually occurred during the last five years according to the different LT relations. A similar analysis of the influence of governing parameters can be carried out, as was done for the PUMA relation, only now it is possible to assess the performance of the GLT relation with respect to the PUMA relation in computing transport rates for different situations.

[m^3/y]	Base case
PUMA	968
GLT	883
Difference	-9%

Table 8.3: Average computed LT over the past 5 years for both relations.

8.2.1. Influence Block Dam

Again the influence of the Block Dam is assessed by means of altering two governing parameters, being the average crest height of the Block Dam and the extra refraction the Block Dam supposedly would generate. Both of these influences are assessed separately below.

Average crest height

The agreement between the both relations could be the result of the reduced transmitted wave height . As explained the Block Dam in front of the DRS reduces the wave height significantly. The overall average of the transmitted wave height $H_{s,t}$ is equal to 0.13 m. This average is taken over the full 5 years of wave data and over the interest area of the DRS. When comparing the transmitted wave height with the overall average of the wave height at the toe of the DRS, which amounts to 0.84 m, one obtains a reduction of 84%. Due to this reduction the wave height could become a less important factor within both LT relations, resulting in less differences in computed transports between the two relations.

To show the reduction of the wave height is not the reason for the agreement between the two relations, the average height of the BD is subsequently lowered by 0.1, 0.25 and 0.4 meters. For each situation the transport rates are then computed for both relations. When the average BD height is lowered, the transmitted wave heights will be less affected by the BD. This will logically result in higher transmitted wave heights and higher transport rates. The output on Longshore Transport rates for both relations is presented in Table 8.4. It appears the GLT relations computes generally lower transports for the different situations of a lowered crest height, i.e. the wave height plays a slightly larger role when it comes to the PUMA relation than for the GLT relation. Nevertheless this difference is marginal, as the increase in Longshore Transport is relatively large.

[m³/y]	Base case	-0.1 m	Increase LT	-0.25 m	Increase LT	-0.4 m	Increase LT
PUMA	968	1137	15%	1444	49%	1825	92%
GLT	883	1025	14%	1279	45%	1592	88%
Difference	-9%	-10%		-11%		-13%	

Table 8.4: Results of computed LT rates for a lowered crest height of the BD.

Refraction

Here the influence of the extra refraction, which would be present according to PUMA, due to the BD is assessed. As a result of visual observations of PUMA during scale model testing, PUMA stated the BD would generate 20% more refraction (Projectorganisatie Uitbreiding Maasvlakte, 2009). The influence of this reduction in wave angle constitutes an approximate decrease of transport rates of 15-20 %, according to both LT relations. This is presented in Table 8.5. For the GLT relation the computed transport decreases more than the transport for the PUMA relation. It appears the GLT relation takes the wave incidence more into account than the PUMA relation does.

[m³/y]	Base case	20% refraction	Decrease LT
PUMA	968	823	-15%
GLT	883	714	-19%
Difference	-9%	-13%	

Table 8.5: Results of computed LT rates for a reduced wave angle due to the BD of 20%.

8.2.2. Influence storm events

As discussed in Chapter 7, a difference in LT can be the result of a difference in occurred storm events over that period. Here a similar run for both the GLT and PUMA relation is carried out as was executed in Section 7.2.3. A one in hundred year design storm is put into the wave climate and transport rates are computed. This is done for both a situation of a 1:100 year design storm consisting of low water levels and one for high water levels. The exact parameters for both design storms are obtainable from Appendix B. The computed transport rates for the GLT and PUMA relation are presented in Table 8.6.

[m³/y]	Base case	LWL Storm	Increase LT	HWL Storm	Increase LT
PUMA	968	1678	73%	1910	97%
GLT	883	1522	72%	1648	87%
Difference	-9%	-9%		-14%	

Table 8.6: Results of computed LT rates as a result of a 1:100 design storm.

What is obtainable from Table 8.6, is the severe increase of computed transport rates for both storms. Remarkable is that for a low water level storm the increase in computed LT is approximately similar for both the PUMA and GLT relation. Apparently the combination of wave height, peak period and wave incidence for a low water level storm have similar Longshore Transport to effect for both LT relations. Only the influence of water level within the high water level storm constitutes a significant difference between the computation of LT rates of the PUMA and the GLT relation.

8.2.3. Influence sea level rise

Here the sole influence of sea level rise is assessed. This is done by increasing the water level by + 0.35 meters, as this is the sea level rise PUMA took into account for the coming 50 years. When using this amount of sea level rise as input for computations of LT for the GLT relation, it is seen the GLT relation is less sensitive for this increase in water level. The GLT relation computes less Longshore Transport compared to the PUMA relations, as can be seen from Table 8.7.

[m³/y]	Base case	+ 0.35 m SLR	Increase LT
PUMA	968	1757	73%
GLT	883	1379	56%
Difference	-9%	-22%	

Table 8.7: Results of computed LT rates as a result of 0.35 m sea level rise.

8.3. Validation of the GLT relation

In the foregoing sections of this chapter it was shown the GLT relation is in theory capable of predicting similar amounts of LT, although being it with a lower approximation of 9% for the period of 2013 to 2018. Now it is possible to compare computed volumes of erosion or accretion to the actual occurred transported volumes along the DRS. In doing so, a similar validation is carried out as was done for the PUMA relation in Sections 7.3-7.5.

In Section 7.3.2 it was explained computed transport rates can not be compared to observed transport rates. The survey data is not accurate enough to extract actual transport rates from the imaging. Therefore calculated and observed gradients in transport over a 100 meter section are compared. First the computed transport gradients over the consecutive survey periods following from the GLT relation are presented in the next section. Thereafter computed gradients over these periods are compared to the observed gradients resulting from the survey imaging, i.e. the displaced volumes per 100 meters along the interest area obtained in Section 7.3.3 of this report.

8.3.1. Computed transport rates over a survey period

Figures 8.2 and 8.3 show the computed transport rates for the PUMA and the GLT relation over the different survey periods. The computed transport rates for both relations again show a similar amount of transport for the same periods. In Section 8.1 of this chapter it was seen the GLT relation computed on average 9% lower transport rates over the last five years. This lower estimation of transport rates by the GLT relation is equally obtained when computing transport rates over the different survey periods.
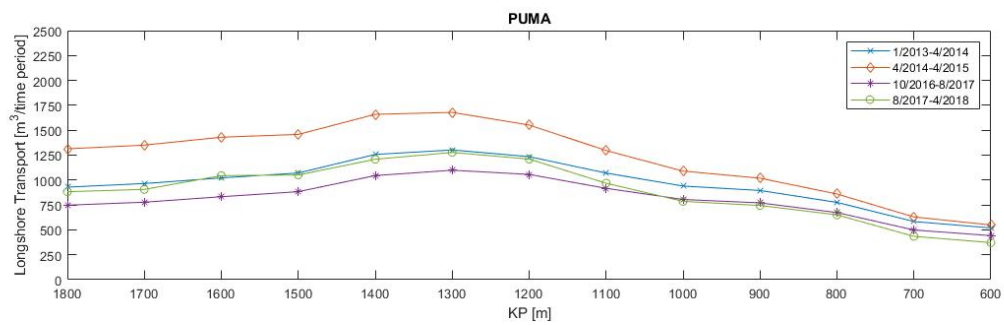
Figure 8.2: Calculated Longshore Transport rates for the PUMA relation over the different survey periods.
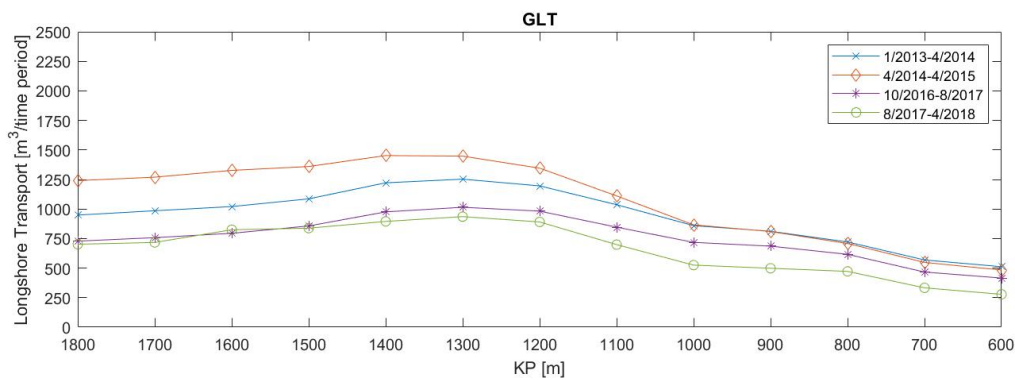
Figure 8.3: Calculated Longshore Transport rates for the GLT relation over the different survey periods.

8.3.2. Calculated versus observed gradients

In order to validate if the GLT relation is able to predict erosion or accretion along the DRS at Maasvlakte 2, gradients in calculated transport are compared to the observed erosion or accretion volumes. As explained a gradient in transport over a certain section is a difference in incoming and outgoing amounts of stones, resulting in erosion or accretion within this section.

The computed gradients in LT, following from the computed transport rates in Section 8.3.1, of both relations are presented in Figures 8.4 and 8.5. When looking at both figures it appears erosion is equally computed by the GLT relation as for the PUMA relation over KP 1800 to KP 1300. Computed erosion volumes are generally lower for the GLT relation than for the PUMA relation. On the other hand the accretion volumes, which are computed over KP 1300 to KP 600 of the interest area, are in the same order of magnitude for both the GLT and the PUMA relation.
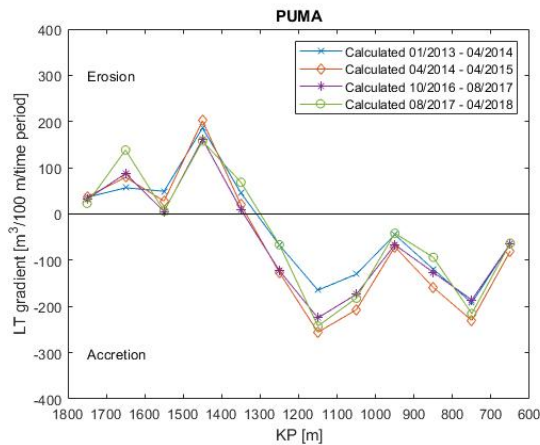
Figure 8.4: Calculated gradients in LT for the GLT relation.
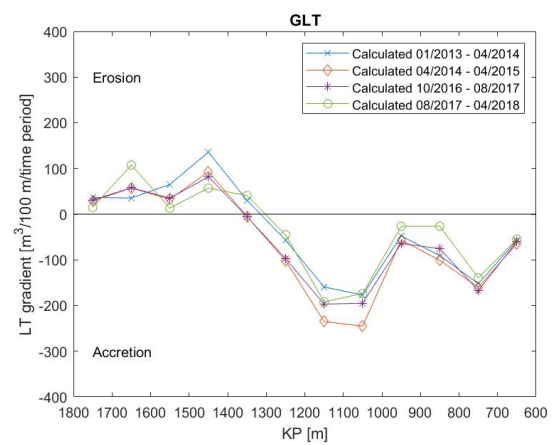
Figure 8.5: Calculated gradients in LT for the GLT relation.

Now a similar comparison of the computed transport gradients in LT with respect to the observed transport gradients can be made, as was done in Chapter 7 for the PUMA relation. Figure 8.6 shows the trend of the gradients in LT for both the PUMA and GLT relation.
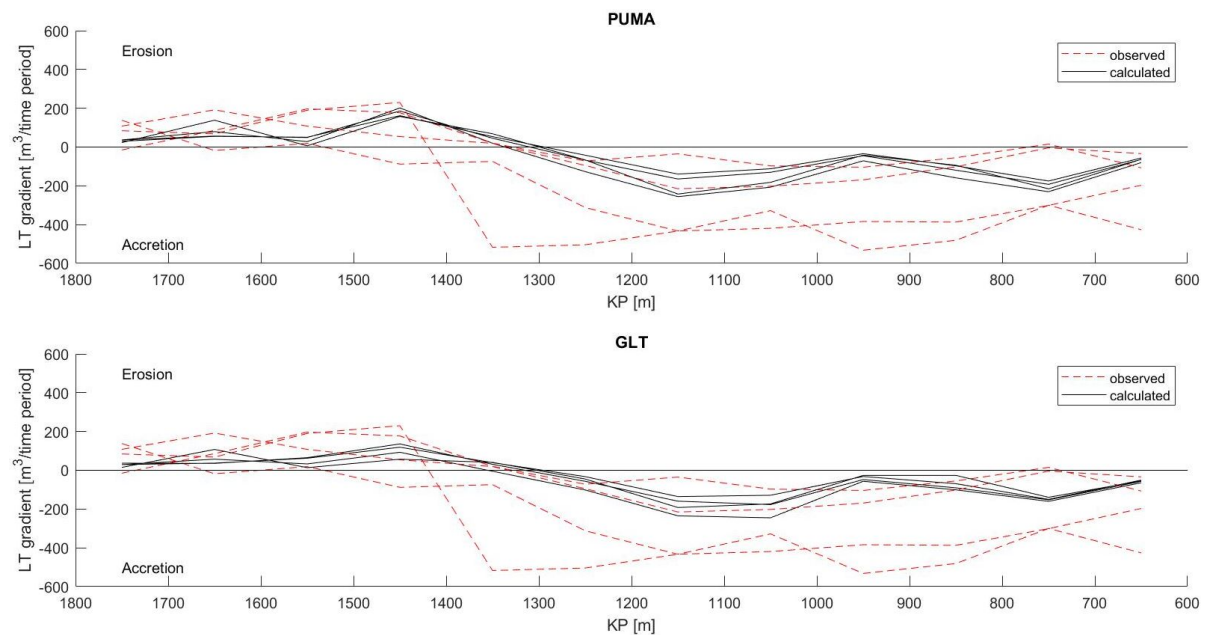
Figure 8.6: Trend in gradients of Longshore Transport for the PUMA and GLT relation.

Again it is obtained both relations perform generally well in predicting erosion along KP 1800 to KP 1300 and accretion along KP 1300 to KP 600. Also obtainable is the ability of both relations to predict the magnitudes of erosion over the different survey periods. With respect to the prediction of accretion, there are differences in fit for different survey periods. Over two survey periods, both relations are very precise in computing accretion and for two other years the occurred accretion seems to be relatively larger than computed values. As explained in Chapter 7 this is probably due to local differences along the DRS which cause stones to accrete. These local differences are not taken into account within both Longshore Transport relations.

In Appendix E the comparison of computed and observed gradients in transport of all survey years and for the both relations are presented. For sake of clarity here only the comparison of the computed gradients of the GLT and PUMA relation with respect to the observed gradients for the most recent survey period of 10/2017 to 08/2018 is presented. This comparison is presented in Figure 8.7. Similarly as for the PUMA relation - observed in Section 7.4.2 - the fit for the GLT relation is remarkably good for this survey period. This implies the GLT relation has similar predictive capabilities as the PUMA relation does.
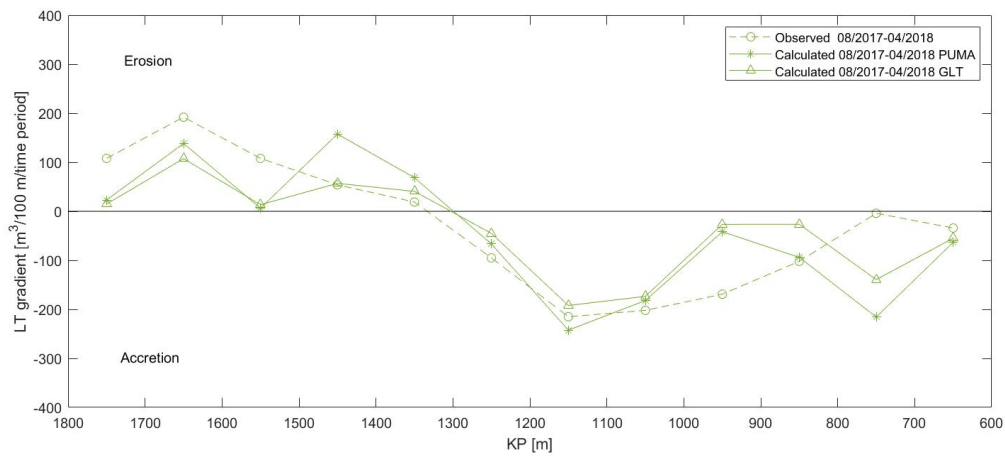
Figure 8.7: Observed LT gradients over 2017 to 2018 versus computed LT gradients for the PUMA and GLT relation.

8.4. Accuracy GLT relation

When one would make use of the GLT relation in a new DRS design it is of interest to know how it performed on different cases. In this research the survey data of the DRS of Maasvlakte 2 is used as a validation of the transport gradients. To quantify the performance of the GLT with respect to the PUMA relation, here the accuracy of the two LT relations is discussed.

Figures 8.8 and 8.9 show the calculated versus the observed gradients for both the PUMA and the GLT respectively. It appears the accuracy of the PUMA and GLT relation is approximately similar. Both figures show calculated transport gradients are computed within a range of approximately a factor 2. This means a calculated gradient can be twice as large or two times as small as the observed gradient in transport. This holds for both LT relations.
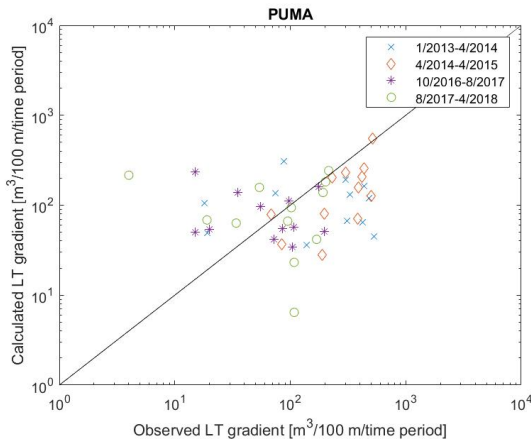
Figure 8.8: Calculated vs. observed gradients in LT for the PUMA relation.
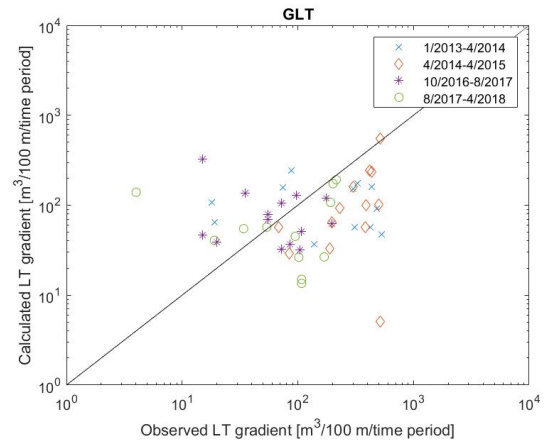
Figure 8.9: Calculated vs. observed gradients in LT for the GLT relation.

In Sections 8.3-8.2 it was seen that on average the GLT relation computes lower transports than the PUMA relation does for similar hydraulic forcing. The same was observed in the previous section. As the PUMA relation computes higher transport rates over the different periods than the GLT does, it is to be expected the gradients in computed transport are lower for the GLT relation. This underestimation of gradients in LT by the GLT relation is not seen when comparing Figures 8.8 and 8.9. Both relations seem to underestimate and overestimate LT gradients a similar amount of times. In other words the 9% difference in computed transport rates for both relation over the period 2013 to 2018 is not seen when comparing transported volumes along the DRS to computed transport gradients. Therewith, both the PUMA and the GLT relation appear to have the same performance in computing gradients in Longshore Transport along the Dynamic Rock Slope of Maasvlakte 2 for the period of 2013 to 2018.

8.5. Conclusions

This chapter shows the non-dimensional General Longshore Transport relation of Tomasicchio et al. (2016) is able to compute similar amounts of transport as the PUMA relation does, being it for the specific case of the Dynamic Rock Slope of Maasvlakte 2 and for the period 2013 to 2018. When averaging over the five years and over the interest area, the GLT relation computes approximately 9% less transport with respect to the computed transport rates following from the PUMA relation.

In order to obtain the influence of different parameters on the computation of transport rates for the GLT relation, hypothetical situations were used as input of the calculation model. When looking at the influence of these governing parameters on the output of computed transport rates one obtains the GLT relation computes transport rates for different situations up to 15% lower than the PUMA relation. Only for the influence of sea level rise, i.e. the sole influence of a water level increase, the GLT relation computes significantly lower transport rates in comparison with the PUMA relation. This difference in computed transports amounts to 22%.

As the GLT relation apparently computes similar Longshore Transport rates as the PUMA relation does for the period of 2013 to 2018, it is seen the GLT relation computes similar volumes of erosion and accretion as the PUMA relation does for this period. Therefore it is concluded within the validation of the GLT relation that it performs equally in predicting erosion or accretion along the interest area of the DRS as the PUMA relation does over the period 2013 to 2018. Both Longshore Transport relations show an accuracy in the order of a factor 2, meaning a computed gradient in transport can be twice as large or two times as small as the observed gradient over that section along the DRS.

8.6. Discussion

Within this chapter the ability of the GLT relation to predict Longshore Transport at the Dynamic Rock Slope of Maasvlakte 2 is assessed. For the computation of the transport following from the GLT relation, a similar computation model - discussed in Chapter 6 - is used as for the PUMA relation, . Therefore all uncertainties which arise when using the calculation model, as explained in Section 6.8, will also apply when calculating Longshore Transport by use of the GLT relation.

On a more general note it must be stated that all conclusions drawn within this chapter that concern the use of the GLT relation, are done for the case of the Dynamic Rock Slope at Maasvlakte 2. Therefore all conclusions drawn within this research are the result of computations resulting from characteristics of this specific case of Dynamic Rock Slope. This special case of Dynamic Rock Slope comprises of the unique Block Dam, which was constructed in front of it. Influences following from this Block Dam have a large effect on the computation of Longshore transport, as was shown throughout this research. The presence of this Block Dam makes it uncertain how the GLT relation performs when applied on a case of Dynamic Rock Slope which does not include a Block Dam.

9

Conclusions and recommendations

In this chapter the final conclusions of this research are presented and recommendations for further research are proposed.

9.1. Conclusions

Here the general conclusions on this research are given by answering the three different research questions. These research questions were set in order to reach the objective of this research. The objective for this research was stated as follows:

> *Analyse where differences in predicted and observed transport rates come from and assess if it possible to validate a non-dimensional relation which describes Longshore Transport at the Dynamic Rock slope of Maasvlakte 2.*

In order to reach the set objective a separate answer on the three research questions is formulated below.

1. Can wave and survey data of Maasvlakte 2 show where the differences in predicted and observed transport rates at the Dynamic Rock Slope at Maasvlakte 2 come from?

PUMA made a prognosis on Longshore Transport at the Dynamic Rock Slope (DRS) of Maasvlakte 2 for the following 50 years after construction. This prognosis was based on calculations resulting from the wave climate of 1979 to 2005. When comparing this historic wave climate to the wave climate of the period 2013 to 2018, it was observed a difference in wave climate has been present. The storm events over the recent data showed less severe storms occurred during the years 2013 to 2018. The period of 2013 to 2018 consisted of approximately 1:5 year storm events, making it a relatively mild period. Computed transport rates show that the wave climate of 2013 to 2018 alone computes 32% less transport over the interest area. The result of this milder wave climate is partly the reason for the lower amount of transport rates computed for the period of 2013 to 2018 with respect to the prognosis of PUMA, for which the wave climate of 1979 to 2005 was used.
A second cause for the lower transport rates over the recent period is the higher placement of the Block Dam in front of the DRS. On average the concrete blocks, out of which the Block Dam in front of the Dynamic Rock Slope consists, were placed approximately 0.4 metres higher along the interest area, than originally was proposed in the design. The average crest height of the Block Dam has a large influence on transport rates along the DRS, as was shown by computing Longshore Transport rates for different situations of average crest heights of the Block Dam. Based on computations following from the hypothetical situation of a lowered Block Dam it was shown transport rates would approximately be 2 times larger, was the design followed exactly.

Through survey data of the DRS at Maasvlakte 2 a validation was executed on the PUMA relation. This validation was done by comparing computed erosion and accretion volumes for the PUMA relation over the period 2013 to 2018 to actual observed displaced volumes along the DRS over this period. In order to compute the erosion and accretion volumes over the period 2013 to 2018, all influencing parameters were set to the situation as they occurred during these five years. It was shown the PUMA relation is able to compute the areas over which erosion or accretion occurs generally well. This fit of the PUMA relation therefore shows that the reason for the differences in Longshore Transport over the period 2013 to 2018 with respect to the prognosis of PUMA are circumstantial, meaning the presence of a mild wave climate and the higher placement of the Block Dam are the cause for the presently lower observed transports over the period 2013 to 2018 and not the predictive abilities of the PUMA relation.

2. Is there a non-dimensional Longshore Transport relation which is able to describe Longshore Transport at the Dynamic Rock Slope of Maasvlakte 2?

The Longshore Transport relation PUMA specifically calibrated for the Dynamic Rock Slope at Maasvlakte 2, is a dimensional relation. This means this relation is only applicable for the characteristics found at the DRS of Maasvlakte 2. Would one want to design a new Dynamic Rock Slope, the PUMA relation becomes inapplicable. Therefore it was investigated if a non-dimensional relation exists which is able to describe Longshore Transport at the DRS of Maasvlakte 2. In order to calibrate the PUMA relation, HR Wallingford executed scale model tests on Longshore Transport (HR Wallingford, 2007a)(HR Wallingford, 2007b)(HR Wallingford, 2009c)(HR Wallingford, 2009d). By means of the results of these tests it was shown in this research that the General Longshore Transport (GLT) relation of Tomasicchio et al. (2016) is able to predict the Longshore Transport rates following from the Wallingford tests.

When looking at the case of the DRS at Maasvlakte 2 for the period of 2013 to 2018, it was concluded that the GLT relation is able to predict Longshore Transport rates in the same order of magnitude as the PUMA relation. On average the GLT shows a lower estimation of computed transport rates of approximately 9% with respect to the PUMA relation over the period of 2013 to 2018. Together with the ability of predicting Longshore Transport at the Wallingford tests this shows the GLT relation is able to predict Longshore Transport at a Dynamic Rock Slope.

3. Is it possible to validate a relation which describes Longshore Transport of stones at the Dynamic Rock Slope of Maasvlakte 2?

In order to assess if both the PUMA and GLT relation are capable of computing Longshore Transport along the DRS over the period of 2013 to 2018, a comparison was made between computed transport rates and actual occurred transport rates along the Dynamic Rock Slope at Maasvlakte 2. It was concluded actual transport rates were not retrievable from the survey imaging of the DRS, therefore gradients in Longshore Transport were assessed. These gradients in Longshore Transport represent displaced volumes of stone along the DRS. From the comparison of the computed displaced volumes, following from both the PUMA and GLT relation, to the actual displaced volumes of stone along the DRS over the period 2013 to 2018, it was seen both relations are equally able to predict erosion or accretion along the interest area of the DRS.

When quantifying the predictive abilities of the Longshore Transport relations, it was seen the scatter between computed and observed displaced volumes was large. Even though both relations perform well in predicting the sections along the interest area of the DRS where erosion or accretion will occur, predicting the magnitude of this erosion or accretion appeared to be more difficult for one survey period to another. Nevertheless it was shown the accuracy of both relations is in the order of a factor 2. Herewith it is concluded both the PUMA relation and the General Longshore Transport relation are validated for the case of the Dynamic Rock Slope at Maasvlakte 2.

9.2. Recommendations

The recommendations of this research are divided into recommendations regarding the Longshore Transport behavior of the Dynamic Rock Slope at Maasvlakte 2 and recommendations for further research.

9.2.1. Recommendations regarding the Longshore Transport behavior of the Dynamic Rock Slope at Maasvlakte 2

- **Acquire more field data on Longshore Transport along the DRS of Maasvlakte 2**
  In this study it was a limiting factor that no actual data on processes behind the Block Dam were available. Would one want to obtain more insight in the actual physical processes leading to Longshore Transport behind the BD, a field test is recommended. Such a field test would preferably be set-up during a storm. When executing such a field test at the DRS, it would be of interest to measure the forcing parameters for Longshore Transport behind the BD. When one would simultaneously measure the alongshore current and actual Longshore Transport during this storm more insight in the processes which lead to Longshore Transport at the DRS of Maasvlakte 2 could be gained. This insight could consequently be used to update the maintenance plan for the DRS.

- **Investigate the effect on Longshore Transport due to the change in wave climate resulting from the morphodynamically active foreshore**
  In Chapter 5 it was observed a difference in nearshore wave climate was present when comparing the wave data over the period 1979-2005 to the period of 2013-2018. It was concluded the difference in wave angle over the different data sets was probably due to change in foreshore of the Dynamic Rock Slope. The effect on the computation of Longshore Transport due to this difference in wave angle - resulting in this difference in wave climate - was not quantified within this research. Therefore it is recommended to investigate which amount the difference in wave angle has on Longshore Transport with respect to the difference in wave climate due to the milder occurred storms.

- **Continuation of a pragmatic approach in maintaining the DRS at Maasvlakte 2**
  Currently the maintenance plan of the DRS at Maasvlakte 2 consists of stone nourishments which are executed every 2.5 years. Yearly an approximation is done on the loss of stone over different sections along the DRS in order to determine where these nourishments are required. This is a rather pragmatic approach as smaller volumes of stone will be nourished if this is possible, and vice versa larger volumes when required. It is advised to maintain this pragmatic approach, only to be aware that there might come a year when more extensive maintenance is required. As it was shown in this research, a singular storm event can directly cause large transport rates, subsequently resulting in larger erosion along the DRS, thereby requiring extensive maintenance. Next to this direct effect of a singular storm, it is expected that such a single storm event can cause a settlement of the Block Dam in front of the DRS. Such a settlement will have a lowered average crest height to effect. A lowered average Block Dam height will indirectly cause higher transport rates over the years following this storm event. Therefore it is advised to monitor the effect of such a storm event and to be prepared for extensive maintenance would this be necessary.

9.2.2. Recommendations for further research

- **Scale model tests with N_s^{**} in DRS section**
  In this research the performance of the GLT relation on the Wallingford test was investigated. The corresponding updated stability numbers of these tests showed the Longshore Transport of the Wallingford tests represented transport at a gravel or sand beach. In order to create more certainty on how the GLT relation performs for a Dynamic Rock Slope, a scale model test would be needed. This scale model test needs to be set-up in such a way that the stability numbers fall in the area of a Dynamic Rock Slope for the updated stability numbers N_s^{**}.

- **Validation of the GLT relation on a DRS which does not include a Block Dam**
  As was obtained in this research, the Block Dam influences the hydraulic forcing severely. This specific case of a Dynamic Rock Slope including a Block Dam introduces large uncertainties within the computation of Longshore Transport. Therefore it is recommended to assess the performance of the GLT

relation on a case of a Dynamic Rock Slope which does not include a Block Dam.

- **More field test data needed for the calibration of design formulas for dynamic rock slopes**
  On a more general note it is proposed more field data is needed for the calibration of design formulas for dynamic rock slopes. At present extensive research has been executed on Longshore Transport for different grain sizes - think of Longshore Transport of sand or Longshore Transport of much larger rock applied at a berm breakwater - as Longshore Transport of these materials is more often present. This has resulted in more data and eventually more reliable design formulas on these subjects. As the appliance of a Dynamic Rock Slope within a breakwater design becomes more commonly applied, it is of interest to acquire more insight in the processes of Longshore Transport at different cases of dynamic rock slopes.

Bibliography

A. Alikhani, G.R. Tomasicchio, and J. Juhl. Berm breakwater trunk exposed to obilique waves. *Coastal Engineering Proceedings*, 1(25), 1996.

Alkyon. Aanbieding Contract I van aanleg Maasvlakte 2 Buitencontour; Vaststelling hydraulische randvoorwaarden. Technical report, A1502RVWr1r4, Alkyon, Marknesse, The Netherlands, 2007.

R. A. Bagnold. An approach to the sediment transport problem from general physics. In *US Geological Survey 422-I*, pages 11–137. 1966.

James A Bailard. An energetics total load sediment transport model for a plane sloping beach. *Journal of Geophysical Research: Oceans*, 86(C11):10938–10954, 1982.

E. W. Bijker. Mechanics of sediment transport by the combination of waves and current. *Design and Reliability of Coastal Structures, 23rd International Conference on Coastal Engineering*, pages 147–174, 1992. doi: uuid: 4574aaa1-9246-4981-8305-c3a932e4ce03.

A. J. Chadwick. Field measurements and numerical model verification of coastal shingle transport. *Advances in Water Modelling and Measurement*, pages 381–402, 1989.

CETMEF CIRIA, CUR. *The rock manual: The use of rock in hydraulic engineering (2nd edition)*, volume C683. London, United Kingdom, 2007.

Coastal Engineering Research Center (US). *Shore protection manual: Volume I*, volume I. Corps of Engineers, Vicksburg, US, 1984.

K. D'Angremond, J. W. Van der Meer, and R. De Jong. Wave transmission at low-crested structures. In *Coastal Engineering*, pages 2418–2427. 1996.

H. C. Frijlink. Discussion of bedload movement formulas of Kalinske, Einstein, and Meyer-Peter and Muller and their application to recent measurements of bedload movement in the rivers of Holland. *English translation of a publication by Frijlink, originally published in the Comptes rendus 2ième Journée Hydraulique, Grenoble, 1952; translation by US Bureau of Reclamation, august 1953.*, 1952. doi: uuid: e3a97534-e3da-4970-a074-5e9db6c89b33.

B. Hofland and M. Van Gent. Maasvlakte 2 Harde Zeewering, Stenig Duin + Blokkendam: Meetrapport van aanvullend 2D schaalmodelonderzoek Scheldegoot Proevenseries 1 t/m 10. Technical report, 1001804-016, Deltares, Delft, The Netherlands, 2011a.

B. Hofland and M. Van Gent. Maasvlakte 2 Harde Zeewering, Stenig Duin + Blokkendam: Meetrapport van aanvullend 2D schaalmodelonderzoek, Scheldegoot, Proevenseries 11 t/m 21. Technical report, 1001804-019, Deltares, Delft, The Netherlands, 2011b.

HR Wallingford. Contract 1 of Maasvlakte 2 Construction Soft Sea-defence, Section Noordelijke Beeindiging: Physical model tests on wave-induced long- shore stone drift (1:20 limestone). Technical report, EX 5528, HR Wallingford, Wallingford, United Kingdom, 2007a.

HR Wallingford. Contract 1 of Maasvlakte 2 Construction Soft Sea-defence, Section Noordelijke Beeindiging: Physical model tests on wave-induced long- shore stone drift (1:20 anthracite). Technical report, EX 5474, HR Wallingford, Wallingford, United Kingdom, 2007b.

HR Wallingford. Maasvlakte 2; Cobble sea defence: Additional spectral wave measurements of drift test conditions 2007. Technical report, EX 5808B, HR Wallingford, Wallingford, United Kingdom, 2009a.

HR Wallingford. Maasvlakte 2: Cobble sea defence expert support: Expert opinion on calibration and validation of Damgaard & Soulsby formula for alongshore cobble drift. Technical report, EX 5808A, HR Wallingford, Wallingford, United Kingdom, 2009b.

HR Wallingford. Maasvlakte 2 Cobble sea defence Physical model of alongshore cobble drift: Test Series 7 and 8 with 15° and 45° sea-states. Technical report, EX 5858 2b, HR Wallingford, Wallingford, United Kingdom, 2009c.

HR Wallingford. Maasvlakte 2 Cobble sea defence Physical model of alongshore cobble drift: Basic Test Series with 30° sea-states. Technical report, EX 5858 2a, HR Wallingford, Wallingford, United Kingdom, 2009d.

R.Y. Hudson. *Wave forces on breakwaters*. ASCE, 1953.

R. Irribarren Cavanilles. *Una fórmula para el cálculo de los diques de escollera*. Madrid, Spain, 1938.

J.W. Kamphuis. On Understanding Scale Effect in Coastal Mobile Bed Models. In *Physical Modelling in Coastal Engineering*, pages 141–162. A. A. Balkema, Rotterdam, The Netherlands, 1985.

A. Lamberti and G. R. Tomasicchio. Stone mobility and longshore transport at reshaping breakwaters. *Coastal Engineering*, 29(3-4):263–289, 1997.

J-P. Latham. Degradation model for rock armour in coastal engineering. *Quarterly Journal of Engineering Geology and Hydrogeology*, 24(1):101–118, 1991.

J. McCowan. On the highest wave of permanent type. *The London, Edinburgh, and Dublin Philosophical Magazine and Journal of Science*, 38(233):351–358, 1894.

Patrick Mulders. Breakwaters Under Construction Exposed To Oblique Waves. Technical report, Msc Thesis, Delft University of Technology, 2010.

Port of Rotterdam. Factsheet Harde Zeewering, 2018a. URL `https://www.maasvlakte2.com/nl/index/show/id/484/harde-zeewering`.

Port of Rotterdam. Maasvlakte 2, 2018b. URL `https://www.maasvlakte2.com/nl/index/show/id/109/aanleg`.

Projectorganisatie Uitbreiding Maasvlakte. Harde Zeewering: Calibratie van golftransmissieformule voor variant SD+B. Technical report, puma-p-jwm-mo06, PUMA, Rotterdam, The Netherlands, 2009.

Projectorganisatie Uitbreiding Maasvlakte. Breuksteensuppletie van Stenig Duin in Onderhoudsperiode 2024 - 2038. Technical report, puma-p-mon-ono17, PUMA, Rotterdam, The Netherlands, 2010a.

Projectorganisatie Uitbreiding Maasvlakte. Breuksteensuppletie van Stenig Duin in Onderhoudsperiode 2019 - 2023. Technical report, puma-p-mo-ono16, PUMA, Rotterdam, The Netherlands, 2010b.

Projectorganisatie Uitbreiding Maasvlakte. Harde Zeewering: Hydraulische ontwerpstorm condities van Stenig Duin + Blokkendam. Technical report, puma-l-mja-ono04, PUMA, Rotterdam, The Netherlands, 2011a.

Projectorganisatie Uitbreiding Maasvlakte. Harde Zeewering: Hydraulische jaarrond condities van Stenig Duin + Blokkendam. Technical report, puma-l-mja-ono02, PUMA, Rotterdam, The Netherlands, 2011b.

Projectorganisatie Uitbreiding Maasvlakte. Harde Zeewering: Breuksteen suppletie van Stenig Duin in Instelperiode. Technical report, puma-p-mon-ono13, PUMA, Rotterdam, The Netherlands, 2011c.

Projectorganisatie Uitbreiding Maasvlakte. Harde Zeewering: Gewichtsverlies van breuksteen van Stenig Duin. Technical report, puma-p-jwm-ono02, PUMA, Rotterdam, The Netherlands, 2011d.

Projectorganisatie Uitbreiding Maasvlakte. NMO prognose van langsverlies breuksteen (jaarrond & ontwerpstorm) van Stenig Duin. Technical report, puma-p-jwm-ono04, PUMA, Rotterdam, The Netherlands, 2012.

Projectorganisatie Uitbreiding Maasvlakte. Harde Zeewering: Analyse zakking (klei-)kruin Stenig Duin Instelperiode. Technical report, puma-o-pbg-mi02, PUMA, Rotterdam, The Netherlands, 2015.

Projectorganisatie Uitbreiding Maasvlakte. Harde Zeewering: Specificaties voor steen suppletie. Technical report, puma-bc1-pbg-mip01, PUMA, Rotterdam, The Netherlands, 2016.

Projectorganisatie Uitbreiding Maasvlakte. Samenvatting bevindingen Instelperiode (2013-2018): Laagdikte en volume Stenig Duin. Technical report, puma-bc-pbg-mi902, PUMA, Rotterdam, The Netherlands, 2018.

R. L. Soulsby and J. S. Damgaard. Bedload sediment transport in coastal waters. *Coastal Engineering*, 52(8): 673–689, 2005.

G. R. Tomasicchio, A. Lamberti, and F. Guiducci. Stone movement on a reshaped profile. *Proceedings of the Coastal Engineering Conference*, 2:1625–1640, 1994.

G. R. Tomasicchio, F. D'Alessandro, G. Barbaro, and G. Malara. General longshore transport model. *Coastal Engineering*, 71:28–36, 2013.

G.R. Tomasicchio, F. D'Alessandro, G. Barbaro, F. Ciardulli, A. Francone, and S.M. Kurdistani. General model for estimation of longshore transport at shingle/mixed beaches. *Proceedings of the Coastal Engineering Conference*, 35:1–9, 2016.

J. P. van den Bos and H. J. Verhagen. Breakwater design (edition 2018). Technical report, Delft University of Technology, Delft, The Netherlands, 2017.

J. W. Van der Meer. Static and dynamic stability of loose materials. *Coastal Protection. Balkema*, 1990a.

J. W. Van der Meer and K. W. Pilarczyk. Dynamic stability of rock slopes and gravel beaches. In *Coastal Engineering*, pages 1713–1726. 1986.

J. W. Van der Meer and J. J. Veldman. Singular points at berm breakwaters: scale effects, rear, round head and longshore transport. *Coastal Engineering*, 17(3-4):153–171, 1992.

J.W. Van der Meer. *Rock Slopes and Gravel Beaches under Wave Attack*. PhD thesis, Delft University of Technology, 1990b.

J.W. Van der Meer, B. Wang, A. Wolters, B. Zanuttigh, and M. Kramer. Oblique wave transmission over low-crested structures. In *Coastal Structures 2003*, pages 567–579. 2004.

E. van Hijum. Evenwichtsprofielen en langstransport bij scheve regelmatige golfaanval. Technical report, Delft Hydraulics, Delft, The Netherlands, 1977.

E. van Hijum and K.W. Pilarczyk. *Gravel Beaches: Equilibrium profile and longshore transport of coarse material under regular and irregular wave attack*. Delft Hydraulics laboratory, 1982.

E. Van Wellen, A. J. Chadwick, and T. Mason. A review and assessment of longshore sediment transport equations for coarse-grained beaches. *Coastal Engineering*, 40(3):243–275, 2000.

C. K. Wentworth. A Scale of Grade and Class Terms for Clastic Sediment. *The journal of Geology*, 30(5):377–392, 1922.

A
Stability number

In this Appendix the development of the stability number is explained in more detail. First a list of symbols which solely apply to this appendix is given.

List of symbols regarding Appendix A

α	[°]	Slope angle.
B	[m]	Buoyancy.
d_n	[m]	Nominal diameter of the sediment.
F	[N]	Force.
g	[$m^3 kg^{-1} s^{-2}$]	Gravitational constant.
H	[m]	Wave height.
H_s	[m]	Significant wave height.
W	[kg]	Weight of the sediment.
μ	[-]	Friction coefficient.
ρ_w	[kg/m^3]	Specific density of water.
ρ_s	[kg/m^3]	Specific density of the sediment.
Δ	[-]	Relative density $\left(\Delta = \frac{\rho_s - \rho_w}{\rho_w} \right)$.
$N_s (= H_o)$	[-]	Stability number.

Irribaren derived the first equation that eventually led to the stability number (Irribarren Cavanilles, 1938). This stability number is derived from a balance of forces of a stone on a slope with angle α. Here the overview of van den Bos and Verhagen (2017) is used. The different forces that were distinguished are the weight of the rock, the buoyancy, the wave force and the frictional resistance. These forces are presented in Figure A.1.
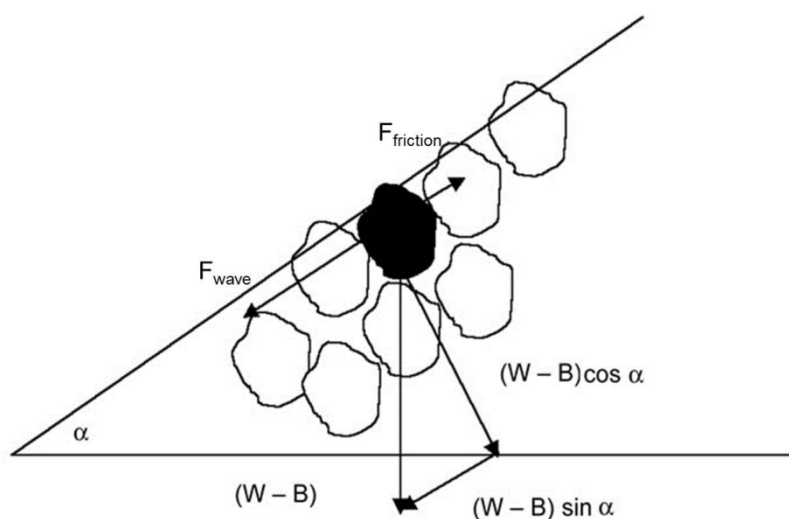
Figure A.1: Equilibrium of forces of a stone on a slope. (van den Bos and Verhagen, 2017).

The different forces are set by Irribarren using the following relations:

$$F_{wave} = \rho_w g d_n^2 H \tag{A.1}$$

$$F_{friction} = \mu F_{normal} = \mu(W - B)cos\alpha \tag{A.2}$$

Relationships A.1 and A.2 leave multiple characteristics unaltered. Think of the shape of the rock and the wave period. Furthermore only drag forces are taken into account and not acceleration forces.

The weight and buoyancy are derived as:

$$B = \rho_w g d_n^3 \qquad W = \rho_s g d_n^3 \tag{A.3}$$

When taking the equilibrium along the slope, at the moment of incipient motion, with the wave force directed downward as in Figure A.1, F_{force} and the component of the submerged weight $(W - B)sin\alpha$ are balanced only by the friction force $F_{friction}$. The friction force can be expressed in the normal force, perpendicular to the slope:

$$F_{friction} = \mu F_{normal} = \mu(W - B)cos\alpha \tag{A.4}$$

μ is the internal friction coefficient describing the friction between the slope and the rock. The final equilibrium becomes:

$$F_{wave} + (W - B)sin\alpha < \mu(W - B)cos\alpha \tag{A.5}$$

This formula can be rewritten to the form:

$$\frac{F_{wave}}{W - B} = \frac{H}{\Delta d_n} < \mu cos\alpha - sin\alpha \tag{A.6}$$

The same derivation can be done for uprush instead of downrush of the wave force, resulting only in a sign change.

$$\frac{F_{wave}}{W - B} = \frac{H}{\Delta d_n} < \mu cos\alpha + sin\alpha \tag{A.7}$$

The group of parameters $\dfrac{H}{\Delta d_n}$ will later be used by researchers as Hudson (1953), van Hijum and Pilarczyk (1982) and Van der Meer and Pilarczyk (1986) in order to assess stability of breakwaters .

$$\frac{H_s}{\Delta d_n} = H_o = N_s \tag{A.8}$$

Nowadays this group of parameters is also known as the stability number N_s or H_o.

B

Longshore Transport prognosis PUMA

This appendix gives a detailed explanation of the prognosis on Longshore Transport which PUMA made regarding the Dynamic Rock Slope at Maasvlakte 2. Again, the list of symbols solely used in Appendix B is given.

List of symbols regarding Appendix B

A	[-]	A certain constant.
B	[m]	Crest width.
C_t	[-]	Wave transmission coefficient.
d	[m]	Crest height.
Dir_{av}	[°N]	Average direction.
$Dir_{10\%}$	[°N]	10% of the direction.
$Dir_{90\%}$	[°N]	90% of the direction.
h_i	[m]	Water depth in front of the Block Dam.
h_t	[m]	Water depth behind the Block Dam.
H_s	[m]	Significant wave height.
$H_{s,i}$	[m]	Incoming significant wave height.
k_s	[-]	Abraision resistance index.
$L_{0,p}$	[m]	Deep water wavelength.
L_{BK}	[m]	Riblength of concrete cubes.
M	[kg]	Mass at a certain moment in time.
M_0	[kg]	Mass at starting moment.
R_c	[m]	Freeboard.
S	[kg/s]	Longshore Transport.
SLR	[m]	Sea Level Rise.
SWL	[m] $\pm$ NAP]	Still Water Level.
$T_{m-1,0}$	s	Wave period calculated from the first negative moment of the spectrum
T_p	[s]	Peak wave period.
T_i	[s]	Time.
X	[-]	Factors leading to degradation
z_{BK}	[m]	Settlement block dam.
α	[°]	Slope angle.
φ	[°]	Wave angle.
φ_i	[°]	Wave angle of the incoming waves.
φ_t	[°]	Wave angle of the transmitted waves.
ξ_p	[-]	Breaking parameter.
KP	[-]	Section along the Hard Sea Defence.
MDE	[-]	Micro-Deval.
SMT	[-]	Scale model test.
SP	[-]	Setting Period.
YFA	[-]	Year of Final Acceptance.

PUMA generally took four steps to realise their prognosis and corresponding maintenance plan. These consecutive steps are treated separately below.

B.1. Step 1: Offshore to nearshore wave transformation

As is often the case in wave analysis, PUMA distinguished two separate hydraulic conditions; year-round conditions and storm conditions (Projectorganisatie Uitbreiding Maasvlakte, 2011a)(Projectorganisatie Uitbreiding Maasvlakte, 2011b). Both hydraulic conditions were established by analysing historical wave data of Rijkswaterstaat, measured at the Europlatform. This platform is situated in the North Sea, approximately 50 km to the east of MV2. The data contained wave measurements from 1979 up to 2005.

B.1.1. Hydraulic year-round conditions

Four main external forcing parameters are necessary in order to estimate LT in step 3. These are water level, wave height, wave period and wave direction.

In order to asses the water levels which are to be expected at the hard sea defence of MV2, the water levels of the station Hoek van Holland were assessed. With this astronomical tide data of Hoek van Holland from 1980 to 2007, the water levels of Table B.1 were established.

	High water level [m+NAP]	Low water level [m+NAP]	Tidal difference [m]
Average tide	1.11	-0.63	1.74
Average spring tide	1.30	-0.60	1.90
Average neap tide	0.88	-0.60	1.48
HHWS/LLWS	1.46	-0.84	-

Table B.1: Characteristic water levels

For the estimation of wave height and wave period the wave data of the Europlatform were translated by Svasek and Alkyon using the model SWAN (Alkyon, 2007). The offshore wave data was transformed to 36 wave conditions along the toe of the DRS, one for every section of 100 meters. An example of a wave condition at location KP1400 is graphically represented in Figure B.1. In the Figure wave direction is indicted by the different slices, wave height is indicated by color and occurrence is indicated by the length of a slice.
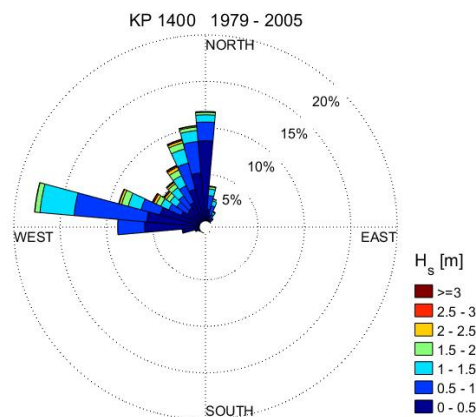
Figure B.1: Year-round wave rose at location KP1400.

B.1.2. Hydraulic design storm conditions

Besides the year-round conditions, Alkyon determined a set of hydraulic design storm conditions (Alkyon, 2007) (Projectorganisatie Uitbreiding Maasvlakte, 2011a). Again these design storm conditions are derived from offshore wave data, subsequently transformed from the offshore Europlatform to nearshore wave conditions at the toe of the DRS. To do so the DRS was divided in four parts containing 15 wave locations. The division of these parts is show in Table B.2 and correspond to Figure B.2. The 15 wave locations are depicted as blue squares in Figure B.2, starting with P1 at the most eastern part of the DRS and increasing to P15 in westerly direction.

Section name	Code	KP	Wave locations
HZ Transition MV1	HZa	-0.170 - 0.190	P1 - P2
HZ East	HZo	0.190 - 0.850	P3 - P5
HZ Middle	HZm	0.850 - 3.000	P6 - P12
HZ West	HZw	3.000 - 3.495	P13 - P15

Table B.2: Division of sections and wave locations along the DRS.

In order to be able to execute scale model tests, different design storm conditions had to be determined. Three design storm conditions were derived:

1. *Normative design storm conditions at high water including SLR for 50 years.*
   The resulting wave parameters per sections are presented in Table B.3. Different conditions are set for the 1:10, 1:100, 1:1.000 and 1:10.000 year design storm. According to the contractual requirements of the Port of Rotterdam a sea level rise (henceforth "SLR") of 0.35 m for a period of 50 years had to be taken into account.

2. *Normative design storm conditions at low water excluding SLR.*
   To asses the stability of the construction at the toe of the block dam the normative design storm conditions at low water were necessary. The resulting wave parameters per sections are presented in Table B.4.

3. *Normative design storm conditions between low and high water.*
   For the estimation of design storm conditions above low water (2.05 m+NAP) to high water an interpolation to the considered water levels was made, hereby keeping the wave steepness constant.
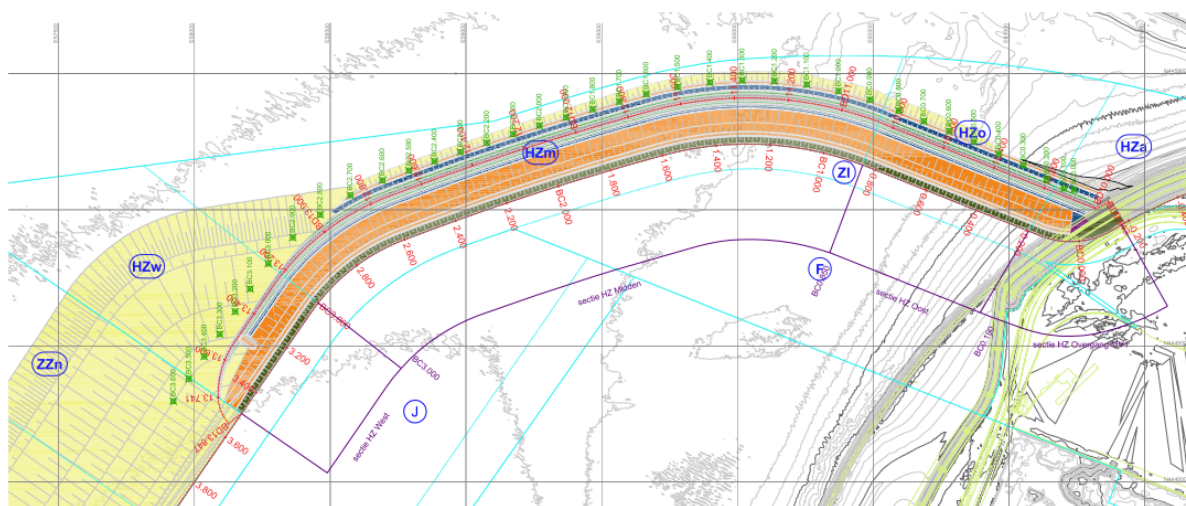
Figure B.2: Topview of the DRS with the layout of the different sections and wave locations (Projectorganisatie Uitbreiding Maasvlakte, 2011a).

	1:10 yr						1:100 yr					
Section	H_s [m]	$T_{m-1,0}$ [s]	Dir_{av} [°N]	$Dir^*_{10\%}$ [°N]	$Dir_{90\%}$ [°N]	w.l.** [m+NAP]	H_s [m]	$T_{m-1,0}$ [s]	Dir_{av} [°N]	$Dir_{10\%}$ [°N]	$Dir_{90\%}$ [°N]	w.l. [m+NAP]
HZa	4.80	9.1	328	317	340	3.24	5.75	10.1	329	318	337	3.87
HZo	5.25	9.1	310	293	332	3.10	6.20	9.9	311	294	331	3.75
HZm	5.65	9.2	302	281	327	3.10	6.65	10.1	304	283	328	3.75
HZw	5.75	9.1	297	273	326	3.10	6.75	10.1	301	275	327	3.75

	1:1.000 yr						1:10.000 yr					
Section	H_s [m]	$T_{m-1,0}$ [s]	Dir_{av} [°N]	$Dir_{10\%}$ [°N]	$Dir_{90\%}$ [°N]	w.l. [m+NAP]	H_s [m]	$T_{m-1,0}$ [s]	Dir_{av} [°N]	$Dir_{10\%}$ [°N]	$Dir_{90\%}$ [°N]	w.l. [m+NAP]
HZa	6.50	10.9	329	319	336	4.56	7.05	11.4	329	324	335	5.30
HZo	6.90	10.7	314	297	331	4.44	7.45	11.3	319	307	332	5.30
HZm	7.40	10.9	308	286	328	4.44	7.95	11.6	317	300	330	5.30
HZw	7.50	10.9	308	282	328	4.44	8.05	11.6	317	297	331	5.30

Table B.3: Hydraulic design storm conditions at high water with 50 years of SLR (Projectorganisatie Uitbreiding Maasvlakte, 2011a).
*Dir = direction   **w.l. = water level

	1:10 yr						1:100 yr					
Section	H_s [m]	$T_{m-1,0}$ [s]	Dir_{av} [°N]	$Dir_{10\%}$ [°N]	$Dir_{90\%}$ [°N]	w.l. [m+NAP]	H_s [m]	$T_{m-1,0}$ [s]	Dir_{av} [°N]	$Dir_{10\%}$ [°N]	$Dir_{90\%}$ [°N]	w.l. [m+NAP]
HZa	4.60	9.1	328	315	339	0.40	5.35	9.9	327	315	335	0.91
HZo	5.00	8.9	309	293	331	0.41	5.80	9.8	310	295	329	0.94
HZm	5.40	9.1	301	281	327	0.40	6.25	10.0	306	285	328	0.95
HZw	5.50	9.1	299	275	327	0.41	6.35	10.0	306	280	328	0.96

	1:1.000 yr						1:10.000 yr					
Section	H_s [m]	$T_{m-1,0}$ [s]	Dir_{av} [°N]	$Dir_{10\%}$ [°N]	$Dir_{90\%}$ [°N]	w.l. [m+NAP]	H_s [m]	$T_{m-1,0}$ [s]	Dir_{av} [°N]	$Dir_{10\%}$ [°N]	$Dir_{90\%}$ [°N]	w.l. [m+NAP]
HZa	5.95	10.6	327	317	334	1.43	6.30	11.1	327	317	333	1.97
HZo	6.35	10.5	311	296	328	1.47	6.70	10.9	312	297	329	2.02
HZm	6.85	10.7	309	289	327	1.49	7.20	11.3	312	293	329	2.04
HZw	6.90	10.8	311	290	328	1.50	7.30	11.4	314	297	330	2.04

Table B.4: Hydraulic design storm conditions at low water excluding SLR (Projectorganisatie Uitbreiding Maasvlakte, 2011a).

B.2. Step 2: Block dam transmission

In front of the DRS a block dam, constituted out of the recycled Maasvlakte 1 armour units, is situated. The concrete armour units are square shaped and positioned rather precise during construction. The block dam is of great influence to the wave characteristics which are imposed on the DRS behind it. The dam alters three main external forcing parameters: wave height, wave period and wave direction, all depicted in Figure B.3. The four parameters were transformed from the toe of the block dam to the breaker line behind the dam. By means of scale model tests executed by HR Wallingford and Deltares these parameters were assessed and PUMA used the outcomes in their prognosis (Projectorganisatie Uitbreiding Maasvlakte, 2009). These outcomes will be presented separately below.
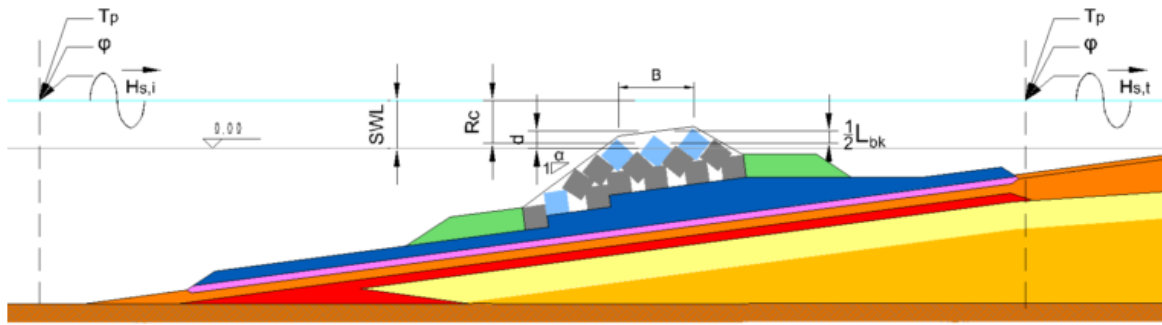
Figure B.3: Visualisation of governing parameters at the block dam of the DRS. (Projectorganisatie Uitbreiding Maasvlakte, 2009)

B.2.1. Wave height

First an foremost the wave height will be reduced by the block dam. Resulting from a literature study, PUMA proposed the wave transmission formula of D'Angremond et al. (D'Angremond et al., 1996) as most applicable. Following Van der Meer et al. and taking wave incidence into account by multiplying with a cosine to the $\frac{2}{3}$ power (Van der Meer et al., 2004), the formula reads:

$$C_t = \left(-0.4\frac{R_c}{H_{s,i}} + \left(\frac{B}{H_{s,i}}\right)^{-0.31} \cdot (1 - e^{-0.5\xi_p}) \cdot 0.64\right)\cos^{\frac{2}{3}}\varphi \quad \text{with limits} \quad 0.075 < C_t < 0.8 \quad \text{(B.1)}$$

where

$$\xi_p = \tan\alpha\left(\frac{H_{s,i}}{L_{0,p}}\right)^{0,5} \quad \text{(B.2)}$$

$$R_c = a - \text{SWL} - 0.5 \cdot L_{BK} - z_{BK} \quad \text{(B.3)}$$

Formula B.1 was calibrated using scale model tests (henceforth "SMT") executed by HR Wallingford and Deltares for the estimation of wave height transmission at the block dam (Hofland and Van Gent, 2011b)(Hofland and Van Gent, 2011a)(HR Wallingford, 2009a). Six constants were calibrated to form Equation B.4. The constants A1 to A6 are presented in Table B.5.

$$C_t = \left(A1\frac{R_c}{H_{s,i}} + \left(A2 \cdot \frac{B}{H_{s,i}}\right)^{A3} \cdot (1 - e^{A4 \cdot \xi_p})\right)\cos^{A5}\varphi \quad \text{with limits} \quad 0.075 < C_t < 0.8 \quad \text{(B.4)}$$

where

$$R_c = d - \text{SWL} - A6 \cdot L_{BK} - z_{BK} \quad \text{(B.5)}$$

The deviation between calculated and measured values for the data used in the calibration of Equation B.4-B.5 had a lower and upper limit of respectively -10% and +13%.

Parameter	Specific calibrated value[-]	Original value[-]
A1	-0.34294	-0.40
A2	0.47609	0.64
A3	-0.27492	-0.31
A4	-0.50000	-0.50
A5	0.10007	0.67
A6	0.50000	0.50[1)]

Table B.5: Calibrated parameters A1 to A6 of the wave transmission equation.
1) Assumption made by PUMA, parameter was not established by D'Angremond et al. (1996).

B.2.2. Wave period

Besides wave height, also the wave period changes due to wave transmission through the block dam of MV2. As Van der Meer et al. (2004) stated, the peak period of the waves will only slightly decrease. However the spectrum changes considerably. For the lower frequencies the energy decreases and for the higher frequencies it increases. Due to this the average period decreases. The peak period at the toe and at the breaker line was measured in multiple tests. The results showed little alterations of the peak period over the block dam (Projectorganisatie Uitbreiding Maasvlakte, 2009). Therefore PUMA chose not to take any peak period alterations into account in their transmission assessment.

B.2.3. Wave direction

During the SMT it was not possible to measure the wave direction behind the block dam, thereby making it impossible to measure the change in wave direction. PUMA made an assumption to account for this wave direction alternation. Would the water depth at the toe be the same as that of the depth at the breaker line, then the decrease in wave angle would be approximately 20%; as presented in Equation B.6.

$$\varphi_b = 0.8 \cdot \varphi_t \tag{B.6}$$

However, there is a difference in water depth between the toe and breaker line. Due to this difference the above-mentioned reduction of wave incidence is not complete. To compensate for this reduction Snell's law is used:

$$\frac{\sin\varphi_t}{\sqrt{h_t}} = \frac{\sin\varphi_b}{\sqrt{h_b}} \tag{B.7}$$

B.3. Step 3: Longshore Transport estimation

In order to translate the governing wave climate at the breaker line of the DRS to Longshore Transport values, more insight in this process was needed. Therefore, PUMA asked Wallingford to assess the Longshore Transport process of cobblestones which was to be expected at the DRS, and come up with a theoretical formula which could represent this process.

B.3.1. Calibration of the DS97 formula

HR Wallingford chose the force-balance method out of the different available approaches regarding Longshore Transport of coarse materials (HR Wallingford, 2009b).

The DS97 formula, Equation C.2-C.5 - for the estimation of LT rates of coarse material - was taken by Wallingford and altered for the specific case of the DRS at MV2. This theoretical approach was calibrated using scale model tests. This resulted in a non-dimensionless semi-empirical formula:

$$S = p_1 \left(H_s - p_2\right)^{p_3} \cdot sin\left(p_4 \cdot \varphi\right)^{p_5} \cdot \left(T_{p,b} - p_6\right)^{p_7} \tag{B.8}$$

Using non-linear regression on the results of the SMT executed by Wallingford, the seven p-coefficients in Equation B.8 were established. The resulting values are presented in Table B.6. HR Wallingford stated that the LT rates estimated using the SMT can vary stochastically with $\pm 50\%$ (Projectorganisatie Uitbreiding Maasvlakte, 2012). PUMA compared the calculated LT values using Equation B.8 with the measured LT values and concluded a maximum deviation of 24% was acceptable.

Coefficient	Year-round conditions	Storm conditions
p_1	6.21	169
p_2	0.00	1.60
p_3	3.60	1.57
p_4	2.00	2.00
p_5	0.86	1.24
p_6	6.00	6.00
p_7	0.10	0.24

Table B.6: Regression coefficients.

The calibration of p-coefficients results in an equation for the estimation of LT that is twofold.

For year-round conditions, i.e. Longshore Transport up to 150 kg/s:

$$S = 6.21 \cdot (H_s - 0.00)^{3.6} \cdot \sin(2.00 \cdot \varphi)^{0.86} \cdot (T_p - 6.00)^{0.10} \qquad \text{for } S < 150 kg/s \tag{B.9}$$

For design storm conditions, i.e. Longshore Transport upward of 150 kg/s:

$$S = 169 \cdot (H_s - 1.60)^{1.57} \cdot \sin(2.00 \cdot \varphi)^{1.24} \cdot (T_p - 6.00)^{0.24} \qquad \text{for } S > 150 kg/s \tag{B.10}$$

B.3.2. Estimation of Longshore Transport

Following the year-round wave conditions which were estimated for 35 sections of the DRS, the year-round Longshore Transport was determined. In order to asses both the LT rates for the first year and that of the following 50 years of the maintenance period, two situations were assessed (Projectorganisatie Uitbreiding Maasvlakte, 2012):

1. Year of Final Acceptance (hereafter "YFA") of the DRS with a crest height block dam of + 2.60 m NAP.

2. 50 years after YFA with a crest height block dam of + 2.00 m NAP.
   The difference in this situation is that of the crest height of the block dam. After 50 years a settlement of 0.6 meters was accounted for. The relative water level on which all wave characteristics are imposed will be higher, resulting in more wave energy present behind the block dam.

This was done by taking the year-round wave conditions and translating these values to the theoretical breaker line and inserting the outcomes in Equation B.9-B.10. This resulted in the gross Longshore Transport which was calculated for every section (KP0.200 - KP3.500) using the year-round wave conditions of 1979-2005. The results are presented in Figure B.4. The grey lines present the LT per year and the red lines are the average values of the LT per year.
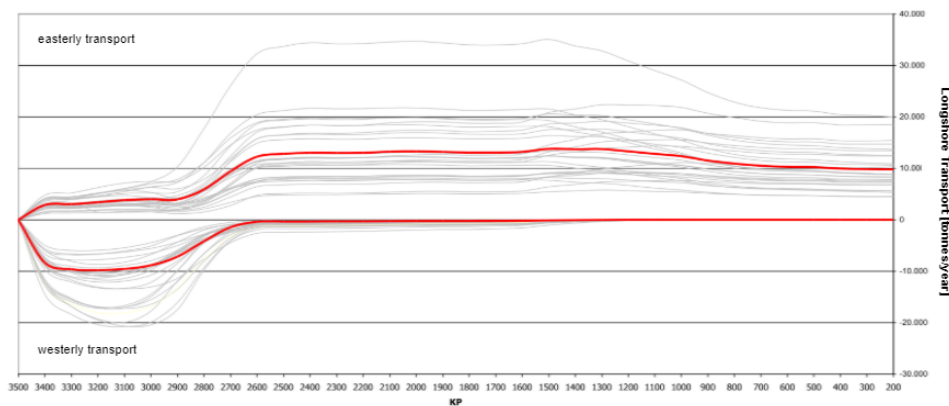
Figure B.4: Bruto LT, crest height block dam + 2.0 m NAP including SLR (Projectorganisatie Uitbreiding Maasvlakte, 2012).

Following from the gross transport rates, the net LT rates are determined and shown in Figure B.5. Multiple conclusions can be drawn from this figure. It was expected that accumulation of stone would occur at the both endings of the DRS. Also, in the eastern part of the DRS predominant easterly directed transport was expected and at the western part of the DRS decrescent westerly directed transport was expected.

By taking the derivative of the netto LT rates the gradients in LT were established. In this respect negative gradients imply net erosion and positive gradients imply net accretion. The year-round average of gradient transport in LT is presented in Figure B.6. The surface area of the negative gradients in Figure B.6 results in the expected longshore losses per year, which amounts 7.6 kton/year.

In conclusion:

1. YFA with a maximum crest height block dam of + 2.60 m NAP: 7.6 kton/year

2. 50 years after YFA with a crest height block dam of + 2.00 m NAP: 23.0 kton/year
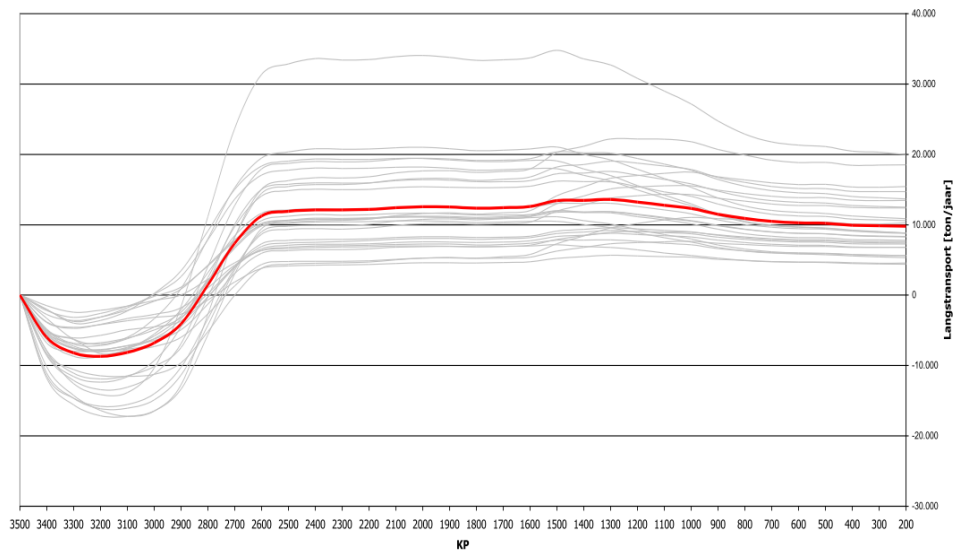
Figure B.5: Netto LT, crest height block dam + 2.0 m NAP including SLR (Projectorganisatie Uitbreiding Maasvlakte, 2012).
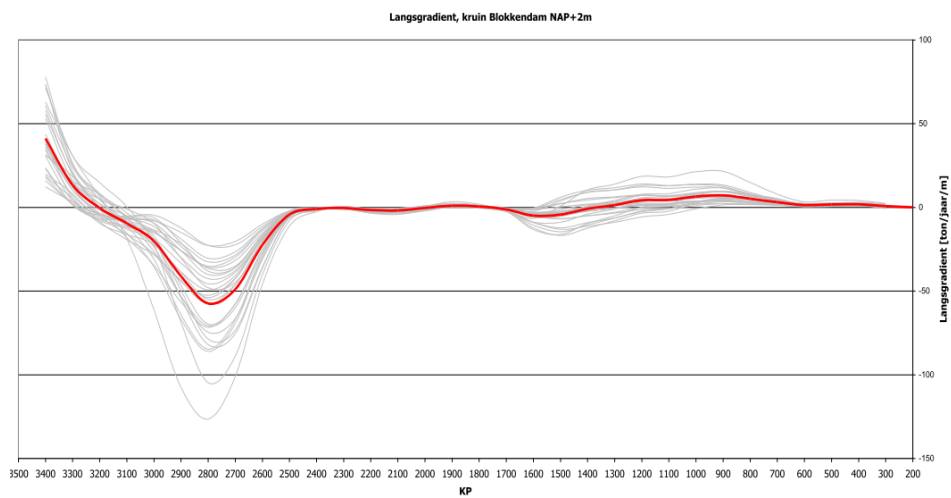
Figure B.6: Gradients in LT, crest height block dam + 2.0 m NAP including SLR (Projectorganisatie Uitbreiding Maasvlakte, 2012).

B.4. Step 4: Setting nourishment volumes

The final step was for PUMA to set the stone nourishment volumes for the maintenance period. The first five years of the maintenance period is called the 'Setting Period' and will henceforth be referred to as SP. Following PUMA's assessment multiple processes contribute to the necessary volumes for nourishment(Projectorganisatie Uitbreiding Maasvlakte, 2011c):

1. Losses of stone in cross-shore direction.

2. Erosion and accretion along the DRS due to the Longshore Transport of stones.

3. Degradation of stones in the swash-zone of the DRS.

4. Year efficiency.

The second process is, obviously, governing. For sake of clarity all processes are assessed separately.

B.4.1. Stone losses

The DRS at MV2 contains two curved sections. Because waves will attack the DRS from multiple directions normally loss of sediment - in this case cobblestones - from the DRS would logically take place. However, the block dam is situated in front and at the both ending sections, thereby enclosing the DRS. In a sense the DRS is a confined space from which stones can not escape. PUMA therefore chose to rely on this confinement and did not take any significant stone losses into account.

B.4.2. Longshore Transport

As seen in Section B.3 a redistribution of stone along the DRS will occur due to wave incidence. This LT process is the main contribution to the nourishment volumes. The estimation of LT rates along the DRS, see Figure B.6, results in an average year-round longshore stone loss of 7.6 kton/year in year one after construction. This volume needs to be compensated by stone nourishments.

B.4.3. Stone degradation

Due to rolling and breaking of the quarry rock, stones will degrade. Degradation of the stones is assessed by PUMA in (Projectorganisatie Uitbreiding Maasvlakte, 2011d). Degradation of stone can occur due to multiple reasons:

1. Weight loss by means of the hydraulic loading, i.e. the year-round we conditions and subsequent currents.

2. Weight loss as a result of handling activities like dismantling, relocation and nourishing.

3. Weathering of the stones due to cyclic behavior like freezing-thaw, dry-wet and hot-cold.

PUMA concluded that the first reason will not be of influence as the stones are relatively sheltered by the block dam. Also the stones that will be used are classified as *good* (CIRIA, CUR, 2007). The remaining degradation causes are assessed by usage of the Micro-Deval (henceforth "MDE") method. This method estimates degradation based on the following equation (Latham, 1991):

$$\frac{M}{M_0} = 0.05 exp\left(-30\left(\frac{k_s}{X}\right)T_i\right) + 0.95 exp\left(\left(\frac{k_s}{X}\right)T_i\right) \tag{B.11}$$

Here M is the mass of the rock at some moment in time and M_0 is the mass at starting point. Within X nine factors that lead to degradation are taken into account. k_s is the intrinsic resistance of the stone against wear.

By means of this formula PUMA showed the degradation of rock would not be higher than the requirement of a maximum weight loss of 5% per year.

B.4.4. Year efficiency

Contractors always take efficiency into account. When it comes to nourishment volumes the year efficiency accounts for any unexpected loss of stone during nourishment activities. PUMA set a year efficiency of 95%, effectively multiplying necessary stone volumes with a factor of 1.14.

B.4.5. Final maintenance plan

The nourishment campaign comprised of nourishments every 2.5 years. To finally translate all above-mentioned requirements to actual nourishment volumes a minor computation was presented. First the yearly wave-driven Longshore Transport was assessed as being 7.6 kton/y in the first year increasing linearly to 23.0 kton/y in year 50 after YFA. Besides wave-driven Longshore Transport PUMA accounts for local erosion along the DRS. According to (Projectorganisatie Uitbreiding Maasvlakte, 2012) the local erosion per meter would be approximately 10% over the sections KP2.500 - KP3.200, so for the full length of the DRS, which is 4 times the length of this section, 40% of local erosion is taken into account. This results in 3 kton/y, bringing the total nourishment for the first year at 10.6 kton/y. The local erosion is expected to increase linearly because of the expected wear of 5% per year. Remaining requirements demand the nourishment volumes for the first 2.5 years - which will be applied at year 0 - to be: $(10.6+11.1+0.5\cdot11.5)\cdot1.14 = 31.2$ kton/y. The final maintenance campaign for the DRS is presented in Table B.7.

Nourishment campaign [year after construction]	Wave-driven [kton/y]	Local erosion/wear [kton/y]	Total [kton/y]	Proposed nourishment [kton/y]
0	-	-	-	31.2
1	7.6	3.0	10.6	-
2	7.9	3.2	11.1	-
3 (2016)	8.2	3.3	11.5	34.3
:	:	:	:	:
5 (2018)	8.9	3.6	12.5	37.6
:	:	:	:	:
8 (2021)	9.8	3.9	13.7	40.4
:	:	:	:	:
10 (2023)	9.8	3.9	13.7	43.8
:	:	:	:	:
:	:	:	:	:
25 (2038)	23.0	9.2	31.2	61.7

Table B.7: Determination of nourishment volumes. (Projectorganisatie Uitbreiding Maasvlakte, 2010a) (Projectorganisatie Uitbreiding Maasvlakte, 2010b) (Projectorganisatie Uitbreiding Maasvlakte, 2011c)

Longshore Transport methods

This appendix briefly treats two of the three Longshore Transport methods. As explained in Section 3.1, three methods are presently accepted for assessing Longshore Transport:

1. Energetics method; divided into the energy flux approach and the stream power approach.

2. Force-balance method.

3. Dimensional analysis method.

This thesis makes use of the LT relations following from the Dimensional analysis method, therefore this appendix will briefly treat the Energetics and Force-balance method. First a list of symbols, which are used solely within this appendix, is given.

List of symbols regarding Appendix C

a	[-]	Porosity index.
A	[-]	A constant.
d	$[m]$	Grain diameter.
$f_{w,r}$	[-]	Wave friction factor.
$f_{w,sf}$	[-]	Friction factor for sheet flow conditions.
g	$[m^3 kg^{-1} s^{-2}]$	Gravitational constant.
H_s	$[m]$	Significant wave height.
$H_{s,b}$	$[m]$	Significant wave height at breaking.
K	[-]	Constant of proportionality.
P_{ls}	$[J/m \cdot s]$	Longshore component of wave power.
Q	$[m^3/s]$	Longshore Transport in volume per unit time.
s	[-]	Ratio of densities of sediment and water.
T	[s]	Time.
α	[°]	Slope angle
ρ_s	$[kg/m^3]$	Specific density of the sediment.
ρ_w	$[kg/m^3]$	Specific density of water.
γ_b	[-]	Breaker index ($=H_b/h_b$).
β	[°]	Wave angle.
β_b	[°]	Wave angle at breaking.
θ	[-]	Shields parameter.
θ_{cr}	[-]	Value of θ at threshold of motion.
θ_m	[-]	Time-mean of the Shields parameter.
θ_{max}	[-]	Maximum value of the Shields parameter.
θ_w	[-]	Oscillatory part of the Shields parameter.
τ_0	$[N \cdot m^{-2}]$	Bed shear-stress.
DS97	[-]	Damgaard and Soulsby formula.

C.1. Energetics method

The first sub-category within the energetics method, i.e. the energy flux approach, determines the LT rate based on longshore wave power, P. The most common equation following from this approach is the CERC equation (Coastal Engineering Research Center (US), 1984):

$$Q = K \cdot P_{ls} = \frac{\rho_w K \sqrt{g/\gamma_b}}{16(\rho_s - \rho_w)(1-a)} H_{s,b}^{2.5} sin(2\beta_b) \tag{C.1}$$

Equation C.1 includes both bed load and suspended sediment transport and is therefore mostly applied at beaches consisting of relatively fine sediment, i.e. sand. The influence of sediment size is not taken into account in the CERC equation, making it less applicable to estimate LT rates when it comes to coarser sediment, like the cobblestones applied at MV2. As LT of coarser sediment is almost entirely due to bedload transport, the CERC formula will practically always overestimate the litoral drift of coarser sediments like gravel, cobble or shingle.

The second energetic based sub-category is the stream power approach, first introduced by Bagnold and extended by Bailard (Bagnold, 1966)(Bailard, 1982). This theory argues that a part of the stream power is issued to the displacement of sediment, both bed and suspended sediment. Again, this approach is mostly applied to sandy sediments. Bailard acknowledged his derivation was likely to over-estimate the LT of coarser material. Therefore this theory will not be discussed any further.

C.2. Force-balance method

The second LT method is that of the force-balance, which derives the sediment transport mainly from the present bed shear stresses. The Kalinski-Frijlink formula was the first of its kind (Frijlink, 1952). This formula describes the stirring up of sediments after which the actual sediment transport takes place. Bijker adapted this formula for the usage in hydrodynamic models (Bijker, 1992). With respect to LT of coarser sediment the work of Damgaard and Soulsby firstly used the force-balance method to derive a total longshore bedload transport formula (henceforth "DS97") (Soulsby and Damgaard, 2005). A combination of current-dominated - Q_{x1} - and wave-dominated - Q_{x2} - transport results in the analytical DS97 formula for LT:

$$Q_{b,1} = \text{sign}\{\beta_b\}\max\{|Q_{x1}|,|Q_{x2}\} \tag{C.2}$$

$$Q_{x1} = \begin{cases} 0.0175 A_4 \frac{\sqrt{g\gamma_b \tan\alpha} H_{s,b}^{5/2}}{(s-1)} \left(\sin(2\beta_b) - \frac{5}{3}\theta_{cr}\right)\sqrt{|\sin(2\beta_b)|} & \text{for } \sin(2\beta_b) > \frac{5}{3}\theta_{cr}^* \\ 0 & \text{for } \sin(2\beta_b) \leq \frac{5}{3}\theta_{cr}^* \end{cases} \tag{C.3}$$

$$Q_{x2} = \begin{cases} A_4(0.0208 + 0.00425\cos(2\alpha)) \frac{g^{3/8} d^{1/4} \gamma_b^{3/8} H_{s,b}^{19/8}}{T^{1/4}(s-1)} sin(2\beta_b) & \text{for } f_{w,r}/f_{w,sf} > 1 \\ A_4(0.00417 + 0.00083\cos(2\alpha)) \frac{g^{2/5} \gamma_b^{3/5} H_{s,b} b^{13/5}}{(\pi T)^{1/5}(s-1)^{6/5}} sin(2\beta_b) & \text{for } f_{w,r}/f_{w,sf} \leq 1 \end{cases} \tag{C.4}$$

where $\quad \theta_{cr}^* = \theta_{cr} \frac{8(s-1)d}{\gamma_b H_s \tan\alpha} \quad$ and subject to the threshold condition

$$Q_{b,1} = 0 \quad \text{for} \quad \theta_{max} \leq \theta_{cr} \quad \text{where} \quad \theta_{max} = \sqrt{(\theta_m + \theta\cos\alpha)^2 + (\theta_w\sin\beta)^2} \tag{C.5}$$

In above-mentioned formulas θ represents the Shields parameter:

$$\theta = \frac{\tau_0}{g\rho(s-1)d} \tag{C.6}$$

D

SWAN transformation

This appendix provides more background information on the SWAN transformation which was executed in order to obtain the nearshore wave climate at the Dynamic Rock Slope of Maasvlakte 2. First a list of symbols is given which are solely applicable within this SWAN transformation appendix.

List of symbols regarding Appendix D

U_{10}	[m/s]	Sustained wind speed at 10m above the (sea) surface. Sustained means averaged over 1 hour.
U_{dir}	[°N]	Wind direction associated with sustained wind speed, defined as coming from with regards to North.
H_{m0}	[m]	Significant wave height, Averaged wave height H of the 1/3 highest waves. Except in shallow water, H_s is accurately approximated by H_{m0}, defined as 4 times the standard deviation of the vertical surface displacement (4 times the square root of spectral moment m0, see below).
$S(f,\theta)$	$[m^2/Hz]$	The spectral density describes the distribution of the variance of the sea surface elevation with frequency f and direction θ. It is often referred to as wave spectrum.
$D(\theta)$	[-]	Directional distribution function: $S(f,\theta) = S(f).D(\theta, f)$.
σ	[°]	One-sided directional width of the spectrum (directional spreading or directional standard deviation).
s	[-]	Spreading index of a cos^{2s} directional spreading function.
m_p	[-]	For any integer p, mp is the integral over frequency f of fp multiplied by the wave spectrum, with f frequency in cycles per unit time. Remark: m0 is the total variance of sea surface elevation.
$T_{mp,q}$	[s]	$T_{mp,q}$= (mp/ mq)1/(q-p) with mp and mq spectral moments, and p and q two distinct integers. Here, $T_{m-1,0}, T_{m0,1}$ and $T_{m0,2}$, are referred to as energy wave period (T_m), mean spectral wave period $(T_{m0,1})$ and spectral mean zero-crossing wave period (T_z) respectively. The latter set of symbols denotes the variables stored in the delivered file.
T_p	[s]	Peak wave period, the period corresponding to the frequency where the spectral density reaches its maximum.
T_z	[s]	Mean Zero up crossing period. T_z is approximated by T_z $T_{m0,2}$ (see Moment-based wave period below).
θ_0	[°N]	Principal wave direction. The direction derived from the first-order directional Fourier moments (sine and cosine-weighted moments) of the directional wave spectrum. Wave direction is defined as coming from. It can also be defined for (a) limited range(s) of frequencies and represented as a function of frequency.
θ_p	[°N]	Peak wave direction, this is the wave direction corresponding to the peak wave frequency.
L	[m]	Deep water wave length: $\frac{gT_p^2}{2\pi}$.
γ	[-]	JONSWAP peakedness parameter.
MSL	[-]	Mean Sea Level.
CD	[-]	Chart Datum.

D.1. Input data

Here a short explanation of the validation of the wave data provided by Rijkswaterstaat and the KNMI is given. The requested data contained hourly data of three parameters; wave height, peak period and wave angle. Besides this data wind data was downloaded from `http://projects.knmi.nl/klimatologie/onderzoeksgegevens/potentiele_wind/`. This data comprised of hourly data for wind speed and direction. All the above-mentioned input data for SWAN was for the period of 1/1/2013 to 1/5/2018 and was measured at the Europlatform, situated in the North Sea. The exact RD coordinates of the Europlatform are: 9.963 447.601.

Multiple reasons can cause gaps in the data. A minor explanation will be given on how these gaps within the data were filled. First a separation of data gaps was made. Gaps smaller than 2 days were linearly interpolated. The gaps larger than 2 days were assessed and filled with hindcast data. This hincast data calculates the data through a larger model. The hindcast data was three-hourly, therefore it was linearly interpolated to hourly data. Next the hindcast data was laid next to the original data in order to see if there was a good comparison. If this was the case the gap was filled with this data, otherwise the larger gap was again linearly interpolated.

D.2. SWAN transformation set-up

Here the SWAN transformation set-up will be discussed in more detail.

D.2.1. Introduction

The objective of this transformation is to transform the ambient climate from offshore to nearshore in the area presented in Figure D.1. The method of transformation is the wave transformation matrix approach (hereafter also reffered to as "WTM"). The WTM approach relies on wind and wave parameters (e.g. U_{10}, U_{dir}, H_{m0}, T_p and θ_0). The offshore climate is first investigated and discretized with a limited number of representative nodes (sets of integrated parameters) which are in turn used as boundary conditions in a wave propagation model. The set of computational results is then combined in transfer functions for each nearshore locations. These transfer functions (or transformation matrices) are then combined with the offshore climate to derive the nearshore climate at each output locations. Used properly, this approach limits the number of computations and can produce a reliable nearshore climate.

The model used for the transformation is SWAN 41.01. SWAN is a two-dimensional, thirdgeneration, spectral wave model. SWAN solves the energy balance equation in the computational domain. The wave energy is discretized in a frequency and directional domain at each node of the spatial computational grid, and allowed to propagate in space and evolve in time. The following wave processes can be represented in the model:

- Wave propagation in time and space, shoaling, refraction due to current and depth; frequency shifting due to currents and non-stationary depth;

- Wave generation by wind;

- Three- and four-wave interactions;

- Whitecapping, bottom friction and depth-induced breaking;

- Dissipation due to vegetation;

- Wave-induced set-up;

- Transmission through and reflection (specular and diffuse) against obstacles;

In this transformation, SWAN is used in stationary mode with uniform offshore boundary conditions.
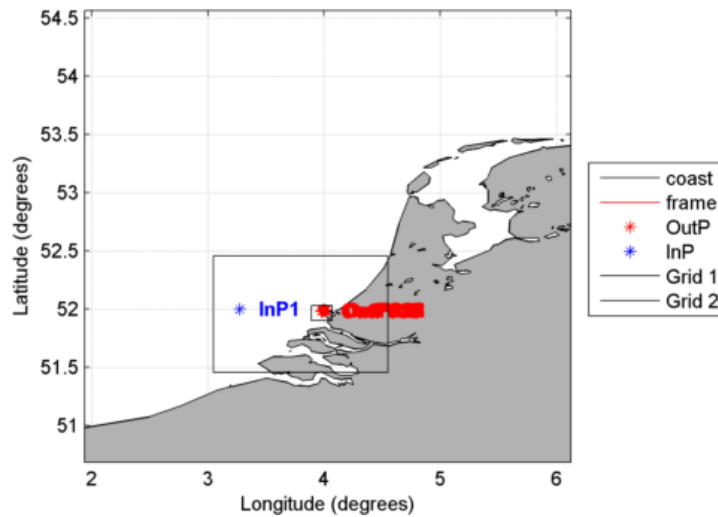
Figure D.1: Area of interest for the SWAN transformation.

D.2.2. Units and conventions

Units are expressed using the SI convention if not stated otherwise:

- length or distance (wave height, surface elevation, water depth) in metres – surface and wind speed elevations are given with regard to MSL – water depths are given with reference to MSL

- wave periods are given in seconds,

- speeds are given in metres per second,

- Wind and wave directions are defined as "coming from" relative to true north positive clockwise.

- The coordinates are given in WGS84

- All dates and times are given with reference UTC.

The spectral shapes presented in this report refer to the JONSWAP spectral shape, defined as:

$$S(f,\theta) = S(f).D(\theta,f) \tag{D.1}$$

where $D(\theta)$ is the directional distribution function:

$$D(\theta) = G_0 cos^n(\theta - \theta_p) \tag{D.2}$$

and where the function $S(f)$ is defined as:

$$S(f) = \alpha \cdot g^2 (2\pi)^{-4} \cdot f^{-5} \cdot exp\left(-\frac{5}{4}\left(\frac{f^{-4}}{f_{peak}}\right)\right) \cdot \gamma^{exp\left(-\frac{1}{2}\left(\frac{f/f_{peak}-1}{\sigma_f}\right)\right)} \tag{D.3}$$

where:

- α: scale parameter;

- f_{peak}: peak frequency;

- γ: peakedness parameter;

- σ_f: equal to 0.07 for $f < f_{peak}$ and equal to 0.09 for $f > f_{peak}$, not to be confused with the directional spreading value.

The directional spreading σ is computed as conventionally for pitch and roll buoy data and integrated over all frequencies as follows:

$$\sigma^2 = \left(\frac{180}{\pi}\right)^2 \int_0^{2\pi} \left(2sin\left(\frac{\theta-\overline{\theta}}{2}\right)\right)^2 D(\theta)d\theta \tag{D.4}$$

$$\left(\sigma \cdot \frac{\pi}{180}\right)^2 = 2\left(1 - \sqrt{\left(\frac{\int sin(\theta)S(f,\theta)dfd\theta}{\int S(f,\theta)dfd\theta}\right)^2 + \left(\frac{\int cos(\theta)S(f,\theta)dfd\theta}{\int S(f,\theta)dfd\theta}\right)}\right) \tag{D.5}$$

D.2.3. Offshore Data

In this section, the offshore data used as a basis for this transformation is presented. At this stage, 1 offshore point has been analyzed before the discretization of the offshore climate. The coordinates of these points are presented in Table D.1. The tidal data used here was extracted from the database at the location: Lon=3.2499, Lat=51.9803.

-	Lon [°E]	Lat [°N]	Origin	Depth [m]
lnP1	3.2751	51.9978	External	29.0

Table D.1: Offshore point specifications.

The wind and wave roses for the offshore point are presented in Figures D.2 and D.3.
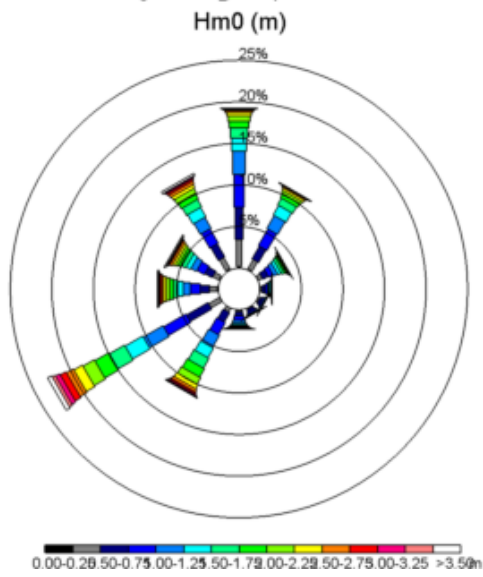
Figure D.2: Wave rose at lnP1.
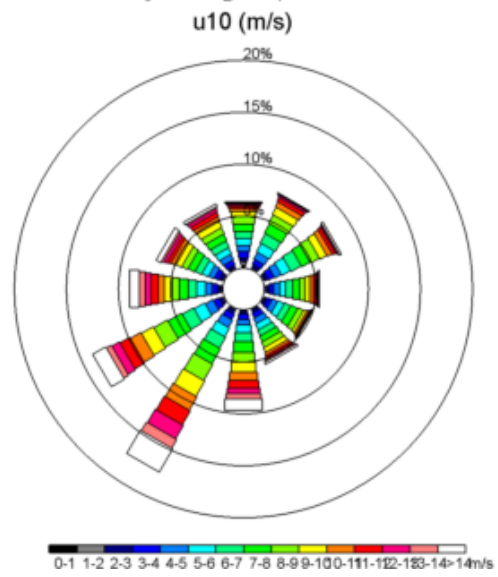
Figure D.3: Wind rose at lnP1.

The exceedance distributions for all year and each of the offshore point selected is presented in Figures D.4 and D.5.
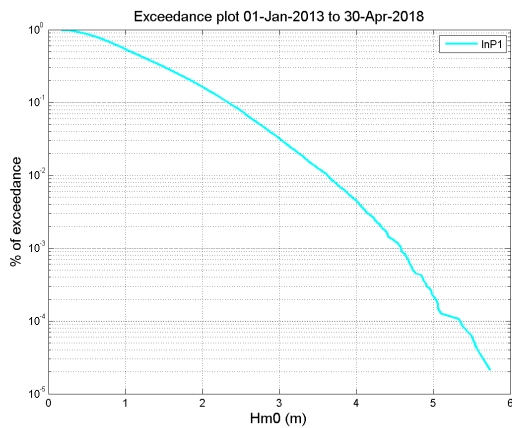
Figure D.4: Plot of exceedance of H_{m0}.
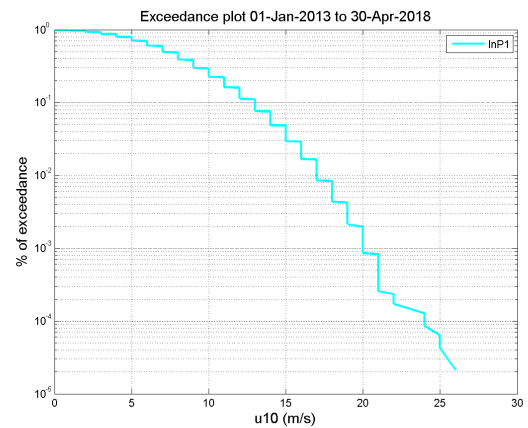
Figure D.5: Plot of exceedance of u_{10}.

D.2.4. Climate discretization

The discretization of the offshore climate is described in this chapter. A Total sea state method was chosen for this transformation. For each parameter (H_{m0}, T_p, θ, u_{10}, water level), the bins selected to discretize the climate are presented below. For the total sea state:

- H_{m0} (m): [0.1 1.25 2.5 3.75 6.25]

- θ (degrees): [0 30 60 90 120 150 180 210 240 270 300 330]

- T_p4 (s): [2 4 6 8 12 16 20]

- Water level (m): [0]

- U_{10} (m/s): 0.1 6.5 13 19.5 26

- Spreading (degrees): [30]

The total number of runs based on this discretization is: 1320. This number takes into account the number of deactivated nodes: 780.

The discretization of the climate is presented in Figures D.6 to D.8. In those figures, the red dots represent the nodes of the transformation matrix and the blue points show those that are deactivated.
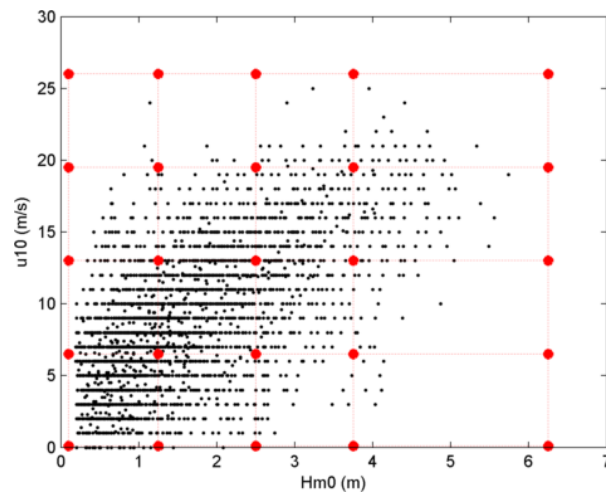
Figure D.6: Climate discretization of H_{m0} / U_{10} (the number of samples in this figure has been reduced to save plotting/saving time).
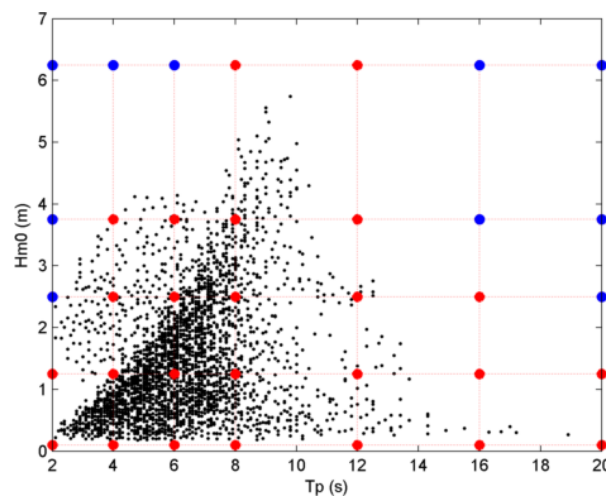
Figure D.7: Climate discretization of H_{m0} / T_p (the number of samples in this figure has been reduced to save plotting/saving time).
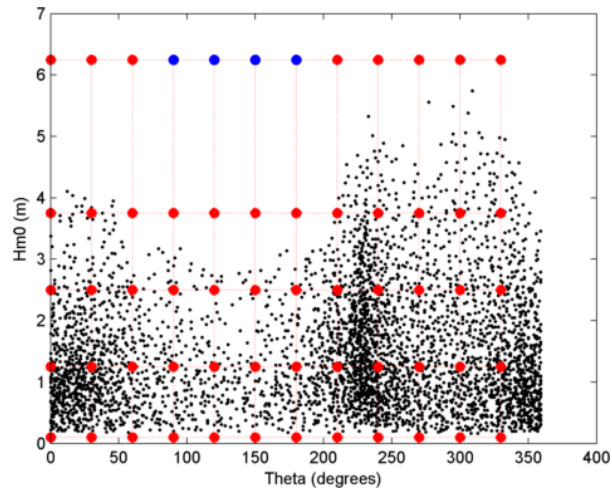
Figure D.8: Climate discretization of H_{m0} / / $theta$ (the number of samples in this figure has been reduced to save plotting/saving time)

D.2.5. Grid design

The number of grids used for this project is: 2. These grids are regular. In order to produce the SWAN bathy-metric files, the samples were automatically interpolated based on: MV2Land200.xyz, MV2Voorland20x20.xyz, emodnet mean CD1m.xyz. The bathymetry of the grids are presented in Figures D.9 and D.10.
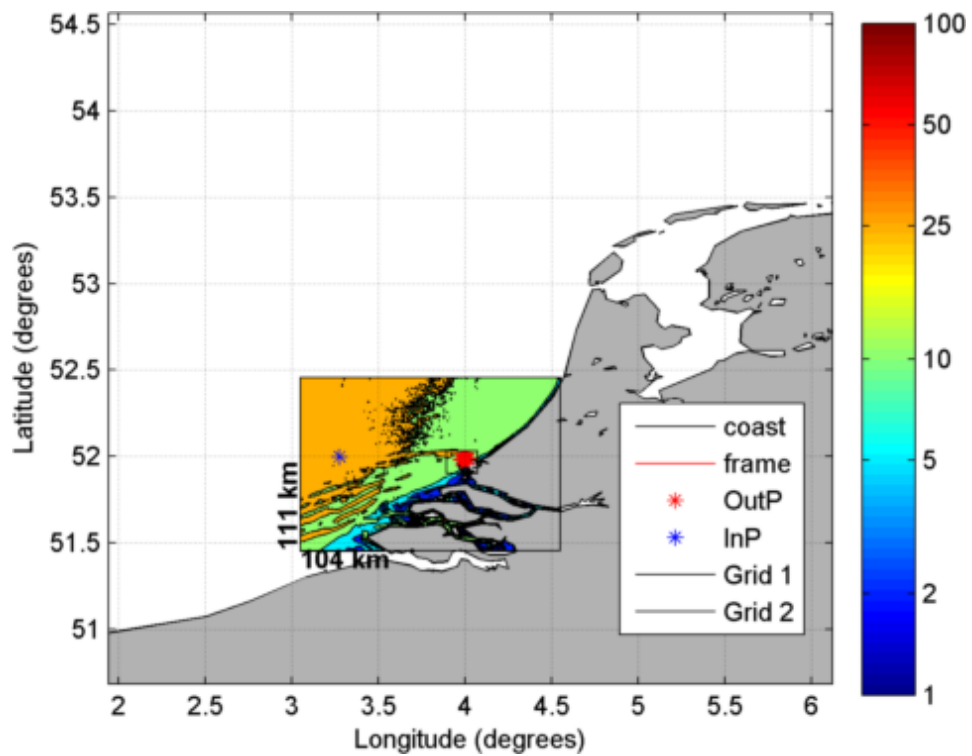
Figure D.9: Bathymetry of the grid A01.

The grid A01 has the characteristic below for SWAN.
CGRID REGULAR 3.048400 51.457000 0.000000 1.500000 1.000000 150 200 CIRCLE 36 flow=0.034500
fhigh=1.000000 msc=37
The grid resolution is 717 m in the x direction and 527 m in the y direction. Samples used for this grid were:
MV2Land200.xyz MV2Voorland20x20.xyz emodnet mean CD1m.xyz

The grid B01 has the characteristic below for SWAN.
CGRID REGULAR 3.891500 51.900100 0.000000 0.180000 0.130000 180 260 CIRCLE 36 flow=0.034500
fhigh=1.000000 msc=37
The grid resolution is 71 m in the x direction and 53 m in the y direction. Samples used for this grid were:
MV2Land200.xyz MV2Voorland20x20.xyz emodnet mean CD1m.xyz
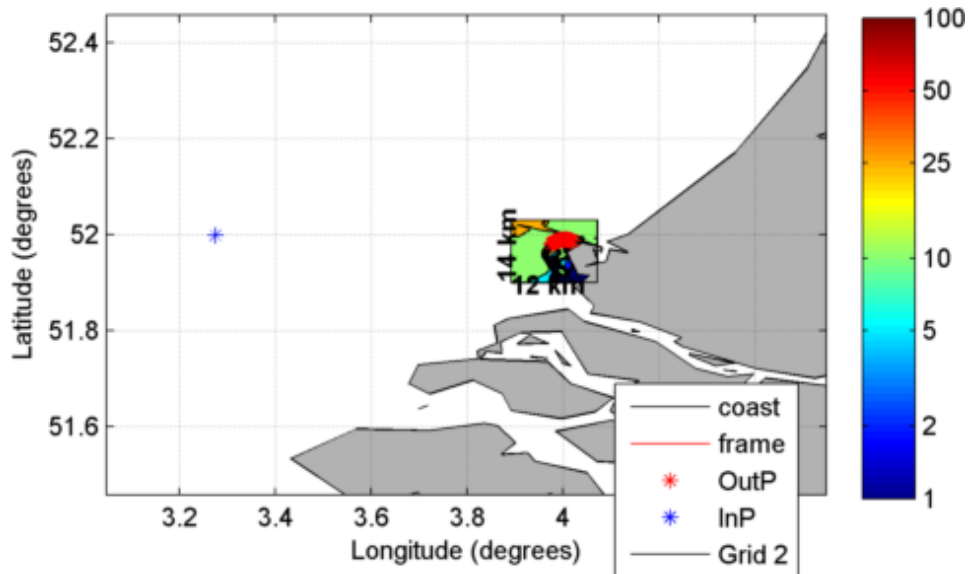
Figure D.10: Bathymetry of the grid B01.

D.3. Output Data
Here specifics regarding the output data of the SWAN transformation are given.

D.3.1. Output points
Table D.2 shows all the output points and their corresponding coordinates and depths along the toe of the DRS.

| Location Toe | Coordinates | | | | Depth outpout point [m] | | |
KP	RD		Lat.	Lon.	Svasek	Current	Difference
200	61140	445112	51.98646	4.02078	10.81	7.99	2.82
300	61054	445164	51.98692	4.01951	12.09	9.95	2.13
400	60963	445206	51.98728	4.01817	15.67	11.14	4.53
500	60872	445250	51.98766	4.01684	15.21	13.51	1.70
600	60780	445288	51.98798	4.01549	16.53	13.60	2.92
700	60687	445325	51.9883	4.01412	17.39	13.72	3.67
800	60595	445364	51.98863	4.01277	15.85	14.99	0.86
900	60488	445404	51.98898	4.01121	15.72	14.48	1.24
1000	60373	445436	51.98924	4.00952	15.56	14.39	1.17
1100	60256	445460	51.98944	4.00781	16.35	14.61	1.74
1200	60137	445473	51.98954	4.00608	16.58	15.16	1.42
1300	60018	445475	51.98953	4.00434	16.96	14.78	2.18
1400	59899	445468	51.98945	4.00261	16.57	14.34	2.23
1500	59780	445451	51.98928	4.00089	15.75	14.10	1.65
1600	59664	445425	51.98902	3.99921	17.09	13.72	3.36
1700	59565	445397	51.98876	3.99777	15.87	13.32	2.55
1800	59467	445369	51.98849	3.99635	15.47	12.70	2.77
1900	59369	445339	51.9882	3.99494	15.57	13.13	2.44
2000	59271	445309	51.98791	3.99352	15.60	12.52	3.07
2100	59174	445278	51.98762	3.99212	15.83	12.95	2.87
2200	59077	445246	51.98731	3.99071	15.87	12.07	3.79
2300	58980	445212	51.98699	3.98931	16.03	11.58	4.46
2400	58884	445178	51.98667	3.98792	16.25	11.89	4.36
2500	58790	445144	51.98635	3.98656	16.60	11.24	5.37
2600	58692	445108	51.98601	3.98515	16.89	10.75	6.14
2700	58574	445053	51.98549	3.98345	15.36	9.64	5.72
2800	58463	444982	51.98484	3.98185	11.83	5.81	6.03
2900	58362	444898	51.98406	3.9804	8.13	4.30	3.83
3000	58272	444802	51.98318	3.97912	6.82	4.04	2.78
3100	58205	444709	51.98234	3.97817	5.69	3.56	2.13
3200	58150	444626	51.98158	3.9774	4.58	3.42	1.16
3300	58093	444543	51.98083	3.97659	3.32	2.74	0.58
3400	58036	444461	51.98008	3.97578	2.05	2.12	-0.07
3500	57979	444379	51.97933	3.97498	1.49	1.34	0.14

Table D.2: Output points of the SWAN transformation with corresponding coordinates and depth.

D.3.2. Nearshore wave roses

Here the wave roses for four different output locations along the toe of the DRS are shown. The wave roses show the wave height to wave direction distribution for every 400 meters along the interest area of the DRS.
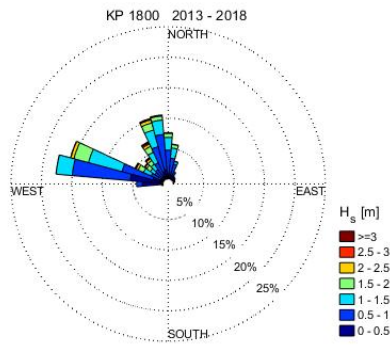
Figure D.11: Wave rose at the toe of KP 1800.
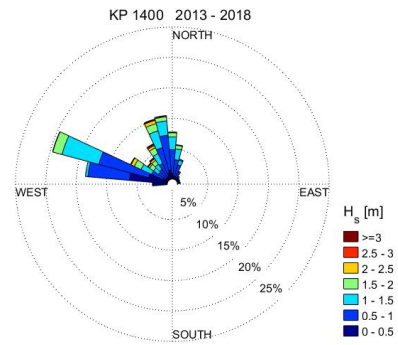
Figure D.12: Wave rose at the toe of KP 1400.
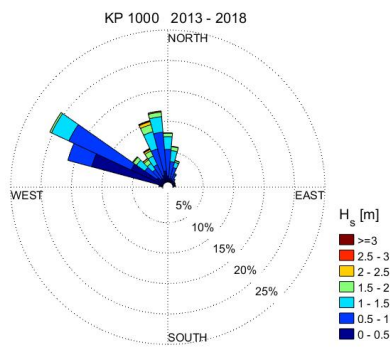
Figure D.13: Wave rose at the toe of KP 1000.
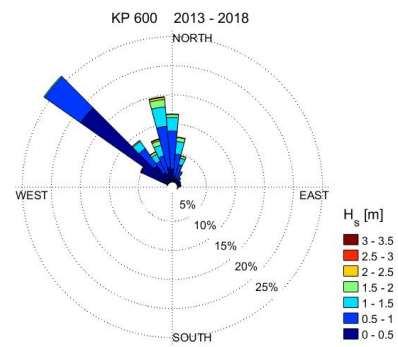
Figure D.14: Wave rose at the toe of KP 600.

D.3.3. Storm events

Here the full lists of the storm events following from the analysis of the nearshore wave data are presented.

Year-Month	H_s max. [m]	$T_{m-1,0}$ max. [s]	Direction mean [° N]	Water level max. [m + NAP]
2013-10	4.05	9.15	359	1.88
2013-10	3.93	8.29	235	1.51
2014-7	3.72	7.92	338	1.45
2015-3	3.51	7.68	258	1.88
2015-7	4.29	8.27	296	1.54
2015-11	3.87	8.18	241	1.72
2015-11	3.97	8.52	320	1.64
2016-1	3.68	7.96	253	1.60
2016-1	4.87	9.22	323	1.81
2016-2	3.51	8.18	218	1.83
2016-3	3.65	7.80	292	1.24
2017-1	4.15	9.08	307	2.22
2017-2	4.18	8.75	263	1.82
2017-6	3.74	7.87	223	1.56
2017-9	3.54	7.72	230	1.64
2017-10	3.63	8.56	305	1.66
2017-12	3.64	7.29	294	1.64
2018-1	3.58	8.76	325	1.97

Table D.3: Low water level storms 2013-2018.

Year-Month	H_s max. [m]	$T_{m-1,0}$ max. [s]	Direction mean [° N]	Water level max. [m+NAP]
2013-9	4.09	8.76	327	2.08
2013-12	4.08	9.32	314	3.01
2014-10	4.31	8.68	303	2.77
2015-1	3.54	7.63	273	2.12
2018-1	3.70	7.09	254	2.11

Table D.4: High water level storms 2013-2018.

E

Longshore Transport output

In this appendix the validation of the PUMA and the GLT relation for the four different survey periods are given. Figure E.1 shows the observed versus the calculated Longshore Transport (LT) gradients per 100 meters for the PUMA relation and Figure E.2 shows this comparison for the General Longshore Transport (GLT) relation. Within the figures "TP" stands for Time Period.
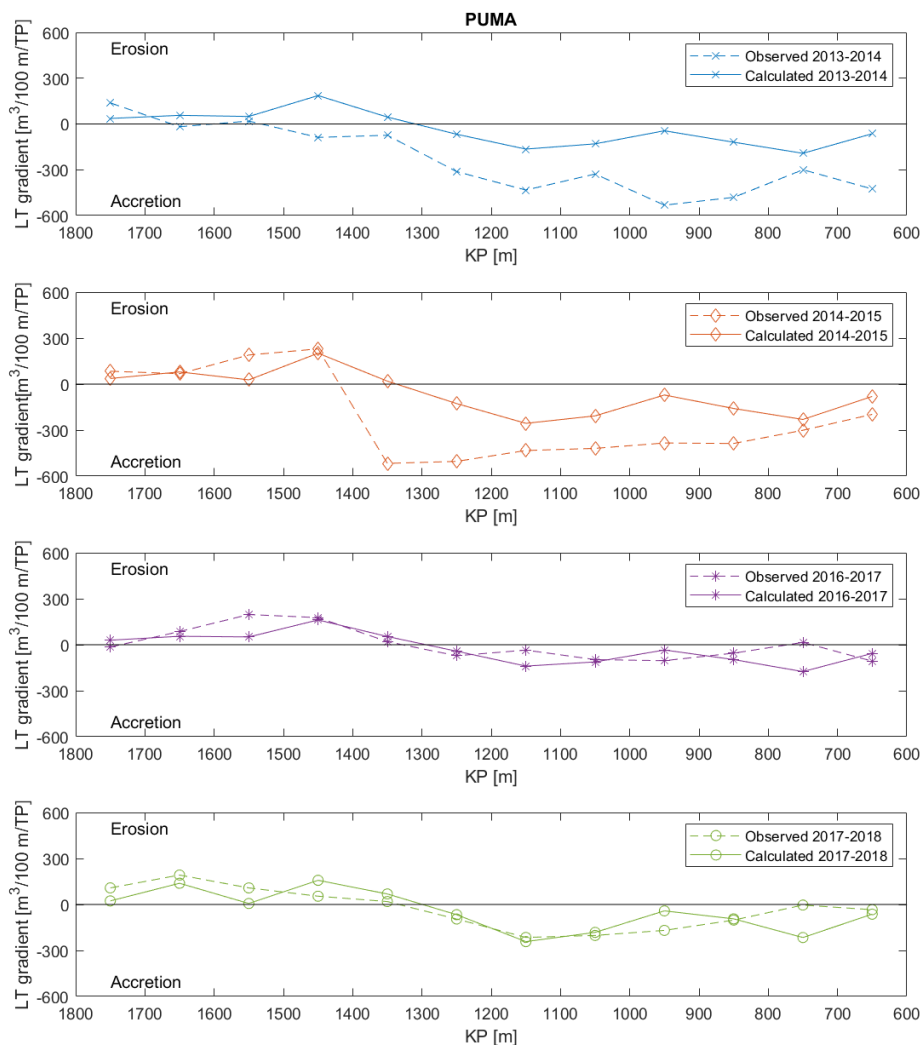
Figure E.1: Observed versus calculated LT gradients by means of the PUMA relation, for the four different survey periods.
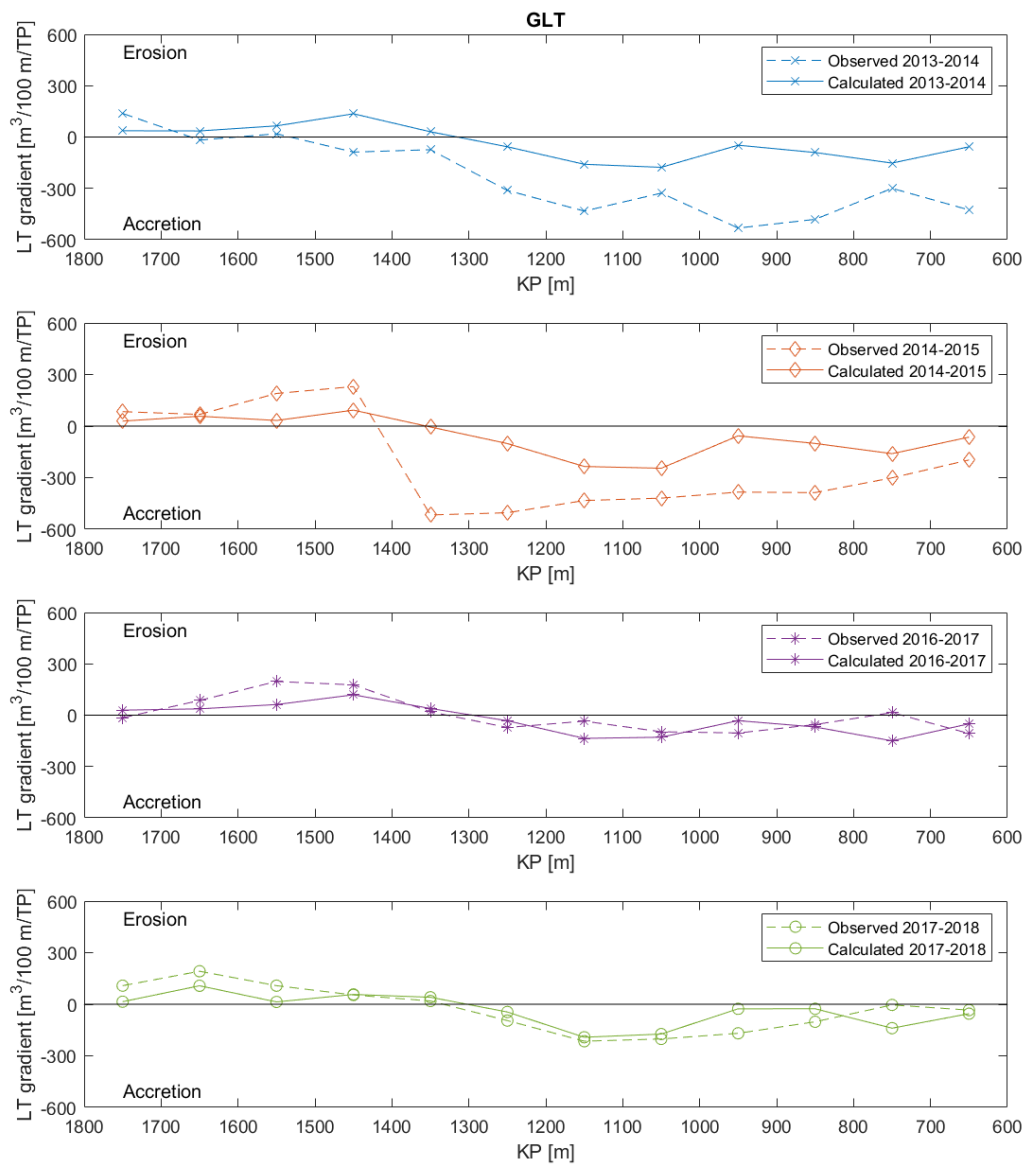
Figure E.2: Observed versus calculated LT gradients by means of the GLT relation, for the four different survey periods.